# Generation of Colo Rectal Cancer targeting TRAIL fusion proteins and a Mesenchymal Stem Cell line for *in situ* expression of these proteins

Von der Fakultät Energie-, Verfahrens- und Biotechnik der Universität Stuttgart zur Erlangung der Würde eines Doktors der Naturwissenschaften (Dr. rer. nat.) genehmigte Abhandlung

Vorgelegt von

**Irene Marini**

aus Frosinone (Italien)

Hauptberichter: Prof. Dr. Klaus Pfizenmaier

Mitberichter: Prof. Dr. Steffen Rupp

Tag der mündlichen Prüfung:
15 December 2016

Institut für Zellbiologie und Immunologie
Universität Stuttgart
2016

*To my family*

*and Andrea*

# Table of content

# Abbreviations

| | |
|---|---|
| **°C** | degree Celsius |
| **aa** | amino acid |
| **Ab** | antibody |
| **ALT** | alanine aminotransferase |
| **amp** | ampicillin |
| **APS** | ammonium persulfate |
| **BM** | Bone marrow |
| **BSA** | bovine serum albumin |
| **BZB** | bortezomib |
| **cFLIP** | cellular FLICE inhibitory protein |
| **CRC** | colorectal cancer |
| **CSCs** | cancer stem cells |
| **Da / kDa** | (kilo) Dalton |
| **DAPI** | 4',6-diamidino-2-phenylindole |
| **Db** | diabody |
| **DcR** | decoy receptor |
| **DD** | death domain |
| **DISC** | death-inducing signal complex |
| **DMSO** | dimethyl sulfoxide |
| **DNA** | deoxyribonucleic acid |
| **dNTP** | deoxyribunucleoside triphosphate |
| **DR** | death receptor |
| **e.g.** | exempli gratia / for example |
| **EC50** | mean effective concentration |
| **ECL** | enhanced chemiluminescence |
| **EDTA** | ethylenediaminetetraacetate |
| **EGFR** | epidermal growth factor receptor |
| **ELISA** | enzyme-linked immunosorbent assay |
| **f.c.** | final concentration |
| **FBS** | fetal bovine serum |
| **FCS** | fetal calf serum |
| **Fig.** | figure |
| **FITC** | fluorescein isothiocyanate |
| **G418** | Geneticin |
| **h** | hour |
| **His6** | hexahistidyl |
| **HPLC** | high performance liquid chromatography |
| **HRP** | horse radish peroxidase |
| **hu** | human |
| **i.p.** | intraperitoneal |
| **i.v.** | intravenous |
| **IBMX** | 3-isobutyl-1-methylxanthine |
| **IF** | immunofluorescence |
| **IMAC** | immobilized metal ion affinity chromatography |

| | |
|---|---|
| **IPTG** | isopropyl-β-D-thiogalactopyranoside |
| **LB** | lysogeny broth |
| **M** | molar |
| **m** | milli ($10^{-3}$) |
| **mAb** | monoclonal antibody |
| **mBMSC** | mouse bone marrow stromal cell |
| **MFI** | mean fluorescence intensity |
| **MHC** | Major Histocompatibility Complex |
| **min** | minutes |
| **mMSC** | mouse mesenchymal stromal cells |
| **MSCs** | mesenchymal stromal cells |
| **mTNF** | membrane-bound TNF |
| **mTRAIL** | membrane-bound TRAIL |
| **MW** | molecular weight |
| **n** | nano ($10^{-9}$) |
| **NOD-SCID** | Non-Obese Diabetic-Severe Combined Immunodeficiency |
| **OD** | optical density |
| **p** | pico ($10^{-12}$) |
| **P** | passage |
| **p.t.** | peritumoral |
| **pAb** | polyclonal antibody |
| **PAGE** | polyacrylamide gel electrophoresis |
| **PBST** | phosphate buffered saline tween |
| **PCR** | polymerase chain reaction |
| **PE** | Phycoerythrin |
| **Pen/Strep** | Penicillin/Streptomycin |
| **ph** | Potential of hydrogen |
| **PI** | propidium iodide |
| **rpm** | rotation per minute |
| **RT** | room temperature |
| **s.c.** | subcutaneous |
| **scFv** | single-chain fragment variable |
| **SCs** | stem cells |
| **scTRAIL** | single-chain TRAIL |
| **SDS** | sodium dodecyl sulfate |
| **SDS** | sodium dodecyl sulfate |
| **SDS-PAGE** | SDS polyacrylamide gel electrophoresis |
| **SEC** | size exclusion chromatography |
| **SEM** | standard error of the mean |
| **SM** | Smac mimetic |
| **TEMED** | N,N,N',N'-tetramethylethyl-diamine |
| **TGF-β** | transforming growth factor β |
| **TNF** | tumor necrosis factor |
| **TNFR** | TNF receptor |
| **TRAIL** | TNF-related apoptosis-inducing ligand |
| **TRAILR** | TRAIL receptor |
| **Tris** | tris-(hydroxymethyl)-amino-methane |

| | |
|---|---|
| **v/v** | volume by volume |
| **VH** | variable heavy chain domain |
| **VL** | variable light chain domain |
| **WB** | Western blotting |
| **WT** | wild type |
| **Zeo** | Zeocin |
| **α** | anti- |
| **α-MEM** | Alpha Minimum Essential Medium Eagle |
| **ε** | molecular extinction coefficient |
| **µ** | micro ($10^{-6}$) |

# Summary

Despite extensive studies aimed to increase the outcomes of cancer therapies, the conventional treatments still show lack of selectivity, short *in vivo* half-life and innate or acquired resistance. In this context, the discovery of cancer stem cells (CSCs), a small population within the tumor (<2-5 %) derived from normal stem cells after genetic/epigenetic alterations, defined new perspectives in the field of tumor therapy. In fact, due to their particular features, such as quiescent status and stemness properties, emerging data suggest a key role of CSCs in chemotherapy resistance, tumor relapse and metastasis formation. A promising strategy is the targeted delivery of anticancer proteins to CSCs, such as TNF-related apoptosis inducing ligand (TRAIL), in order to improve the therapeutic effects.

Based on these new findings, in the first part of this study, two novel antibody single-chain (sc)TRAIL fusion proteins with hexavalent TRAIL assembly, targeting the cancer stem cell markers CD133 and LGR5, were generated and characterized ($Db_{\alpha CD133}$-scTRAIL and $Db_{\alpha LGR5}$-scTRAIL). The biochemical analyses demonstrated for both fusion proteins integrity and correct dimeric assembly. The binding functionality of the scTRAIL fusion proteins to the targets was confirmed by flow cytometry analysis. Furthermore, in order to investigate the bioactivity of the fusion proteins, TRAIL-mediated cell death induction was verified by *in vitro* assays. A significant increase of cell death induction was observed for both proteins which exerted even a more potent antitumoral effect in combination with the sensitizer Bortezomib, resulting in a ~4-fold increased bioactivity. Interestingly, a significant benefit of the targeting domains, in terms of enhanced binding rate or bioactivity, was not observed for both TRAIL fusion proteins in comparison with a non-targeted TRAIL fusion protein. This is probably due to the particular cell lines tested, a moderate affinity of the targeting domain or to a low antigen expression on the two analyzed tumor cell lines.

An alternative approach to enhance the efficacy of therapeutics is based on normal adult stem cells used as carrier system for the *in situ* production of proteins, resulting in higher local concentration and reduction of general side effects caused by systemic administrations. This method, which exploits unique properties of adult stem cells, such as mesenchymal stem cells (MSCs), including tumor homing capacity and immunosuppressive ability, is currently exploited as transient expression system for therapeutic proteins in clinical applications. In the second part of this work, this novel stem cell based approach for colon cancer treatment was investigated. Different from the published work, here, I investigated the potential use of MSCs as delivery vector for the

stable expression of the pro-apoptotic protein $Db_{\alpha EGFR}$-scTRAIL. First, the insensitivity of MSCs to TRAIL activity was verified, showing a complete resistant phenotype even in the presence of sensitizers, confirming the huge advantage of these cells. Then, the bioactivity of $Db_{\alpha EGFR}$-scTRAIL secreted by MSCs was analyzed and a potent cell death induction, caused by TRAIL apoptotic pathway activation, was observed in combination with bortezomib. Importantly, all MSC properties and characteristics were maintained after stable transfection over time in *in vitro* cultivation. Finally, using xenotransplantation mouse tumor models, I could demonstrate the therapeutic activity of $Db_{\alpha EGFR}$-scTRAIL produced by MSCs when injected peritumorally, in combination with Bortezomib. In fact, a significant tumor volume reduction and a survival rate of 80% was observed in comparison with all control groups. Interestingly, no hepatotoxic or general side effects were revealed during the entire period of treatment, indicating the safety of this novel therapeutic approach.

# Zusammenfassung

Trotz großer Fortschritte in der Onkologie gibt es für viele Tumorerkrankungen noch unzureichende therapeutische Ansätze, wofür u.a. Tumorheterogenität, konstitutive oder erworbene Resistenz des Tumors gegenüber dem Therapeutikum, fehlende Selektivität der Wirkstoffe und kurze in vivo-Halbwertszeit ursächlich sein können. In diesem Zusammenhang ist die Entdeckung von Krebsstammzellen (cancer stem cells, CSC), einer kleinen Population innerhalb des Tumors (2-5 %), die sich von normalen Stammzellen nach genetischen und epigenetischen Veränderungen ableiten, interessant. Krebsstammzellen wird aufgrund ihrer besonderen Stammzell-ähnlichen Eigenschaften eine Schlüsselrolle in der Therapieresistenz, insbesondere im Hinblick auf Tumorrückfall nach primärem Ansprechen sowie Metastasierung, zugeschrieben. Aufgrund der Unempfindlichkeit von Krebsstammzellen gegenüber konventioneller Chemotherapie könnte die gezielte Behandlung mit hochpotenten Proteintherapeutika, wie dem Apoptose-induzierenden Liganden TRAIL, eine erfolgversprechende neue Strategie darstellen.

Basierend auf diesen aktuellen Erkenntnissen wurden im ersten Teil dieser Arbeit zwei neue, zielspezifische Antikörper-TRAIL-Fusionsproteine auf der Basis von einzelkettigem, single-chain (sc)TRAIL entwickelt. Die Fusionsproteine besitzen, die Spezifität für die Krebsstammzellmarker CD133 oder LGR5 sowie eine hexavalente Anordnung von TRAIL mit Hilfe des sogenannten Diabody-Formates ($Db_{\alpha CD133}$-scTRAIL und $Db_{\alpha LGR5}$-scTRAIL). Die biochemischen Analysen zeigten eine korrekte Assemblierung der jeweiligen Diabody-scTRAIL-Moleküle als Dimer, d.h. jedes Fusionsprotein-Molekül enthält zwei funktionelle, einzelkettige scTRAIL-Moleküle. Die spezifische Bindung der TRAIL-Fusionsproteine auf den Zielzellen wurde mittels Durchflusszytometrie-Analyse und die Bioaktivität durch in vitro Apoptose-Induktion bestätigt. In beiden Fällen, $Db_{\alpha CD133}$-scTRAIL und $Db_{\alpha LGR5}$-scTRAIL, führte die simultane Inkubation der Zellen mit dem Proteasom-Hemmstoff Bortezomib (Velcade) zu einer signifikanten (~4-fachen) Erhöhung der Apoptose . Überraschenderweise wurde aber für die untersuchten Zelllinien in den in vitro Experimenten kein Vorteil der zielspezifischen scTRAIL-Fusionsproteine gegenüber einem funktionell äquivalenten, nicht zielspezifischen scTRAIL-Fusionsprotein festgestellt. Die Gründe hierfür bleiben unklar, könnten aber in einer unzureichenden Expression des Zielproteins bzw. unzureichenden Affinität der scFv-Domäne für das Zielantigen begründet sein.

Ein alternativer Ansatz, um die Wirksamkeit von Therapeutika zu verbessern, basiert auf normalen adulten Stammzellen, die als Trägersystem für eine in situ-Produktion von

Proteintherapeutika genutzt werden sollen., Die Verwendung dieser Zellen stellt vor allem unter dem Gesichtspunkt einer höheren lokalen Wirkstoff-Konzentration und Verringerung von allgemeinen Nebenwirkungen, wie sie bei systemischer Verabreichung oft beobachtet werden, einen Vorteil dar. Die einzigartigen Eigenschaften von adulten Stammzellen, insbesondere der mesenchymalen Stammzellen (MSCs), wie beispielsweise Tumor-Homing-Kapazität und Gewebeverträglichkeit, machen diese Zellen zu einem attraktiven Werkzeug in der Tumortherapie. Im zweiten Teil dieser Arbeit, wurde deshalb ein Stammzell-basierter Ansatz für die Tumor-Behandlung in einem Darmkrebs-Modell untersucht. Insbesondere wurde die Verwendung von MSCs als stabiles Expressionssystem für die in situ-Herstellung des pro-apoptotischen Proteins $Db_{\alpha EGFR}$-scTRAIL getestet. Es konnte gezeigt werden, dass die verwendete MSC-Linie unempfindlich gegenüber TRAIL und dem Antikörper-scTRAIL-Fusionsprotein und damit als Producer-Linie geeignet ist. Stabile Produktions-Klone konnten isoliert und in Langzeitkultur gehalten werden. Das sezernierte Produkt, $Db_{\alpha EGFR}$-scTRAIL, wies die erwarteten Eigenschaften bezüglich Apoptoseinduktion auf den entsprechenden Zielzellen auf. Von besonderer Bedeutung war die Beobachtung, dass die stabilen MSC-Klone alle phänotypischen und funktionellen Eigenschaften einer mesenchymalen Stammzelle beibehielten. Schließlich konnte in einem Xenotransplantations-Tumormodell der Maus die therapeutische Aktivität der peritumoral applizierten, $Db_{\alpha EGFR}$-scTRAIL produzierenden MSCs gezeigt werden, wobei die Wirkung durch zusätzliche Gabe des sog. „Apoptose-Sensitizers“ Bortezomib deutlich gesteigert werden konnte. In dieser Behandlungsgruppe wurde im Beobachtungszeitraum (52 Tage) die stärkste Tumorvolumenreduktion und eine Überlebensrate von 80% festgestellt, im Vergleich zu den Kontrollgruppen (PBS 0%, Kontroll-MSC plus Bortezomib 50%, TRAIL-MSC ohne Bortezomib 60%). Interessanterweise wurden in den behandelten Tieren keine erhöhten Leberwerte oder allgemeine Nebenwirkungen festgestellt, was darauf hinweist, dass die Verwendung von mesenchymalen Stammzellen zu einem gut verträglichen Therapieverfahren entwickelt werden kann.

# 1 Introduction

## 1.1 Colorectal cancer

Cancer is the second cause of death worldwide and colorectal cancer (CRC) is the fourth most common lethal malignancy with over one million new cases every year (Siegel et al., 2014). The normal intestinal epithelium presents a well-defined structure that consist of crypts and finger-like protrusions (villi) with a hierarchical organization. Due to the function of the organ, the homeostasis of this tissue is finely regulated.

The CRC carcinogenesis is a multistep process that requires the accumulation of specific genetic mutations involved in various signal transduction pathways that maintain the correct intestinal homeostasis. The progression from normal colon tissue to adenoma, carcinoma and finally to metastatic cancer requires the sequential alteration of protective pathways regulated by adenomatous polyposis coli (APC), p53 and transforming growth factor β (TGF-β) and the activation of oncogenes such as K-Ras and B-Raf (Markowitz et al., 2009 and Lampropoulos et al., 2012) (Figure 1). An important characteristic of CRC is its high heterogeneity which can explain the wide range of different responses of patients to clinical therapy of tumors that are pathologically similar (Budinska et al., 2013).

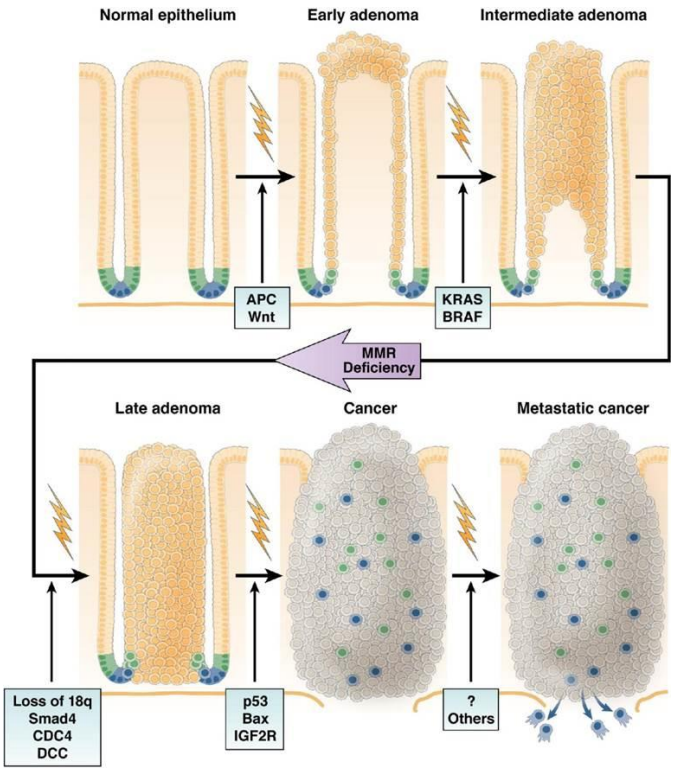


**Figure 1 Schematic representation of colon carcinogenesis**
Mutations on APC gene, negative regulator of the Wnt pathway, leads to hyper proliferation and formation of an early adenoma. Alterations on BRAF and KRAS genes occurs at the stage of intermediate adenoma. Late adenoma results after loss of heterozygosity at 18q, including Smad 4, cell division cycle 4 (CDC4) and DCC. The invasive state, finally, occurs after mutations on p53, Bax, and/or insulin-like growth factor receptor 2 (IGF2R) genes. Taken from Todaro et al., 2010.

Currently, the conventional strategies used to treat CRC are basically four: surgery, chemotherapy, radiotherapy and targeted therapies. Despite of the fact that surgical resection and additional therapy can cure early stage of primary tumors, the metastatic stage is mostly incurable because of its systemic distribution and resistance to conventional therapies. For this reason, more than 90% of cancer-related deaths can be ascribed to recurrence and not to primary lesions (Gupta et al., 2006 and Steeg et al., 2006). In particular for patients with newly diagnosed metastatic colon cancer the 5 year prognosis continues to be less than 20% (Jemal et al., 2011).

### 1.1.1 Stem cells and intestinal stem cell niche

Stem cells (SCs) are defined as undifferentiated cells with indefinite ability for self-renewal and differentiation into various cell types. The first identification was reported in 1963 by Becker and Siminovitch (Becker et al., 1963 and Siminovitch et al., 1963). Stem cells can divide through two different mechanisms: symmetric division giving rise to two daughter cells identically to the mother cell that maintain the self-renewal capacity or through the asymmetric division producing one cell that is identical to the mother cell whereas the other one is a more specialized cell. Based on their ability to differentiate into various distinct cell types/tissues, i.e. their plasticity, stem cells are classified as totipotent, pluripotent and multipotent. The totipotent stem cells are found in the zygote and can generate a new individual on their own. The pluripotent stem cells can give rise to almost all body tissues but they lost the ability to form extraembryonic tissues like placenta. While the multipotent stem cells, also called adult stem cells (ASCs), can generate different cell types according to their location. These multipotent stem cells can be isolated from different adult tissues such as blood, epidermal and intestinal tissue characterized by rapid regeneration, where they contribute to maintain the tissue homeostasis (Beddington et al., 1989). In particular the colon, the last part of the digestive system, consists of millions of crypts and each one contains about 2000 cells (Potten et al., 1992 and Booth et al., 2000) which undergo turnover every 2-5 days in normal condition and increasing following tissue damage with an average of $10^{10}$ cells produced daily (Brittan et al., 2002). This complex process is regulated by adult stem cells located at the very base of the crypt. This specific environment is called Stem Cell Niche and consists of cellular and extracellular components that ensure the optimal condition for SC maintenance. In particular, the niches control the SC's fate, regulating the correct balance between self-renewal and differentiation, through the secretion of various cytokines, growth factors and direct interactions (Todaro et al., 2010). SCs in the niche divide mainly through asymmetric division generating one daughter identically to the mother that remains within

the niche and the other one that leaves the niche and differentiates along the crypt axis towards the luminal surface where it undergoes apoptosis (Todaro et al., 2010). Intrinsic and extrinsic factors have been shown to regulate SC niches. Merlos-Suarez et al. reported that ephrinB (EphB) pathway is involved in the cell compartments organization and in the regulation of migration of epithelial cells along the crypt axis (Merlos-Suarez et al., 2008). Intestinal subepithelial myofibroblasts (ISEMFs), located at the base of the crypt, are key regulators of intestine SCs by secreting a wide range of morphogenetic factors (Todaro et al., 2010). But the entire intestinal homeostasis is finely regulated by a complex crosstalk network of pathways such as Wingless/Int (Wnt), Notch and Hedgehog which control the balance between proliferation, differentiation and self-renewal. In particular for Wnt pathway there is a decreasing gradient of expression from the base to the top of the crypt. For this reason Wnt proteins are mainly present at the bottom of the crypt where they interact with receptors on epithelial cells resulting in nuclear translocation of β-catenin. Nuclear β-catenin induces the expression of EphB receptors which interact with ephrin ligands distributed along the crypt axis, enhancing the proliferation rate. In addition to Wnt signal Notch contributes to potentiate proliferation and inhibits differentiation at the bottom of the crypt (Holmberg et al., 2006). While Hedgehog pathway seems to be a Wnt suppressor, probably through BMP's activity. In fact, there is a decreasing gradient of BMP expression from the top to the base of the crypt which neutralizes the proliferative effect of Wnt and maintains the differentiation state in the apical part of the crypt (Medema et al., 2011). This intricate network of finely regulated pathways defines the environment which controls the crucial balance between proliferation, differentiation and self-renewal in the intestinal tissue. In this context, obviously, the alteration/deregulation of a single factor can significantly increase the risk of carcinogenesis.

### 1.1.2 Colorectal Cancer Stem Cells (CSCs)

According to the traditional model of tumorigenesis, called the stochastic model, every cell within the tumor population is able to initiate and propagate tumor development, following multiple genetic mutations. However in the last several years evidence was obtained supporting the idea that only a small fraction of cells, with stemness characteristics, possess the unique property of tumor initiation. This concept has generated a new model for carcinogenesis called Cancer Stem Cell (CSC) model (Huang et al., 2008). Indeed, CSCs have been isolated from different types of tumor, including colon. In particular the existence of colon CSCs was reported for the first time in 2007 by the research groups of O'Brien and De Maria (De Maria et al., 2007 and O'Brien et al., 2007) using CD133

glycoprotein as marker. Both research groups, independently, observed that only a small population of cancer cells, positive for CD133 expression, was able to initiate tumor growth during serial transplantations in immunodeficient mice recapitulating the original tumor, while negative cells were not able to do so. CSCs show similar properties with normal SCs such as slow cycling, high expression of anti-apoptotic proteins and ATP-binding cassette (ABC) transporters, which could explain the failure of canonic anticancer treatments which, on the contrary, target differentiated and proliferating cells (Scopelliti et al., 2009). Based on these features, CSCs could play a key role in cancer recurrence after radio/chemotherapy, due to the fact that they are resistant to standard treatments and possess cancer-initiating potential.

Despite initial description of CD133 as a potential CSC marker, CD133 expression is not restricted to CSCs only, but also expressed in differentiated colonic epithelium, with 0,4-2,1% expression in healthy tissue versus 8.9-15.9% in cancer (Catalano et al., 2012). For this reason, several additional molecules have been proposed as putative colon CSCs markers including CD44, CD24, CD166, Lgr5 and ALDH-1 (Vaiopoulos et al., 2012). A combination of these markers is likely more suitable for the identification and isolation of true colon CSCs (Haraguchi et al., 2008).

### 1.1.3 Colorectal CSC markers: CD133 and Lgr5

Several studies reported that the expression of CSC markers in CRC has prognostic significance (Coco et al., 2012 and Zhang et al., 2012), consequently targeting these cells is suggested to enhance the success of cancer therapy. As mentioned above, the first putative colon CSC marker reported was CD133 (De Maria et al., 2007 and O'Brien et al., 2007). It is a pentaspan transmembrane glycoprotein implicated in the organization of plasma membrane, with two large N-glycosylated extracellular loops, two small intracellular domains and a cytoplasmic C-terminal domain as show in figure 2A (Yin et al., 1997). Although its function in tumor progression remains still unclear, CD133 could play a role in cell polarity through cell-cell and cell-matrix contact (Giebel et al., 2004). In fact, CD133 was reported to be localized at the lipid rafts on the cell membrane contributing to the activation of signalling cascades (Simons et al., 2000). This glycoprotein seems to be involved into stem cell properties maintenance such as the balance between symmetric and asymmetric cell division (Bauer et al., 2008). Therefore, Pilati et al. suggested that CD133 mRNA levels of circulating tumor cells could have a prognostic value in advanced colorectal cancer (Pilati et al., 2012). In particular, they analyzed different genes finding out that only the expression levels of CD133 correlate with patients' survival. In fact, the CD133 expression was significantly higher in the liver

metastasis in comparison with primary colon cancer and normal tissue. The transcriptional level of CD133 was negatively correlated with disease-specific survival indicating its predictive power in CRC.

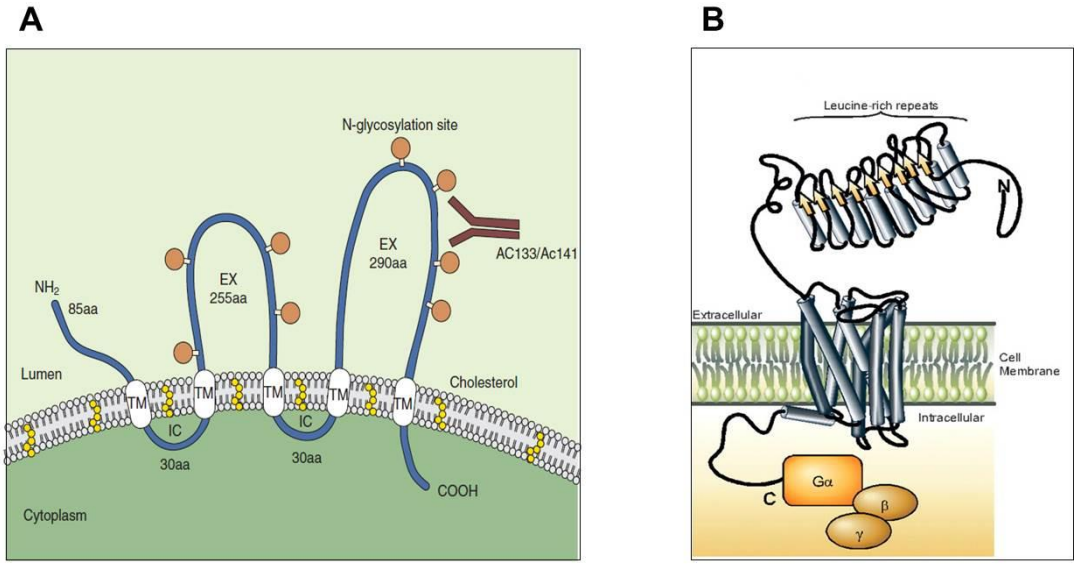


**Figure 2 Structure of CD133 and Lgr5**
(A)The predicted structure of CD133 consists of an 85 amino acid (aa) N-terminal extracellular domain, five transmembrane domains (TM) with two extracellular loops (EX) of 255 aa and 290 aa, two 30 aa intracellular domains, and a 50 aa cytoplasmatic tail. Eight N-linked glycosylation sites are the binding sites of antibodies (AC133 and AC141). Taken from (Catalano et al., 2012). (B) Lgr5 is predicted to encode a 7-transmembrane protein with a large extracellular domain for ligand binding and a short cytoplasmic tail for coupling to G-proteins. Taken from (Barker et al., 2008).

Among all the proposed putative CSC markers Leucine-rich repeat-containing G-protein coupled receptor 5 (Lgr5), a Wnt target gene, is considered one of the most promising (Barker et al., 2008). Its structure consists of seven transmembrane loops, a large extracellular domain for ligand binding and a short cytoplasmic tail for coupling to G-proteins as show in figure 2B (Barker et al., 2008). For a long time Lgr5 was considered as an orphan receptor, but in 2011 de Lau et al. identified for the first time R-spondin as ligand for Lgr5 (de Lau et al., 2011). Although its specific function is still under debate, the expression of Lgr5 is exclusively restricted to the base of the intestinal crypt, where the intestinal SC niche is located (Barker et al., 2007). Additionally, due to the fact that Lgr5 is a target of the Wnt pathway, this protein is probably involved in maintenance of the correct SC niche environment.

First evidence that Lgr5 is a specific CSC marker and that it can be used to isolate CSCs from colorectal cancer, was reported in 2012 by Kemper et al. They demonstrated that three new monoclonal antibodies against Lgr5 can identify the CSC population in human colorectal cancer. In fact, the CRC cells selected for high expression levels of Lgr5 were more clonogenic and tumorigenic than CRC cells which showed low Lgr5 expression

levels. Kemper and colleagues (Kemper at al., 2012) also observed that the overexpression of Lgr5 induced a higher clonogenic growth *in vitro*, indicating that this protein is a new functional marker for colorectal CSCs identification.

## 1.2 Apoptosis

Apoptotic cell death is a physiological process genetically controlled that maintains the body homeostasis eliminating damaged or stressed cells in a way that is expected to cause the slightest damage and no inflammation (Garg et al., 2010). The canonic therapeutic strategies for tumor treatment such as chemotherapy, radiotherapy and new protein drugs all operate via inducing programmed cell death in cancer cells. Two forms of apoptosis have been found: the intrinsic and the extrinsic apoptotic pathways (Figure 3). The intrinsic pathway, also known as mitochondrial pathway, is activated in response to cellular stress including DNA damage, oxidative stress, chemotherapy and radiotherapy. It is mainly regulated by the balance between the members of the Bcl superfamily which consists of pro-apoptotic proteins as Bak and Bax; and the anti-apoptotic members like Bcl-2, Bcl-XL and Mcl-1. A crucial sensor of cellular damage is the tumor suppressor protein p53 which can regulate the expression of the genes of pro-apoptotic proteins such as Puma, Noxa, Bax and Apaf-1 inducing cell death via the intrinsic pathway (Vousden et al., 2002). In particular, the pro-apoptotic proteins induce the permeabilization of the mitochondrial outer membrane and consequently the release into the cytosol of co-factors of apoptosis like cytochrome c and Smac/Diablo. The cytochrome c and dATP induce Apaf-1 and caspase 9 to assemble the apoptosome in which caspase 9 is activated and in turn can activate downstream effectors such as caspase 3, 6, 7 to further catalyze the effector phase of apoptosis (Sprick et al., 2000 and Ashkenazi et al., 2008). SMAC/Diablo can indirectly promote apoptosis by inhibition of the members of the IAPs (inhibitor of apoptosis) family such as XIAP, cIAP1 and cIAP2. The IAPs are in fact able to ubiquitinate the initiator caspase 9 and the effectors caspase 3 and 7, thereby leading to proteasomal degradation of these critical mediators of apoptosis and thus suppress cell death (Falschlehner et al., 2007).

The extrinsic apoptosis pathway is activated by binding of a death ligands to transmembrane receptors called Death Receptors (DRs) that transduce a signal from outside into the cell. The interaction between ligands and DRs induces their oligomerization that is crucial for the recruitment of the adaptor protein Fas-associated death domain (FADD) to the intracellular death domains (DD) of these receptors. FADD in turn recruits the pro-caspases 8 and 10 forming the death-inducing signalling complex (DISC). At the DISC through an auto-catalytic cleavage caspases 8 and 10 are activated

and in turn can directly cleave caspase 3 which itself cleavages other caspases and various critical cellular substrates, foremost the Caspase activated DNAse Inhibitor (ICAD) leading to irreversible DNA cleavage and subsequent cell death (Sprick et al., 2000 and Kruyt et al., 2008).

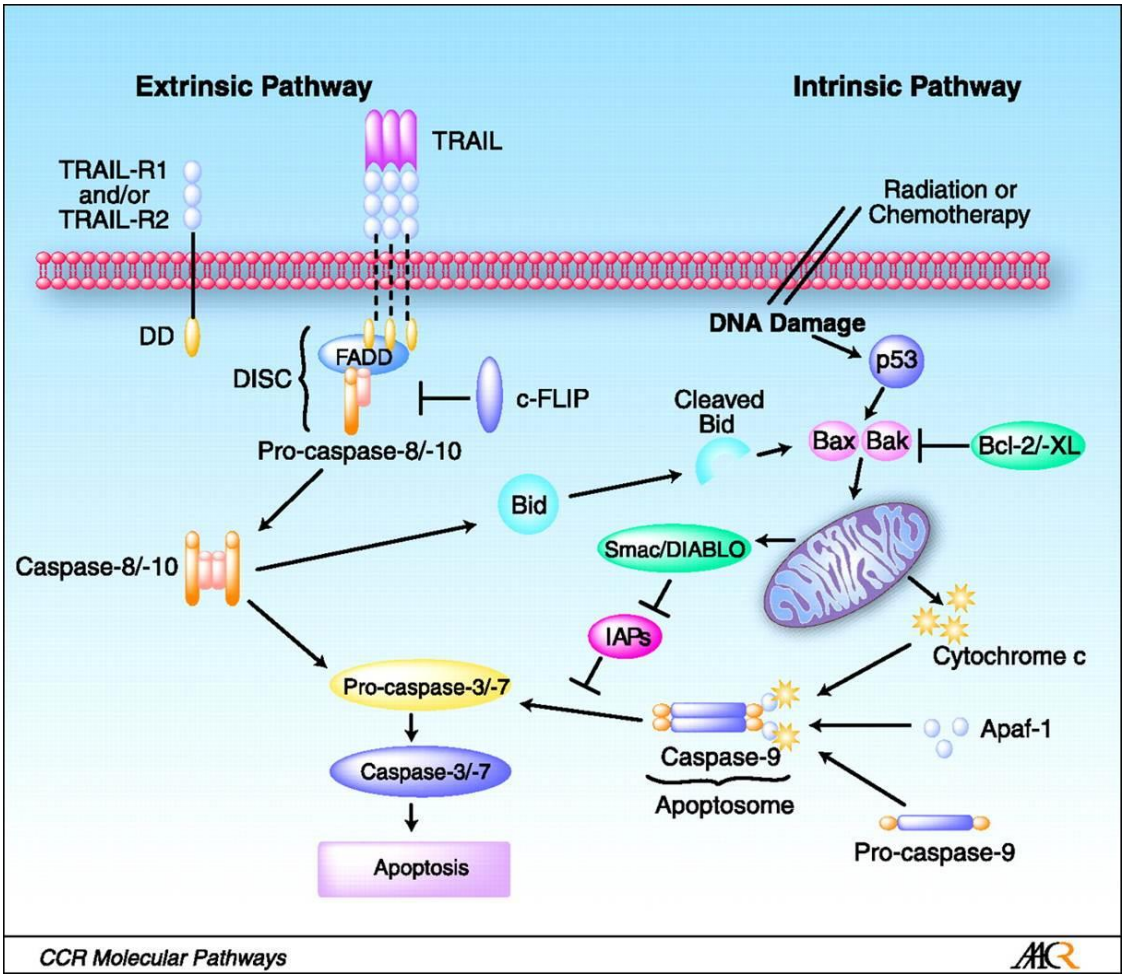


**Figure 3 Intrinsic and Extrinsic pathways of apoptosis**
The extrinsic pathway is triggered by the binding of apoptosis-inducing ligands to pro-apoptotic receptors (TRAIL-R1 and TRAIL-R2) resulting in oligomerization of the receptors. The death-inducing signaling complex (DISC) is composed of the Fas-associated death domain (FADD), which binds to the death domain (DD) of the receptor and recruits the pro-caspases 8 and 10 undergoing auto-activation by proteolytic cleavage (caspases 8 and 10). The initiator caspases 8 and 10 activate the downstream effector caspases 3 and 7, which execute apoptosis in the cells. The intrinsic pathway is triggered by cellular stress, such as DNA damage or by radiotherapy and chemotherapy, resulting in a p53-dependent upregulation of pro-apoptotic proteins, like Bax and Bak. These proteins induce the permeabilization of mitochondrions resulting in a release of cytochrome c and Smac/DIABLO into the cytosol. The apoptosome is composed of Apaf-1, cytochrome c and caspase 9, exhibiting the activation of the effector caspases 3 and 7. Smac/DIABLO also activates apoptosis indirectly by inhibiting the subfamily of inhibitors of apoptosis (IAPs). The cross-talk between the extrinsic and the intrinsic pathway is performed by the pro-apoptotic protein Bid, which can be cleaved and activated by caspase 8. This protein induces apoptosis by inhibiting the anti-apoptotic proteins Bcl-2 and Bcl-XL and by activating the pro-apoptotic proteins Bax and Bak. Taken from (Carlo-Stella et al., 2007).

Based on *in vitro* studies, cells have been classified in two categories of differing in the pathway used for apoptosis induction. In type 1 cells the cell death is triggered via the extrinsic pathway upon activation of the DRs. While in the type 2 cells, the induction of

caspase 3 activation by DISC is insufficient to trigger apoptosis and they need an additional amplification step via the mitochondrial pathway (Ozören and El-Deiry, 2002).
The link between the extrinsic and the intrinsic pathways is represented by the pro-apoptotic protein Bid, a member of the Bcl2 family. Bid can be cleaved by active caspase 8 into a truncated form (tBid). Cleaved Bid translocates to the mitochondria and interacts with Bax and Bak inducing their oligomerization and the release of Cytocrome c and SMAC/Diablo and the consequent activation of the downstream effectors caspases (Kruyt et al., 2008).

## 1.3 TNF-Related apoptosis inducing ligand: TRAIL

TNF-Related apoptosis inducing ligand (TRAIL), also known as Apo2L, is a member of the TNF superfamily. The tumor necrosis factor (TNF) was the first death ligand discovered in 1975 and used for anticancer treatment (Carswell et al., 1975). Although TNF showed cell death induction in some cancer types, it soon became clear that its major function was in the pro-inflammatory process and this activity could explain the high toxicity observed after systemic administration of TNF (Tracey et al., 1987; Tracey et al., 1988; Roberts et al., 2011). Afterwards, the death receptor (DR) FAS/Apo1 (CD95) was proposed as anticancer target, based on the finding that two antibodies targeting this receptor induced apoptosis in various cancer cell lines (Trauth et al., 1989 and Itoh et al., 1991). Unfortunately, similar to the TNF outcomes, tumor treatment with systemic administration of CD95 agonistic antibodies caused fulminant and lethal hepatotoxicity (Ogasawara et al., 1993). Few years later TRAIL was identified based on its sequence homology to the others members TNF and CD95 (Wiley et al., 1995 and Pitti et al., 1996). In this case, in contrast to TNF and CD95 results, TRAIL showed antitumoral activity *in vivo* without inducing toxicity during systemic treatment (Ashkenazi et al., 1999 and Walczak et al., 1999). This new member apparently possesses the unique ability to induce apoptosis selectivity in cancer cells and not in normal cells.
TRAIL is a homotrimeric molecule which can bind five types of receptors: TRAIL-Receptor 1 (TRAIL-R1) also called Death Receptor 4 (DR4); TRAIL-R2 (DR5); TRAIL-R3 and TRAIL-R4 also named respectively decoy receptor 1 and 2 (DcR1 and DcR2) and a soluble molecule osteoprotegerin (OPG) (Lemke et al., 2014). Although all the four trans-membrane receptors bind TRAIL, the apoptotic process can be induced only via TRAIL-R1 and TRAIL-R2 due to the fact that DcR1 lacks the intracellular domain and DcR2 contains only a truncated one (Wang et al., 2003). The interaction between TRAIL and the extracellular domains of TRAIL-R1 or TRAIL-R2 induces receptor oligomerization that is crucial for the recruitment of the adaptor protein Fas-associated death domain (FADD) to

the intracellular death domains, the formation of the DISC complex and the caspases activation (Sprick et al., 2000 and Kruyt et al., 2008).

### 1.3.1 TRAIL: combination therapy for tumor treatment

Tumors are heterogeneous populations of cells with a genetic and epigenetic unstable background (Meacham et al., 2014). For this reason cancer cells show different responses to TRAIL. In some case tumor cells are intrinsically resistant to TRAIL induced apoptosis, but they can also acquire resistance to TRAIL during tumor progression (Stuckey et al., 2013). However, many chemotherapeutic agents commonly used in cancer therapy have shown a synergistic effect with TRAIL, such as gemcitabine, doxorubicine, 5-Fluro Uracil (5-FU), cisplatin and irinotecan (reviewed by Newsom-Davis et al., 2009) and they can overrule the constitutive TRAIL resistance of several cancer cell lines (Hellwig et al., 2012). The molecular mechanisms that regulate this sensitization to TRAIL are not yet completely elucidated and are dependent on the different mode of action of the drugs (Dimberg et al., 2013). Novel drugs used in combination with TRAIL are under pre-/clinical evaluation, these so-called Smac mimetics mimic the XIAP (X-linked inhibitor of apoptosis protein) binding site of SMAC/Diablo, thus blocking XIAP as well as cIAP (cellular inhibitor of apoptosis) function and inducing there rapid degradation. These small molecules have shown, in a variety of cancer types, a strong sensitization of tumor cells to TRAIL activity both *in vitro* and *in vivo* (Li et al., 2004; Fakler et al., 2009; Lecis et al., 2010). Another promising agent, which displays antitumoral activity alone or in combination with TRAIL is bortezomib, a proteasome inhibitor, commonly used to treat different kinds of cancers including liver, breast, lung and pancreatic cancer (reviewed by de Wilt et al., 2013).

### 1.3.2 Bortezomib as sensitizer of TRAIL activity

Bortezomib (VELCADE) is a proteasome inhibitor and is currently approved by the Food and Drug Administration (FDA) for the treatment of multiple myeloma and mantle cell lymphoma (Orlowski et al., 2008 and Raab et al., 2009). In particular, bortezomib can reversibly bind the β5 subunit of the 26S proteasome, the major non-lysosomal protein degradation complex, causing the inhibition of the chymotrypsin-like proteolytic activity (Adams et al., 2003). Due to this inhibition polyubiquitinated proteins are accumulated and inefficiently degraded causing cell cycle arrest and the activation of the apoptotic pathway. Bortezomib is a potent sensitizer of TRAIL pro-apoptotic activity and the antitumoral effect of combined treatment was reported *in vitro* and *in vivo* in a broad range of different

cancers (reviewed by de Wilt et al., 2013). The sensitization of bortezomib affects TRAIL signalling pathway at multiple levels. For example, treatment with bortezomib was reported to increase TRAIL-R1 and/or TRAIL-R2 expression in various tumors types, resulting in enhanced apoptotic signalling (Koschny et al., 2007 and Liu et al., 2010). Another crucial effect of bortezomib activity on TRAIL pathway is the enhancement of caspase 8 activation at the DISC complex I (Brooks et al., 2010 and Seki et al., 2010). Furthermore, the inhibition of 26S proteasome affects the expression of various target genes at the transcriptional level by changing the stability of transcription factors like NF-kB. The activity of NF-kB is regulated by the repressor protein IkB, which is controlled by proteasome degradation. Bortezomib administration prevents IkB degradation, which consequently inhibits NF-kB dependent transcription of several anti-apoptotic target genes like c-FLIP, Bcl-XL and XIAP (Kreuz et al., 2001 and Sayers et al., 2003). As reported by Khanbolooki et al, treatments of pancreatic cancer cells with bortezomib as well as with a specific NF-kB inhibitor showed downregulation of XIAP and Bcl-XL expression and TRAIL sensitization (Khanbolooki et al., 2006). Concerning the Bcl-2 family, the effect of bortezomib on this group of proteins is not completely clear and it seems to be cell-type dependent. Nevertheless, Naumann et al. (Naumann et al., 2011) found that treatments with bortezomib stabiles N-terminal and C-terminal fragments of Bid following its cleavage by caspase 8. Furthermore, bortezomib can inhibit degradation of the C-terminal fragment of cleaved Bid via proteasome leading to enhancement of mitochondrial apoptotic pathway.

The efficacy of combined therapy using bortezomib and TRAIL has been explored in several xenograft mice models, e.g. as reported by Wahl et al. (Wahl et al., 2013) in hepatocellular carcinoma treatment and in a colorectal cancer xenograft model by Siegemund et al. (Siegemund et al., 2012).

### 1.3.3 Db-scTRAIL fusion proteins targeting colorectal CSCs

The failure of conventional tumor treatments is mainly due to metastasis formation and recurrence of cancer even after surgery and a long term period of chemo/radiotherapy.

Interestingly, both of these processes seem to be caused and regulated by CSCs. The hypothesis that only tumor-initiating cells are able to form new tumor in a different site, was reported by Dieter et al. and Kreso et al. for CRC (Dieter et al., 2011 and Kreso et al., 2013). They observed that metastasis derived from a subpopulation of cells, located in the primary tumor, which shows specific CSCs properties such as chemotherapy resistance, quiescent status and self-renewal ability. Furthermore, traditional tumor treatments have been generated to target and eradicate proliferating cells, but the small fraction of CSCs

within the tumor is, by and large, not affected and thus may cause cancer recurrence after months or years of apparent remission (Scopelliti et al., 2009).

This complex scenario underlines the need to develop new therapeutic agents targeting specifically CSCs that, potentially also in combination with canonic chemotherapy, could be significantly more efficient in prevention of metastasis formation and tumor regrowth. A new, promising approach to effectively attack malignant cells is based on the proapoptotic ligand TRAIL because of its presumed tumor selective activity and its high tolerability upon systemic administrations in humans (Yee et al., 2007 and Wainberg et al., 2013). However, several clinical trials testing the conventional recombinant TRAIL revealed that the use of this protein is largely ineffective to achieve significant therapeutic effects (Herbst et al., 2010 and Soria et al., 2010). These negative results are mainly due to the low *in vivo* bioactivity of the TRAIL molecules used and their short plasma half-life. In order to overcome these limitations an alternative approach, based on TRAIL fusion proteins targeting tumor markers, was investigated. First, fusion of three TRAIL domains into one polypeptide chain, through short peptide linkers, results in a single chain derivative of TRAIL (sc-TRAIL) which showed higher stability and antitumoral activity (Schneider et al., 2010). Furthermore, as reported by Siegemund et al. (Siegemund et al., 2012), the dimerization of single chain TRAIL (scTRAIL) proteins and an EGFR targeting scFv can be combined to obtain bifunctional fusion proteins, a Diabody-scTRAIL. These constructs maintain the ability to bind TRAIL receptors and simultaneously to target specific cancer antigen, In this example EGFR, resulting in enhancement of apoptotic induction both *in vitro* and *in vivo*.

## 1.4 Mesenchymal Stem Cells

An additional strategy to target and treat efficiently not only primary tumors but also the metastatic sites is the use of stem cell as delivery system for *in situ* expression of therapeutics. Mesenchymal stem cells (MSCs) are adult stem cells, which are currently exploited for different cellular therapies in clinical applications. The discovery of MSCs was reported for the first time in 1960s by Friedenstein et al. (Friedenstein et al., 1966 and Friedenstein et al., 1968) in the stromal compartment of bone marrow (BM) and they were described as clonal fibroblastic stromal cells that formed adherent colonies in culture and had robust osteogenic potential. The term “mesenchymal stem cells“ (MSCs) was defined for the first time by Caplan et al. in 1991 (Caplan et al., 1991) and their potential to multi lineage differentiation into bone, cartilage and fat cells was described in 1999 by Pittenger and colleagues.

In 2006 the International Society of Cellular Therapy (ISCT) has established three minimal criteria for defining MSCs. First, MSCs must show *in vitro* adherence to plastic in standard culture conditions; second, MSCs must express specific surface antigen such as CD9, CD71, CD105 and lack expression of other markers like CD34, CD14 and CD11b. According to the third criteria, MSCs must have the ability to differentiate into osteoblasts, adipocytes and chondroblasts *in vitro* (Dominici et al., 2006). This definition and characterization of MSCs still relies only on *in vitro* culture cell and consequently the localization and the *in vivo* distribution of MSCs are much less known (Hernanda et al., 2014). Nevertheless, in the last years MSCs were isolated from a variety of different organs/tissues such as bone marrow, kidney, adipose tissue, umbilical cord, brain, liver and lung (Zuk et al., 2001; da Silva Meirelles et al., 2006; Choi et al., 2014). The highest level of lineage plasticity has been imputed to bone marrow derived MSCs, which have been described to generate virtually all cell types following implantation into early blastocysts (Jiang et al., 2002). In spite of the fact that MSCs reside in the bone marrow in small number (0.001-0.01% of nucleated cells) (Kawada et al., 2004), they are easy to handle and expand *in vitro* to yield a sufficient number of cells for clinical applications. The most abundant source of MSCs in the human body is the adipose tissue obtained from subcutaneous tissue using simple and non-invasive techniques (Kern et al., 2006). Due to their accessibility and easy expansion protocols, MSCs have been recognized as promising candidates to set up new cellular therapies in regenerative medicine but also for treatment of various other diseases.

### 1.4.1 MSCs properties

In addition to the ease isolation from many different tissues and the convenient expansion *in vitro*, MSCs possess unique biological characteristics that make them an attractive therapeutic agent for treatment of a wide range of different pathologies.

**Multi lineage differentiation potential**

Giving the fact that MSCs belong to the mesoderm lineage they can differentiate in various cell types according to their own original lineage and to the tissue in which they reside. Their ability to generate bone, cartilage, and adipose tissues has been well documented both *in vitro* (Muraglia et al., 2000) and *in vivo* (Aslan et al., 2006). However the differentiation potential of MSCs appears exceptional. In fact, further studies reported that, using cytokine induction and/or gene introduction, MSC differentiate *in vitro* into cells of other lineages including endodermal (hepatocytes and insulin-producing cells) and

ectodermal lineages (neuronal, peripheral glial and epidermal cells) (Prockop et al., 1997; Dezawa et al., 2001; Oyagi et al., 2006; Wu et al., 2006; Karnieli et al., 2007; Dezawa et al., 2004). However the frequency of these differentiation events is generally very low and is considered to correspond to a small, potentially an as yet undefined subpopulation of MSCs. While the capacity to form the three distinct cell types: osteoblasts, chrondrocytes and adipocytes, remains the only reliable functional criterion to define MSCs.

**Immunosuppressive properties**

MSCs are considered immune privileged cells potentially “ignored” by the immune system. This can be explained by the fact that these cells express low levels of major histocompatibility (MHC) class I surface markers and are negative for MHC class II expression. Furthermore, they lack the expression of co-stimulatory molecules such as CD40, CD80 and CD86. Despite the low levels of MHC class I antigens a potential activation of T cells is conceivable, however, in the absence of co-stimulatory molecules the mandatory secondary signals for T cell activation are lacking, thus leaving the T cells anergic (Javazon et al., 2004). Furthermore, despite reduced levels of MHC class I antigens, these are sufficient toprotect MSCs from natural killer (NK) cell-mediated cytotoxicity, because cells that lack MHC class I antigens are targeted and destroyed by NKs (Moretta et al., 2001). In addition, MSCs can secrete a range of immunomodulators, such as nitric oxide (NO), prostaglandin (PGE2), indoleamine 2,3-dioxygenase (IDO), interleukin (IL)-6, IL-10, and HLA-G. These soluble factors are known to negatively modulate the function of various immune cells. In addition, through cell-cell contact and the production of soluble factors, MSCs induce an immunosuppressive environment by generating regulatory T cells (Tregs). The ability of MSCs to induce Tregs has been observed both *in vitro* (Di Ianni et al., 2008 and Ye et al., 2008) and *in vivo* in various models (Zappia et al., 2005; Nemeth et al., 2010; Madec et al., 2010).

**Tumor homing of MSCs**

One of the most important and unique properties of MSCs is their ability to migrate to site of wounds, chronic inflammation and tissue damage as well as to the tumor microenvironment (Spaeth et al., 2008). The first evidence of MSCs’ tumor tropism was reported in 1999 by Maestroni at al., showing also that bone marrow derived MSCs release some soluble factors that inhibit lung carcinoma and melanoma growth in mice. In the past decades the homing potential of MSCs was discovered in almost all tested cancer cell lines: colon cancer (Menon et al., 2007), breast cancer (Kidd et al., 2009),

melanoma (Studeny et al., 2002), pancreatic cancer (Kidd et al., 2010), ovaric cancer (Kidd et al., 2009), lung cancer (Loebinger et al., 2009), Kaposis's sarcoma (Khakoo et al., 2006) and malignant glioma (Sasportas et al., 2009). The mechanism by which MSCs migrate across endothelium and home to the tumor site is not yet fully understood, however it seems to be dependent upon biological properties of the tumor micro-environment (Roisin et al., 2010). Since a tumor can be considered a "wound", its microenvironment resembles a site of chronic inflammation with high concentrations of inflammatory chemokines and growth factors. These factors may be responsible for integration of MSCs into the tumor stroma. Extensive studies have shown that MSCs can be attracted by different cytokine/receptors pairs including SDF-1/CXCR4, SCF/c-Kit, HGF/c-Met, VEGF/VEGFR, PDGF/PDGFR, MCP-1/CCR2, and HMGB1/RAGE (reviewed by Momin et al., 2010). MSCs express a variety of chemokine receptors: CCR1, CCR2, CCR4, CCR6, CCR7, CCR8, CCR9, CCR10, XCR, CXCR1, CXCR2, CXCR3, CXCR4, CXCR5, CXCR6 and CX3CR (Ringe et al., 2007). The production of their respective ligands is a shared characteristic of tumor tissue and thus these receptors may likely play a role in MSCs migration and tumor homing. Other influential signalling pathways have been elucidated and include PI3K signalling (Kendall et al., 2008), urokinase-type plasminogen activator (uPA)-uPA receptor (uPAR) (Vallabhaneni et al., 2011) and matrix metallo-proteinase 1 (MMP1)-proteinase-activated receptor 1 (PAR1) (Gutova et al., 2008). Two recent studies show that human MSCs migrate *in vitro* and *in vivo* toward hepatocellular carcinoma. In one case the chemotaxis is reoriented due to the chemokine CCL15, secreted by the tumor cells, that binds the CCR1 receptor on MSCs (Gao et al., 2016). While in the second one, the monocyte chemoattractant protein-1(MCP-1) expressed by lung cancer cells, interacts with the CCR2 receptor expressed on the surface of human MSCs (Yan et al., 2016).

Additional receptors involved in MSCs migration are Toll-like Receptors (TLR). In particular TLRs1-6 have been identified in primary human MSCs and have been reported that TLR stimulation enhanced the migratory ability of MSCs (Tomchuck et al., 2008).

The migration towards a tumor site *in vivo* is influenced not only by the tumor microenvironment but also by the nature of MSCs such as: heterogeneity of the population, culture conditions of in vitro MSC expansion and the expression of migratory factors. Besides targeting the primary tumor mass, MSCs have been shown to track tumor metastasis sites (Sasportas et al., 2009). Two recent studies, in fact, reported that MSC administration results in strong recruitment within colon cancer lung metastasis (Knoop et al., 2015) and breast cancer lung metastasis (Liu et al., 2015).

Furthermore many tumor microenvironments exhibit hypoxia that results in expression of proangiogenic molecules. The hypoxia-induced transcription factor HIF-1α activates the

transcription of genes, including VEGF, macrophage migration inhibitor factor, tumor necrosis factors, and numerous pro-inflammatory cytokines (Winner et al., 2007), inducing the production of chemokines, such as MCP-1, involved in migration of MSCs toward tumors (Dwyer et al., 2007). These cells are relatively resistant to hypoxic conditions due to anaerobic adenosine triphosphate production (Mylotte et al., 2008) which should give these cells a competitive advantage in the tumor microenvironment.

### 1.4.2 MSCs and clinical applications

Therapeutic use of MSCs is a promising strategy to treat a large number of different diseases. Their feasibility of isolation from different adult tissues and expansion in culture, the capacity to avoid immune rejection and their homing ability are some of the properties that make MSCs a great resource for cell based therapy. One of the first clinical applications of MSCs was in the tissue regeneration field, where they can be used as an alternative to donated organs by offering a renewable cell source for replacement of degenerated tissue. In 1995 Lazarus et al., reported for the first time that MSCs can be safely applied in an oncological indication, too: 15 patients with hematological malignancies were infused with autologous cultured MSCs, resulting in complete remissions (Lazarus et al., 1995). Few years later MSCs were successfully used by Horwitz et al. 1999, to treat children affected by osteogenesis imperfecta. The allogeneic hematopoietic stem cells transplantation and the transplanted bone marrow cells engrafted and generated functional osteoblasts leading to improvement in bone structure and function (Horwitz et al. 1999).

In cardiovascular diseases MSCs have been used to treat acute and chronic myocardial infarction patients, with significant improvements in heart functions (Chen et al., 2006 and Zeinaloo et al., 2011). In addition to autologous MSCs, the efficacy of allogeneic MSCs has also been reported. Allogeneic MSCs were well tolerated with a significant increase in left ventricular ejection fraction and lower incidences of arrhythmia and chest pain (Ichim et al., 2008).

Based on their ability to modulate immune responses, MSCs have also been proposed as a treatment for autoimmune diseases. Thus, the therapeutic role of MSCs was investigated in patients with Crohn's disease, a chronic inflammatory disorder in which the immune system attacks the gastrointestinal tract. The patients were given intralesional treatments of MSCs mixed with fibrin glue, showing signs of significant repair 8 weeks after treatment (Garcia-Olmo et al., 2009). The effect of MSCs has also been documented in systemic lupus erythematosus (SLE), an autoimmune inflammatory disease with multiorgan involvement including the kidney, brain, lung and hematopoietic systems

(Wang et al., 2013). A study published by Sun and colleagues suggested that MSCs derived from SLE patients show functional abnormalities (Sun et al., 2007) and, thus, allogeneic MSC transplantation may be more effective, as compared to autologous MSCs. Clinical support for this reasoning was obtained in a pilot study showing that allogeneic MSC transplantation improved serological markers and stabilized renal functions in refractory SLE patients (Liang et al., 2010). In addition, clinical studies using MSCs revealed the prevention of graft-versus-host disease, which is one of the complications and risks during autologous or allogeneic hematopoietic stem cell transplantation (Figure 4) (Lin et al., 2011).

Furthermore, MSCs have been used to treat liver diseases due to their regenerative potential and immunomodulatory properties. In a phase I to II clinical trial, eight patients with end-stage liver diseases received autologous MSCs that were well tolerated and improved liver functions, demonstrating that MSC therapy is safe, feasible, and applicable in end-stage liver disease (Kharaziha et al., 2009).

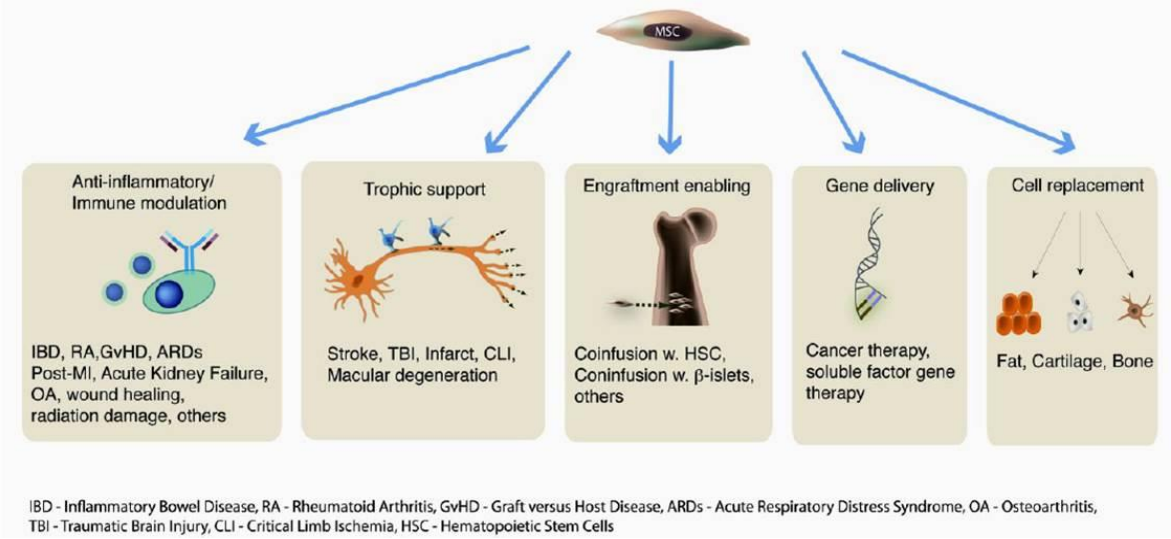


**Figure 4 Multiple modes of action attributed to MSCs**
The potential utility of MSCs resides in their multifunctional properties. They modulate the immune system, enhance engraftment of hematopoietic stem cells, promote tissue healing and contribute to structures such as bone, cartilage, and fat. As culture-expanded cells, they may provide critical trophic support for normal tissue maintenance and protection and recovery from tissue injury. In addition, MSCs can be exploit as cell-based gene delivery system for the expression of antitumoral agents. Taken from (Viswanathan et al., 2014).

### 1.4.3 MSCs as drug delivery system

The lack of selectivity, often resulting in considerable loss of healthy tissue, is one of the main limitations of conventional tumor therapies. Most researchers agree that cell based therapy as targeted delivery system has a promising future, especially for cancer treatments, in order to proactively focus on tumor tissue and to efficiently attack malignant

cells. An encouraging method is based on the use of MSCs as cellular carrier vehicle for the expression of antitumoral peptide/protein based reagents. These cells, in fact, will not only provide a delivery system that is immune privileged (Ye et al., 2008) but they are expected to home to the cancer site, due to their tumor tropism (Studeny et al., 2002), and here serve as a delivery platform to stably express therapeutic proteins, increasing their concentration at the target site. Consequently, a constant *in situ* production can circumvent the short half-lives that all low molecular weight peptide and most non-antibody based protein reagents exhibit. Moreover, the presumed local expression of the therapeutic in the tumor microenvironment would avoid broad systemic action causing potential off target actions, so-called unwanted side effects. Support for the feasibility of the MSC drug carrier concept was obtained in several preclinical studies. An early application of MSCs was the transduction with the Interferon β (IFN-β) gene which shows a wide range of biological activities like anti-proliferative (Johns et al., 1992) and pro-apoptotic (Chawla-Sarkar et al., 2001) effects. However, its *in vivo* therapeutic efficacy has been limited due to toxicity associated with systemic administration. Studeny et al. reported (Studeny et al., 2002) that i.v. administration of MSCs, engineered to express IFN- β (IFN-β-MSCs), significantly prolonged the survival of animals with established metastases of either breast carcinoma or melanoma tumor in the lung. Toxic effects associated with IFN-β were reduced by the delivery of MSCs expressing IFN-β to tumors. In addition Nakamizo et al. (Nakamizo et al., 2005) have observed that IFN-β-MSCs show tropism for human gliomas after either intravascular or local delivery with a significant extension of the survival of animals with established intracranial gliomas.

Others candidates as therapeutic agents secreted by MSCs are the interleukins (ILs), regulators of inflammatory and immune responses. ILs can be used to improve the anti-cancer immune surveillance by activating cytotoxic lymphocytes, natural killer cells, and producing IFN-γ (Studeny et al., 2002). MSCs genetically modified with IL-12, when mixed with melanoma cells, significantly delayed tumor growth in a dose-dependent manner (Shrayer et al., 2002). Likewise, when IL2-expressing MSCs are injected in the vicinity of pre-established melanoma in mice tumor growth was inhibited (Stagg et al., 2004). Furthermore, Chen et al. (Chen et al., 2012) showed that the administration of MSCs transduced with IL-12 suppress metastasis and increase tumor cell apoptosis in mice bearing melanoma, lung cancer and hepatoma.

In addition, the activation of systemically delivered, inactive prodrugs that are converted into biologically active cytotoxic agents by genetically modified MSCs homing to the tumor is an alternative concept. The first example of this strategy was the application of cytosine deaminase (CD), which can convert the nontoxic prodrug 5-fluorocytosine to the antitumoral agent 5-fluorouracil, that can diffuse out of the producer MSCs into

surrounding cells and is selectively toxic only to rapidly proliferating cells (Chang et al., 2010). Another prodrug system that was evaluated is the Herpes simplex virus-Thymidine kinase (HSV-TK) in combination with ganciclovir (GCV). This latter is a nontoxic purine analogue and is phosphorylated by the enzyme HSV-TK and further by endogenous kinases. The final phosphorylated form, GCV-triphosphate, inhibits DNA synthesis and induces cell death via apoptosis (Moolten et al., 1990). In particular, Song et al. have shown that MSCs transduced with HSV-TK significantly inhibit the growth of subcutaneous prostate cancer xenografts as well as metastatic tumor in the presence of prodrug GCV (Chao et al., 2011).

Furthermore MSCs can be engineered to express pro-apoptotic proteins like TRAIL which has the ability to induce apoptosis selectively in cancer cells and leaving normal cells intact (Walczak et al., 2000). The therapeutic efficacy of TRAIL expressed by transduced MSCs for tumor treatment has been shown in different cell lines or mouse models such as colorectal carcinoma (Mueller et al., 2011), gliomas (Ehtesham et al., 2002), lung, breast, and cervical cancer (Loebinger et al., 2009) (Figure 5).

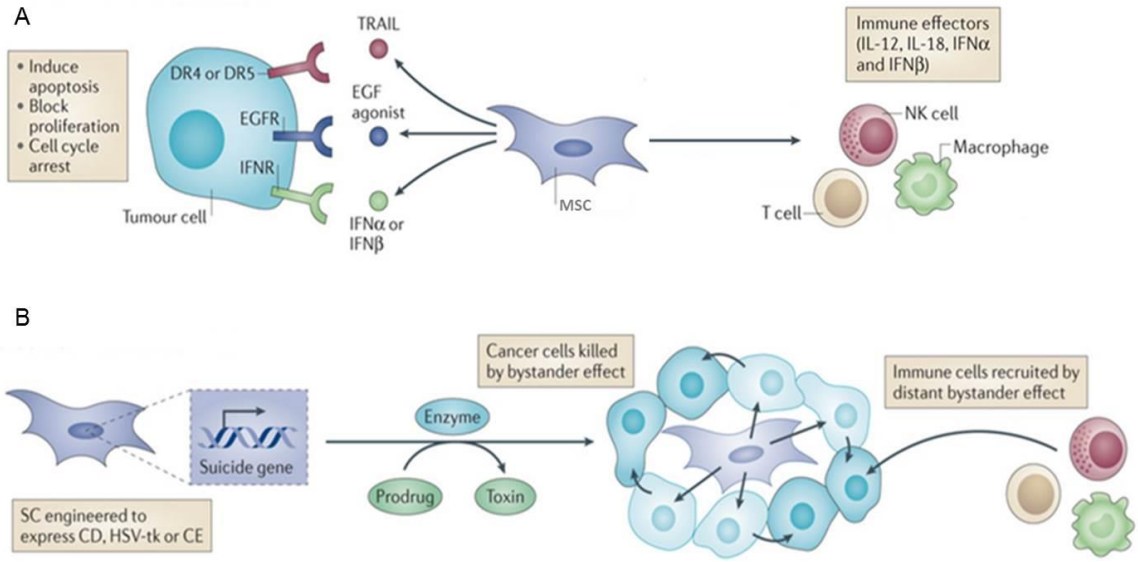


**Figure 5 Using stem cells to promote tumor cell death**
SCs can be modified in various ways to generate antitumour capabilities. (A) SCs can be engineered to secrete therapeutic proteins that function directly on tumor cells or indirectly on cells of the tumor microenvironment. For example, tumor necrosis factor-related apoptosis-inducing ligand (TRAIL), epidermal growth factor (EGF) agonists or interferons (IFNα or IFNβ) can be secreted to function on death receptor 4 (DR4) and DR5, EGF receptor (EGFR) or IFN receptors (IFNRs), respectively. (B) SCs can be engineered to express a suicide gene encoding an enzyme (such as cytosine deaminase (CD), carboxylesterase (CE) or herpes simplex virus thymidine kinase (HSV-tk)) that converts a prodrug into a toxin. This induces suicide of the SCs, and cancer cells are killed by the bystander effect, a phenomenon that describes the movement of toxin from the SCs to adjacent cancer cells via a paracrine mechanism or gap junctions. The distant bystander effect describes the recruitment of host immune cells in response to death or inflammatory signals released from dying cells. Adapted from (Stuckey and Shah, 2014).

A combined approach was also investigated in stem cells based gene therapy, in order to synergize with the delivered agent or to sensitize resistant populations. For example,

delivery of TRAIL mediated by stem cells was combined with various agents such as PI3K-mTOR inhibitor, histone deacetylases (HDACs) inhibitors, short hairpin RNA (shRNA), micro RNA inhibitors as well as bortezomib and cisplatin, resulting in enhanced pro-apoptotic TRAIL mediated activity (reviewed by Stuckey et al., 2013).

### 1.4.4 MSCs: pro-tumorigenic or anti-tumorigenic?

The tumor microenvironment is a complex structure composed of malignant tumor cells, also known as parenchyma, and a stroma compartment. The tumor stroma contains different kind of cells including cancer-associated fibroblasts (CAFs) (Levin 1912), endothelial cells (Greenblatt et al., 1968 and Duda et al., 2006), immune cells (Woods et al., 1997 and Lyden et al., 2001), adipocytes (Andarawewa et al., 2005) and various types of extracellular matrix (ECM) proteins (Levin 1913). These stroma elements play a crucial role in tumor survival, structural support and vascularization. Due to their tumor homing ability, MSCs move to tumor site and incorporate into the tumor stroma compartment, interacting with each other and with cancer cells (Kidd et al., 2009). The exact role of MSCs in the tumor stroma and consequently their effects on tumor progression or tumor inhibition is still controversial. There are conflicting findings in studies concerning the use of MSCs for cell based therapy. In fact, several publications have reported pro-tumorigenic effects of MSCs through different processes such as: promotion of angiogenesis and metastasis formation, suppression of the organism's immune response against tumor cells, induction of epithelial-mesenchymal transition (EMT) and transition to tumor associated fibroblasts (reviewed by Klopp et al., 2011). In contrast to these potentially tumor promoting properties of MSCs, several other studies have demonstrated that these cells can reduce or prevent tumor growth. These anti-tumoral effects are mediated by different ways including inhibition of signalling pathways involved in cell proliferation process like AKT, PI3K and Wnt, downregulation of XIAP (X-linked inhibitor of apoptosis protein) and suppression of angiogenesis (Khakoo et al., 2006; Qiao et al., 2008; Otsu et al., 2009).

The reasons for these reported discrepancies are still unknown, but the dual role of MSCs in support or suppression of tumorigenesis may depend on many factors. The timing of MSCs administration seems to be critical to determinate the final effect on tumor growth. In many studies, antitumoral effects were observed when MSCs were injected into established tumors and when direct contact of MSCs and tumor was avoided using gelatin matrix or intravenous administration of MSCs during tumor initiation (Ohlsson et al., 2003). By contrast, in several publications tumor growth was promoted when MSCs and tumor cells were injected simultaneously (Djouad et al., 2003 and Karnoub et al., 2007). The

heterogeneity of MSCs, furthermore, is probably a critical point as reported by the group of Waterman. In these studies MSCs, which express several TLRs (Toll-like receptors), were separated into two homogenous phenotypes, called MSC1 and MSC2, according to the different downstream TLRs stimulation. The researchers reported that MSC1 exhibited a pro-inflammatory nature, whereas MSC2 an immunosuppressive one (Waterman et al., 2010) and in a cancer model MSC1 treatment reduced primary tumor growth and metastasis, while administration of MSC2 resulted in increase of tumorigenesis and metastasis formation (Waterman et al., 2012). Additionally, the dose of MSC administration and the conditions of their expansion *ex vivo* are variable factors and may contribute to the conflicting results.

Although the impact of MSCs on tumor progression is still unclear, putative tumor-promoting effects of MSCs can be overcome by manipulating their gene expression pattern. For example, MSCs could be engineered to express a suicide gene. With this system, after migration into the tumor and the local expression of antitumor protein, MSCs can be targeted by an agent, like gancyclovir, which induces a selective elimination of the exogenously delivered MSCs.

### 1.4.5 Stem cell delivery of TRAIL

Over the past decades many recombinant versions of TRAIL have been generated to increase its antitumoral activity (Stuckey and Shah 2013), because of very limited clinical efficacy (Herbst et al., 2010 and Soria et al., 2010). This recombinant soluble form of TRAIL shows *in vivo* a short half-life of around 30 minutes (Kelley et al., 2001). This is for most due to dissociation of the homotrimer and rapid kidney clearance (Duiker et al., 2012). Although a lot of different approaches have been investigated to improve the stability and pharmacokinetics of a recombinant protein, like addition of leucine and isoleucine zipper (LZ-TRAIL Walczak et al., 1999 or iz-TRAIL Ganten et al., 2006) or the addition of human serum albumin (Muller et al., 2010), the serum half-life and the specific delivery site still remain a major hurdle of this therapeutic strategy. These problems can be overcome using cell base gene therapy to express and delivery recombinant proteins directly to their site of action, with an increase of their concentration at the target side and a simultaneous reduction of potential side effects. Many types of adult stem cells have been engineered to secrete soluble form of TRAIL and have been transplanted into mice to treat different kinds of tumors as described in Table 1.

| Stem cell type | Form of TRAIL | Tumor type | Combination therapy | Principle findings |
|---|---|---|---|---|
| Human UCB-MSCs | Adenoviral infection of secretable trimeric TRAIL | U87-MG | Irradiation of tumor | Irradiation enhances tumor tropism and therapeutic potential of SCs |
| Human BM-MSCs | Lentiviral infection of secretable TRAIL | Primary + Established human GBM | | Use of real-time imaging to follow migration and therapeutic effect of MSCs on tumor volume *in vivo* |
| Human A-MSCs | Non-viral nucleofection of TRAIL | Rat glioma model | | Reduction of tumor volume and significant survival benefit *in vivo* |
| Rat BM-MSCs | Adenoviral transduction of dodecomeric TRAIL | Renal cell carcinoma (RCC) | Co-expression of herpes simplex virus thymidine kinase | Complete elimination of established RCC *in vivo* |
| Human MSC/Mouse MSC | Secretable TRAIL | Established GBMs | Stem cells express herpes simplex virus thymidine kinase | Stem cells are eliminated after therapeutic effect by addition of the prodrug gancyclovir |
| MSCs | Secretable TRAIL introduced using non-viral PEI(600)-Cyd | Lung metastasis | | Lung tumor homing and reduction in metastasis |
| Mouse NSCs | Lentiviral infection of secretable TRAIL | GBM6/8/12 *in vitro*, Gli36-EGFRVIII *in vivo* | PI-103 (PI3-kinase/mTOR inhibitor | PI-103 augments *in vivo* response of gliomas to TRAIL |
| Mouse NPCs | Lentiviral infection of secretable TRAIL | Human U87 established glioma model | Locked nucleic acid (LNA) anti-miR-21 oligonucleotides | Synergism with TRAIL resulting in eradication of tumor *in vivo* |
| Human MSCs | LV-TRAIL under tet promoter | Pulmonary metastasis model | Conditional expression of TRAIL using Dox | Cleared metastatic disease in lung metastasis model |
| Human A-MSCs | Secretable TRAIL | Malignant fibrous histiocytoma | | Decrease in metastasis |
| Mouse NSC/Human MSC | Secretable TRAIL | Established + Primary GBMs | Stem cells encapsulated in sECM | Increased retention of stem cells within resection cavity |
| Human MSC | Inducible TRAIL | Breast + bone metastasis model | Stem cells encapsulated in silk scaffold | Halts breast cancer growth and decreases degree of bone and lung metastasis |
| Mouse NSC | LV-EGFR-Nanobody TRAIL (ENb2-TRAIL) | Established GBMs | | Target EGFR and TRAIL signaling pathways simultaneously |

**Table 1 Stem cell delivery of TRAIL for cancer therapy**
Abbreviations: UCB-MSCs, Umbilical cord blood-derived mesenchymal stem cells; BM-MSCs, Bone marrow-derived mesenchymal stem cells; A-MSCs, Adipose-derived mesenchymal stem cells; NSCs, Neural stem cells; NPCs, Neural progenitor cells; sECM, synthetic extracellular matrix; EGFR, Epidermal growth factor receptor. Taken from (Stuckey et al., 2013).

As show in the Table 1, a variety of viral vectors have been exploited to introduce TRAIL into mesenchymal stem cells for their use in cell based therapies in animal tumor models. But the safety of these viral systems is still problematic and under controversial debate. In particular there are two major concerns. The first one is the immune response reaction, due to the fact that some viral vectors are immunogenic and show instability of transgene expression, that can cause severe reactions in the patient. The second concern is about the site of integration of the DNA into the genome of the cells, which should not destroy genes essential for the physiologic behavior of the MSCs, otherwise they might themselves generate cancer. Although non-viral methods have lower efficiency compared to viral-based methods, they are safe, non-infectious, and non-immunogenic, have negligible toxicity, can be produced simply on a large scale and have the capacity to carry larger therapeutic genes (Schaffert et al., 2008). Nevertheless, only a small number of studies have used non-viral methods to transfect stem cells with TRAIL (Choi et al., 2011 and Hu et al., 2012). This emphasizes the importance to explore the possibility to use MSCs as delivery vehicle based on non-viral transfection for tumor treatments.

## 1.5 Goals

Despite extensive research aimed to develop new therapeutic strategies against cancer, it still remains one of the first causes of death. Recent evidence reported the existence of a sub-population of quiescent cells within the tumor mass named cancer stem cells. These cells are typically in a quiescent status which makes them resistant to standard anti-cancer therapies such as chemotherapy and radiotherapy. In addition, due to their self-renewal and differentiation abilities, CSCs are considered responsible for tumor initiation and relapse even after apparent complete response to systemic therapy. In this context, targeting the CSC population will be critical to advance the efficacy of cancer treatment. Based on this new finding, in the first part of my thesis, I exploited the strategy of targeting delivery to CSCs of anticancer proteins generating and testing TRAIL fusion proteins directed against two of the most promising CSC markers, CD133 and LGR5.

In the second part, I investigated the feasibility and the safety of a novel cell based therapeutic approach for cancer treatment. This method exploits unique features exert by mesenchymal stem cells, such as tumor homing ability and immunosuppressive properties. Due to these capabilities, several studies tested the mesenchymal stem cell as a delivery system for local expression of therapeutic reagents. Additionally, with this approach the major limitations observed during standard protein therapy, including short half-life and fast renal clearance, can be overcome. Based on these concepts, the second part of my thesis addressed the potential use of MSCs as carrier system for a stable and long *in situ* production of the therapeutic TRAIL protein. In particular the specific aim was to exploit non-viral transfection methods for generation of a stable producer MSC line and investigate their functional activity in various *in vitro* as well as in an *in vivo* tumor model.

# 2 Materials and Methods

## 2.1 Materials

### 2.1.1 Equipment

Table 2: List of instruments used in this thesis

| Equipment | Company |
|---|---|
| Balances: 440-39N, 440-333N and ALJ 120-4 | Kern, Germany |
| Beckman Coulter Avanti J-30I Centrifuge (Rotor J20) (for amounts up to 250 ml) | Beckman Coulter, Krefeld |
| Beckman J2-MC Centrifuge (Rotor JA14) (for amounts up to 250 ml) | Beckman Coulter, Krefeld |
| CK2 (standard light microscope) | Olympus, Hamburg |
| Concentrator (Vivaspin) | GE Healthcare, Germany |
| Cytomics FC 500 (FACS) | Beckman Coulter, Krefeld |
| Eppendorf Centrifuge 5415D (Rotor F45-24-11) (for amounts up to 1.5 ml) | Eppendorf, Hamburg |
| Eppendorf Centrifuge 5415R (Rotor F45-24-11) (for amounts up to 1.5 ml) | Eppendorf, Hamburg |
| EVOS fl inverted fluorescence microscope | AMG, Mill Creek, USA |
| Film Processor Curix 60 | Agfa, Düsseldorf |
| HBT-1-131 (Heat block) | BioTech, Bovenden |
| Incubator for bacteria BD53 | Binder, Stuttgart |
| Incubator for cell culture ($CO_2$ Inkubator 2424-2) | Zapf, Sarstedt |
| Jouan CR422 Centrifuge (low speed for cell culture) | Jouan Quality system |
| Mini-PROTEAN 3 Electrophoresis Cell System | BioRad, Munich |
| MKR 13 (orbital microplate shaker) | HLC BioTech, Bovenden |
| NanoDrop® ND-1000 (Spectrophotometer) | peQLab, Erlangen |
| Neubauer counting chamber 0.0025 $mm^2$ | Marienfeld, Lauda-Königshofen |
| Nuaire IR Autoflow, CO2 Water-Jacketed Incubator | Zapf Instruments |
| pH meter FiveEasy | Mettler Toledo, Giessen |
| Pipettes (1 – 10 µl / 2 - 20 µl / 20 - 200 µl / 100 - 1000 µl) | Gilson / Eppendorf |
| Robo Cycler Gradient 96 (PCR cycler) | Stratagene |
| Sterile bench W90 | Waldner-Laboreinrichtungen, Germany |
| Tecan Infinite M200 (ELISA plate Reader) | Tecan, Grödig, Austria |
| TransBlot SD, Semidry transfer cell | BioRad, Munich |
| Transilluminator Bio View UV light | Biostep, Jahnsdorf |
| Vortex | Sky Line Elmi Ltd., Latvia |
| Water Purification Milli-Q Reference | Millipore, Schwalbach |
| Waterbath | MA6, Lauda, Lauda-Königshofen |
| HPLC-System Waters Alliance 2695 | Waters Cooperation, Milford, USA |

## 2.1.2 Consumables

Table 3: List of consumables used in this thesis

| Consumable | Company |
|---|---|
| 0.2 µm filter for sterile filtration | Sarstedt, Nümbrecht |
| 6-well glass bottom cell culture dishes | MatTek Corporation |
| 96-well E-plates | Roche Diagnostics, Mannheim |
| blotting paper, 3 mm Whatman | Schleicher Schuell, Dassel |
| cell culture dishes | Greiner, Frickenhausen |
| cell culture flasks | Greiner, Frickenhausen |
| cell culture plates | Greiner, Frickenhausen |
| Cryo vials 1ml | Greiner, Frickenhausen |
| D-Tube™ Dialyzer Mini (MW cut-off 6 - 8 kDa) | Calbiochem, Merck, Darmstadt |
| falcon tubes (15 ml and 50 ml) | Greiner, Frickenhausen |
| HPLC columns: BioSep-SEC-S2000, -S3000 or Yarra SEC-3000 | Phenomenex, Aschaffenburg |
| Nitrocellulose Transfer Membrane | Pall Life Sciences, East Hills, USA |
| pipette tips (1 - 20 µl; 20 - 200 µl; 200 - 1000 µl) | Greiner, Frickenhausen |
| pipettes (5 ml, 10 ml and 25 ml) | Greiner, Frickenhausen |
| Poly-Prep® columns | Bio-Rad, Munich |
| Protino® Ni-NTA agarose beads | Machery-Nagel, Düren |
| PVDF blotting membrane | Carl Roth GmbH & Co, Karlsruhe |
| reaction tubes 1.5 ml (standard and safe-lock) | Eppendorf, Hamburg |
| replica dishes | Sterilin Limited, Newport, UK |
| Transwells (24-well plate plus inserts) for cell migration assays, (0.8 µm pore size) | Costar/Vitaris AG, Baar, Germany |
| X-ray films | CEA, Strangnas, Sweden |

## 2.1.3 Chemical and solvent

Table 4: List of chemicals and solvents and used in this thesis

| Chemical and solvent | Company |
|---|---|
| 3, 3', 5, 5'-Tetramethylbenzidine (TMB) | BD Bioscience, Heidelberg |
| Agarose | Carl Roth GmbH & Co, Karlsruhe |
| Alexa Fluor 568® -labeled phalloidin | Molecular Probes /Invitrogen, Carlsbad, USA |
| Ammonium persulfate (APS) | Carl Roth GmbH & Co, Karlsruhe |
| Ampicillin | Roth, Karlsruhe |
| Anti-Flag M2 Affinity Gel | Sigma-Aldrich, München |
| Ascorbic acid-2-phosphate | Sigma-Aldrich, München |
| Bromphenol blue | Serva, Heidelberg |
| Calcium chloride ($CaCl_2$) | Merck, Darmstadt |
| Coomassie Brilliant Blue | SERVA Electrophoresis, Heidelberg |
| Crystal violet | Merck, Darmstadt |
| Dexamethasone | Lonza, Köln |
| Dimethylsulfoxide (DMSO) | Carl Roth GmbH & Co, Karlsruhe |
| Disodium hydrogen phosphate ($Na_2HPO_4$) | Carl Roth GmbH & Co, Karlsruhe |

| Chemical and solvent | Company |
|---|---|
| Dithiothreitol (DTT) | Carl Roth GmbH & Co, Karlsruhe |
| EGF | R&D System |
| Ethanol (EtOH) | Carl Roth GmbH & Co, Karlsruhe |
| Ethidium bromide (EtBr) | Roche Diagnostics, Mannheim |
| Fluoromount-G | Southern Biotech, Birmingham, USA |
| GeneRuler 1 kb (DNA ladder) | Thermo Fisher Scientific, Waltham, USA |
| Glycerol | Carl Roth GmbH & Co, Karlsruhe |
| Glycine | Carl Roth GmbH & Co, Karlsruhe |
| $H_2SO_4$ | Carl Roth GmbH & Co, Karlsruhe |
| Human insulin | Sigma-Aldrich, Deisenhofen |
| Hydrochloric acid (HCl) | Carl Roth GmbH & Co, Karlsruhe |
| IBMX (3-Isobutyl-1-methylxanthine) | Sigma-Aldrich, Deisenhofen |
| Imidazole | Carl Roth GmbH & Co, Karlsruhe |
| Indomethacin | Sigma-Aldrich, Deisenhofen |
| Isopropanol | Carl Roth GmbH & Co, Karlsruhe |
| $KH_2PO_4$ | Carl Roth GmbH & Co., Karlsruhe |
| Methanol (MeOH) | Carl Roth GmbH & Co, Karlsruhe |
| N,N,N,N-Tetramethylethyldiamine (TEMED) | Carl Roth GmbH & Co, Karlsruhe |
| $Na_2HPO_4$ | Carl Roth GmbH & Co., Karlsruhe |
| PageRuler prestained protein ladder | Thermo Scientific, Rockford, USA |
| Paraformaldehyde (PFA) | Carl Roth GmbH & Co, Karlsruhe |
| Peptone | Carl Roth GmbH & Co., Karlsruhe |
| Phenylmethylsulphonyl fluoride (PMSF) | Sigma-Aldrich, München |
| Potassium acetate | Sigma-Aldrich, München |
| Potassium chloride (KCl) | Carl Roth GmbH & Co, Karlsruhe |
| Propidium iodide (PI) | Invitrogen, Karlsruhe |
| Protein G Sepharose beads | KPL, Gaithersburg, USA |
| Sodium azide | Sigma-Aldrich, Taufkirchen |
| Sodium chloride (NaCl) | Carl Roth GmbH & Co, Karlsruhe |
| Sodium dodecyl sulfate (SDS) | Carl Roth GmbH & Co, Karlsruhe |
| Sodium hydroxide (NaOH) | Carl Roth GmbH & Co., Karlsruhe |
| Tris-hydroxymethyl-aminomethane (Tris) | Carl Roth GmbH & Co, Karlsruhe |
| Triton X-100 | Carl Roth GmbH & Co, Karlsruhe |
| Tween 20 | Carl Roth GmbH & Co, Karlsruhe |
| β-Glycerophosphate | Sigma-Aldrich, München |
| β-Mercaptoethanol | Carl Roth GmbH & Co, Karlsruhe |

### 2.1.4 Buffers and solutions

Table 5: List of buffers and solutions used in this thesis

| Buffer and Solution | Composition |
|---|---|
| 1% Alizarin red solution | 100 mg alizarin red solved in 10 ml $H_2O$, pH adjusted to pH 6.4 |
| 10% APS solution | 10% (w/v) APS in $H_2O$ |

| Buffer and Solution | Composition |
|---|---|
| AP buffer | 100 mM Tris pH 9.5, 100 mM NaCl, 5 mM $MgCl_2$ |
| Blocking solution (microscopy) | 5% (v/v) bovine serum, 0.1% (v/v) Tween 20 in PBS |
| Blocking solution (Western blot) | 5% (w/v) milk powder, 0.1 % (v/v) Tween 20 in PBS |
| Blotting buffer | 200 mM glycine, 25 mM Tris base, 20% (v/v),methanol |
| Cell freezing solution | 10% (v/v) DMSO in FCS |
| Competent cell solution A | 0.1 M $CaCl_2$ in 1x PBS |
| Competent cell solution B | 20% (v/v) glycerol, 50 mM $CaCl_2$ in 1x PBS |
| Coomassie blue solution | 0.008% (w/w) Coomassie Brilliant Blue G-250, 35 mM HCl in $H_2O$ |
| Crystal violet staining solution | 20% (v/v) methanol, 0.5% (m/v) crystal violet in $H_2O$ |
| DNA loading buffer (5x) | 25% (v/v) glycerol, 0.02% (w/v) bromphenol blue in 5x TAE buffer |
| ELISA – blocking solution | 2% (m/v) dry milk powder in 1x PBS |
| ELISA – developing solution | 0.1 mg/ml TMP, 100 mM sodium acetate buffer pH 6.0, 0.006% (v/v) $H_2O_2$ |
| ELISA – stopping solution | 1 M $H_2SO_4$ |
| ELISA – washing solution | 0.05% (v/v) Tween20 in 1x PBS |
| Hemalaun solution | 1 g hämatoxylin, 0.2 g $NaIO_3$, 50 g aluminium potassium sulphate, 50 g chloral hydrate, 1 g citric acid, $H_2O$ added to 1 |
| IMAC elution buffer | 250 mM imidazole in 1x sodium phosphate buffer |
| IMAC wash buffer | 35 mM imidazole in 1x sodium phosphate buffer |
| Laemmli SDS sample buffer (5x) | 400 mM Tris, pH 6.8, 500 mM dithiothreitol, 50% (v/v) glycerol, 10% (w/v) SDS, 0.2% (w/v), bromophenol blue |
| Oil red-o solution | 6 parts of 0.5% oil red O solution solved in isopropanol with 4 parts $dH_2O$ |
| PBA | 2% (v/v) FBS, 0.02% (w/v) $NaN_3$ in 1x PBS |
| PBS-Tween | 0.05% (v/v) Tween20 in PBS |
| Periplasmic preparation buffer (PPB) | 30 mM Tris-HCl pH 8.0, 1 mM EDTA, 20% (w/v) sucrose in $H_2O$ |
| PFA | 4% (w/v) in PBS |
| Phosphate Buffered Saline (PBS) | 140 mM NaCl, 2.7 mM KCl, 8 mM $Na_2HPO_4$, 1.5 mM $KH_2PO_4$ |
| SDS-PAGE running buffer | 25 mM Tris pH 8.8, 192 mM glycine, 0.1% SDS, |
| Separating gel solution | 10%, 12,5% or 15% (v/v) acrylamide, 375 mM Tris, pH 8.8, 0.1% (v/v) SDS, 0.1% APS, 0.1% TEMED in $H_2O$ |
| Stacking gel solution | 5% (v/v) acrylamide, 130 mM Tris, pH 6.8, 0.1% (v/v) SDS, 0.1% APS, 0.1% TEMED in $H_2O$ |
| TAE (Tris-Acetat-EDTA) | 40 mM Tris-acetate, 1 mM EDTA, |
| TE buffer (10x) | M Tris-HCl, 10 mM EDTA, pH 7.5 |
| Tris-Acetat-EDTA (TAE), pH 8,0 | 40 mM Tris-acetate, 1 mM EDTA, pH 8.3 |
| Washing solution (Western blot) | 0.05% (v/v) Tween 20 in 1x PBS |

### 2.1.5 Kits

Table 6: List of kits used in this thesis

| Kit | Company |
|---|---|
| BD OptEIA™ human TRAIL ELISA Set | BD Biosciences, Heidelberg |
| MaxDiscovery™ ALT Enzymatic Assay kit | BIOO Scientific, Austin, USA |
| NucleoBond® Xtra Midi | Macherey-Nagel, Düren |
| NucleoSpin® Plasmid | Macherey-Nagel, Düren |
| NucleoSpin®Gel and PCR Clean-up | Macherey-Nagel, Düren |

### 2.1.6 Enzymes

Table 7: List of enzymes used in this thesis

| Enzyme | Company |
|---|---|
| DreamTaq™ Green PCR Master Mix | Fermentas, St. Leon-Rot |
| FastAP™ Thermosensitive Alkaline Phosphatase | Fermentas, St. Leon-Rot |
| Lysozyme | Roche Diagnostics, Mannheim |
| Restriction enzymes: *Bsh*TI (*Age*I), *Not*I, *Sfi*I | Fermentas, St. Leon-Rot |
| T4 DNA ligase | Fermentas, St. Leon-Rot |

### 2.1.7 Cell lines, media and reagents

Table 8: List of cell lines and media used in this thesis

| Cell line | Medium | Origin |
|---|---|---|
| Caco2 | RPMI 1640 + 10% (v/v) FCS | Human colon adenocarcinoma |
| Colo 205 | RPMI 1640 + 10% (v/v) FCS | Human colon adenocarcinoma |
| HCT116 | RPMI 1640 + 10% (v/v) FCS | Human colon carcinoma |
| HEK293T | RPMI 1640 + 5% (v/v) FCS | Human embryonic kidney |
| LoVo | RPMI 1640 + 10% (v/v) FCS | Human colon adenocarcinoma |
| M2 | α-MEM + 10% (v/v) FBS | Mouse bone marrow |

Table 9: List of cell culture reagents, media and antibiotics used in this thesis

| Product | Company |
|---|---|
| 10x Trypsin EDTA | Life Technologies, Darmstadt |
| Alpha-MEM Eagle | Genaxxon bioscience, Ulm |
| Anti TRAIL antibody | Enzo Life Sciences, Lörrach |
| Bortezomib | Velcade®, kindly provided by Dr. Thomas Mürdter (Institute of Clinical Pharmacology, Dr. Margarete Fischer-Bosch Foundation, Stuttgart) |
| FBS (fetal bovine serum) | GE Healthcare Bioscience, Austria |
| FCS (fetal calf serum) | Thermo Fisher Scientific, Waltham, USA |

| Product | Company |
|---|---|
| G418 | Enzo Life Sciences, Lörrach |
| Heparin | B-Brawn, Melsungen |
| Penicillin/streptomycin (100x) | Invitrogen, San Diego |
| Polyethyleneimine (PEI) | Polysciences Europe GmbH, Eppelheim |
| RPMI 1640 and OptiMEM | Invitrogen, San Diego |
| Zeocin™ | Invitrogen, San Diego, USA |

### 2.1.8 Antibodies

Table 10: List of antibodies used in this thesis

| Antibody | Species | Dilution | Company |
|---|---|---|---|
| Alexa Fluor-568 Phalloidin | goat mAb | 1:500 (IF) | Invitrogen, San Diego, USA |
| Anti-CD105-PE | mouse mAb | 1:100 (FC) | BioLegend, London UK |
| Anti-CD133-PE | mouse mAb | 1:50 (FC) | Miltenyi Biotec, Köln |
| Anti-CD44-PE | mouse mAb | 1:100 (FC) | BioLegend, London UK |
| Anti-CD71-PE | mouse mAb | 1:100 (FC) | BioLegend, London UK |
| Anti-CD9-PE | mouse mAb | 1:100 (FC) | BioLegend, London UK |
| Anti-cleaved caspase 3 (Asp 175) | rabbit mAb | 1:1500 (FC) | Cell Signaling, Frankfurt (Main) |
| Anti-FLAG (DYDDDDK) | mouse mAb | 1:200 (WB) | Sigma-Aldrich, St. Louis, USA |
| Anti-Isotype IgG2a-PE | rat mAb | 1:100 (FC) | BioLegend, London UK |
| Anti-LGR5-PE | mouse mAb | 1:50 (FC) | Miltenyi Biotec, Köln |
| Anti-rabbit-FITC | goat mAb | 1:100 (FC) | Sigma-Aldrich, St. Louis, USA |
| Anti-TRAIL | mouse mAb | 1:80 (WB) | R&D Systems, Wiesbaden |

### 2.1.9 Bacteria culture: strain, media and reagents

Table 11: List of bacterial strain used in this thesis

| Bacterial strain | Description |
|---|---|
| *E. coli* TG1 | Genotype: supE thi-1 Δ(lac-proAB) Δ(mcrB-hsdSM)5 (rK– mK–) [F´ traD36 proAB lacIqZΔM15] (Stratagene, La Jolla, USA) |
| *E. coli* DH5α | Genotype: F- endA1 glnV44 thi-1 recA1 relA1 gyrA96 deoR nupG 80dlacZM15 (lacZYAargF) U169, hsdR17(rK - mK +), λ– (Stratagene, La Jolla, USA) |

Table 12: List of bacteria media and reagents used in this thesis

| Medium and reagent | Composition | Company |
|---|---|---|
| Ampicillin | 100 mg/ml in $H_2O$ | Roth, Karlsruhe |
| IPTG | Isopropyl-β-D-thiogalactopyranoside, 1 M in $H_2O$ | Gebru Biochemicals, Gaiberg |

| Medium and reagent | Composition | Company |
|---|---|---|
| LB $_{Amp,Glc}$ agar plates | LB-medium, 2 % (w/v) agar, after autoclaving added ampicillin (f.c.: 100 µg/ml) and 1 % (w/v) glucose | |
| LB-medium | 1 % (w/v) peptone, 0.5 % (w/v) yeast extract, 0.5 % (w/v) NaCl in $H_2O$ | |
| TY-medium | 1.6 % (w/v) pepton, 1 % (w/v) yeast extract, 0.5 % (w/v) NaCl in $H_2O$ | |

## 2.1.10 Vectors and plasmid

Table 13: List of vectors used in this thesis

| Vector | Description and source |
|---|---|
| pAB1 | Vector for prokaryotic expression in periplasm of *E.coli* TG1 (Kontermann et al., 1997) |
| pCR3 | Eukaryotic expression vector (Invitrogen, Karlsruhe) |
| pAB1-4D5 | Murine vector for prokaryotic expression in periplasm of *E.coli* TG1 |

Table 14: List of plasmids used in this thesis

| Plasmid | Description |
|---|---|
| pCR3-$Db_{EGFR}$-scTRAIL | Kindly provided by Dr. M. Siegemund (Siegemund et al., 2012) |
| pCR3-$Db_{EGFR}$-Glyco-scTRAIL | Kindly provided by Dr. M. Siegemund (Siegemund et al., 2012) |
| humanized pAB1- $scFv_{αCD133}$ | Cloned in this work |
| humanized pAB1- $scFv_{αLGR5}$ | Cloned in this work |
| $Db_{αCD133}$-scTRAIL | Cloned in this work |
| $Db_{αLGR5}$-scTRAIL | Cloned in this work |
| murine pAB14D5-$scFv_{αCD133}$ | Cloned in this work |
| murine pAB14D5-$scFv_{αLGR5}$ | Cloned in this work |

## 2.1.11 Primers

All primers were synthesized by Biomers (Ulm), dissolved in $dH_2O$ (f.c.: 50 µM) and stored at -20 °C.

Table 15: List of primers used in this thesis

| Nr. | Primers for cloning | Sequence 5'-3' |
|---|---|---|
| 1 | SfiI-$scFv_{αCD133}$-For | GCACGATCTCAGATCCTCCGCCGCCACTCG |
| 2 | SfiI-$scFv_{αCD133}$-Rev | CCACGTACCGGTCAGGTGCAGCTGGTGCAGTC |
| 3 | NotI-$scFv_{αCD133}$-For | GGGCCCAAGCTTGGTACCCGTTCATTGC |
| 4 | NotI-$scFv_{αCD133}$-Rev | GCGGAGGATCTGAGATCGTGCTGACACAGAGC |
| 5 | SfiI-$scFv_{αLGR5}$-For | CAGAAGAAAGTGAACCGCCTCCACTCGAGACG |
| 6 | SfiI-$scFv_{α\ LGR5}$-Rev | CACGATCTCAGATCCTCCGCCACTCGTTCAC |
| 7 | NotI-$scFv_{α\ LGR5}$-For | CCCTCGTGACAGTCTCGAGTGGCGGAGGATC |

| Nr. | Primers for cloning | Sequence 5'-3' |
|---|---|---|
| 8 | NotI-scFv$_{\alpha\ LGR5}$-Rev | CACGATCTCAGATCCTCCGCCACTCGAGAC |
| 9 | AgeI-Db$_{\alpha CD133}$-scTRAIL-For | ATATATACCGGTCAGGTGCAGCTGGTGCAGTC |
| 10 | AgeI-Db$_{\alpha CD133}$-scTRAIL-Rev | GCTGGATATCAGATCCTCCGCCTCCGCTAG |
| 11 | NotI-Db$_{\alpha CD133}$-scTRAIL-For | GCGGAGGATCTGATATCCAGCTGACCCAGAGC |
| 12 | NotI-Db$_{\alpha CD133}$-scTRAIL-Rev | ATATATGCGGCCGCTCTCTTGATTTCC |
| 13 | AgeI-Db$_{\alpha LGR5}$-scTRAIL-For | ATATATACCGGTGAAGTGCAGCTGGTGGAATCTG |
| 14 | AgeI-Db$_{\alpha\ LGR5}$-scTRAIL-Rev | CTGGATATCTGATCCTCCGCCTCCGCTAG |
| 15 | NotI-Db$_{\alpha\ LGR5}$-scTRAIL-For | GCGGAGGATCAGATATCCAGATGACCCAGAGCC |
| 16 | NotI-Db$_{\alpha\ LGR5}$-scTRAIL-Rev | ATATATGCGGCCGCTCTCTTGATTTCC |

### 2.1.12 Programs and online tools

Table 16: List of programs and online tools used in this thesis

| Programs and online tools | Reference |
|---|---|
| Clone Manager Professional 7 | Scientific & Educational software, Carey, USA |
| ExPASy Prot Param Tool | http://web.expasy.org/protparam/ |
| FlowJo | http://www.flowjo.com |
| GraphPad Prism 5.01 | GraphPad software, La Jolla, USA |
| ImageJ | http://rsb.info.nih.gov/ij/ |
| Microsoft® Word and Excel | Microsoft Corporation |
| RCSB protein databank | http://www.pdb.org/pdb/home/home.do |

## 2.2 Methods

### 2.2.1 Cloning

#### 2.2.1.1 Cloning of Db$_{\alpha CD133}$-scTRAIL and Db$_{\alpha LGR5}$-scTRAIL

The DNA sequences of murine scFv-CD133 and scFv-LGR5 were synthetically produced (Geneart, Regensburg, Germany) according to the patent WO2011149493 (Valera) for CD133 and to the patent WO201016766 (Clevers) for LGR5. Then, both scFv fragments were digested by *Age*I/*Not*I and cloned into the murine vector pAB1-4D5, digested with the same enzymes, resulting in pAB1-4D5-scFv$_{\alpha CD133}$ and pAB1-4D5-scFv$_{\alpha LGR5}$. Then, pAB1-4D5-scFv$_{\alpha CD133}$ and pAB1-4D5-scFv$_{\alpha LGR5}$ were amplified by PCR using the primers (for scFv$_{\alpha CD133}$ Nr. 1, 2, 3, 4; for scFv$_{\alpha LGR5}$ Nr. 5, 6, 7, 8), digested by *Sfi*I/*Not*I and then ligated into the vector pAB1, also digested with *Sfi*I/*Not*I, resulting in humanized pAb1-scFv$_{\alpha CD133}$ (hu-scFv$_{\alpha CD133}$) and pAb1-scFv$_{\alpha LGR5}$ (hu-scFv$_{\alpha LGR5}$). For the generation of scTRAIL fusion proteins, hu-scFv$_{\alpha CD133}$ and hu-scFv$_{\alpha LGR5}$ were amplified by PCR using the

respective template pAb1-scFv$_{\alpha CD133}$ and pAb1-scFv$_{\alpha LGR5}$ and primers (for CD133 Nr. 9, 10, 11, 12; for LGR5 Nr. 13, 14, 15, 16). Subsequently, the PCR products were digested by *Age*I/*Not*I and cloned into the vector pCR3-Db$_{glyco}$-scTRAIL, resulting in Db$_{\alpha CD133}$-scTRAIL and Db $_{\alpha LGR5}$-scTRAIL. Used primers are listed in Table 15.

### 2.2.1.2 Polymerase chain reaction

Polymerase chain reaction (PCR) was used with the aim of amplifying desired sequences, from vector template, with the necessary restriction sites. Usually a PCR reaction contained:

- 5 µl *pfu*-polymerase buffer (10 x) + $MgSO_4$
- 1µl Template (50 ng/µl)
- 1 µl Forward primer (10 pmol/µl)
- 1 µl Reverse primer (10 pmol/µl)
- 2 µl dNTPs (5 mM)
- 1 µl *pfu*-DNA-polymerase (2.5 U/µl)
- $dH_2O$ for a final volume of 40µl

The amplification of DNA was performed using the PCR program described in Table 17. The elongation time was dependent on the resulting PCR product. For the *pfu* polymerase was assumed a synthesis rate of 1000 nucleotides per minute, with a minimal elongation time of 0.5 min. Next, the PCR product was loaded on an agarose gel and separated from primers and template DNA.

Table 17: PCR program

| PCR step | Temperature (°C) | Time (minutes) | Number of cycles |
|---|---|---|---|
| Initial denaturation | 94 | 5 | 1x |
| Denaturation | 94 | 0.5 | 33x |
| Annealing | 50 | 0.5 | 33x |
| Elongation | 72 | dependent | 33x |
| Final elongation | 72 | 5 | 1x |

### 2.2.1.3 Restriction digestion

In a final volume of 50 µl, the vector DNA (5 µg) or the entire DNA purified from agarose gel was digested. For double digests, both enzymes were added to the mixture when temperatures and buffer conditions were the same and incubated for 2 h. Otherwise digestions were performed consecutively with additional purification step. Then, the buffer

exchange was performed with the NucleoSpin Gel and PCR Clean-up kit. Using Fast alkaline phosphatase (1 µl), for 1h at 37°C, the vector DNA was dephosphorylated, after the last digestion step. Finally the fragments obtained were separated and analyzed by agarose gel electrophoresis.

### 2.2.1.4 DNA electrophoresis and gel extraction

The DNA fragments obtained by digestion or after amplification were analyzed and purified by horizontal agarose gel electrophoresis. Gels were prepared by dissolving 1 – 2 % (w/v) of agarose, according to the size of the fragments, in TAE boiling buffer. Next, a final concentration of 1 µg/ml of ethidium bromide was added. DNA was mixed with DNA loading buffer and loaded to the agarose gel (80 V, 30 min). DNA fragments were visualized under ultra violet light and relevant bands were excised and purified according to manufacturer's protocol with a NucleoSpin Gel and PCR Clean-up kit.

### 2.2.1.5 Preparation of chemically competent *E. coli* cells

After overnight culture, *E. coli* TG1 or DH5α were inoculated in 1 l of LB medium (dilution 1:100) and grown, at 37 °C under shaking conditions (170 rpm), until they reached an $OD_{600}$ of 0.5 to 0.6. Next, cells were chilled on ice for 15 minutes, harvested by centrifugation (4000 g, 10 min, 4 °C) and the pellet was resuspended on ice with 50 ml of competent cell solution A (0.1 M $CaCl_2$ in 1x PBS), followed by incubation for 30 minutes on ice. An additional centrifugation step was performed (4000 g, 5 min, 4 °C) and the bacteria pellet was resuspended on ice with 10 ml competent cell solution B (20 % (v/v) glycerol/50mM $CaCl_2$ in 1x PBS). The resulting competent cells were immediately frozen in liquid nitrogen and stored at -80 °C.

### 2.2.1.6 Ligation of DNA fragments and transformation of bacteria

Ligation of DNA fragments and linerarized vector fragments were performed using T4 DNA-ligase with a total DNA amount of 250 ng and a molar ratio of vector to insert of 1:3. For the ligation reaction, 1 U of T4 DNA ligase was incubated with the DNA fragments for 1 h at 25°C, in a final volume of 20 µl. The latter was added to 100 µl of competent *E. coli*, previously thawed on ice, and incubated for 45 min on ice. Next, bacteria were subjected to heat shock at 42 °C for 45 sec and were subsequently placed on ice for 1 min, followed by resuspension in 1 ml of LB medium. After recovery, cells were incubated for 45 min at

37°C. Finally, bacteria were harvested by centrifugation (3000 g, 2 min) and were plated on LB agar plates containing the selective antibiotic and incubated overnight at 37 °C.

#### 2.2.1.7 Plasmid DNA isolation and sequence analysis

One single clone, from the $LB_{Amp,Glu}$ plate or from PCR screening, was inoculated into 5 ml LB medium for Mini preparation or 100 ml for Midi, containing the respective antibiotic. After overnight incubation at 37 °C, bacteria were harvested by centrifugation and DNA was purified according to manufacturer's protocol with the NucleoSpin Plasmid kit and the NuceloBond Xtra Midi kit for Mini and Midi preparation respectively. Sequence confirmation of the final expression vector was performed by GATC Biotech AG (Konstanz, Germany) using the corresponding primers from Table 15.

### 2.2.2 Cell culture

Mouse bone marrow derived MSCs (M2) were kindly provided by Dr. Angelika Hausser (IZI, University of Stuttgart, Germany). These cells were cultivated under sterile conditions, at 37 °C in a 5% $CO_2$ humidified atmosphere, in alpha-MEM supplemented with 10% FBS plus 1% Penicillin/Streptomycin (Pen/Step). MSCs were passaged, using trypsin-EDTA for cell detachment, at a confluence of 70% every 3-4 days if not mentioned otherwise.

Caco2, Colo205, HCT116, HEK293 and LoVo cells were obtained from the ATCC (Manassas, VA, USA) and cultured, at 37 °C and 5% $CO_2$, in RPMI-1640 medium (Invitrogen) supplemented with 10% FCS (Thermo Fisher Scientific), excepting HEK293 where 5% FCS was added to the medium. Before reaching confluence, cells were passaged and maintained in culture for not longer than three month. New cultures of each cell line were established from frozen stocks containing the respective serum supplemented with 10% DMSO which were stored in liquid nitrogen. All cell lines grew in adherent condition.

### 2.2.3 Cell transfection

All cell lines were transfected with polyethyleneimine (PEI) using a ratio 1:3 for DNA and PEI. The day before, 1 million cells were seeded in a 6-well plate in a final volume of 2 ml and allowed to adhere overnight. The next day, cell culture medium was removed and 1.5 ml of serum free Opti-MEM was added. Then, 300 µl of Opti-MEM were incubated with 12

µg of PEI for 5 min a RT. Next, 4 µg of plasmid DNA was added to the mixture and vortexed. After 20 min incubation, the mix was carefully added drop-wise to the cells. After overnight incubation at 37 °C Opti-MEM was removed and cells were transferred into a flask and allowed to grow in cell culture medium for 24 h. Next, in order to select the transfected cells, G418 (f.c.: 150 µg/ml and 250 µg/ml for MSCs or 200 µg/ml for HEK293) was added to the medium. After establishment of stably transfected cell pools (2-3 weeks), cells were used for further studies.

### 2.2.4 Single clone selection

In order to obtain single clone cell lines, 18 h after PEI transfection, MSCs or HEK393 cells were immediately seeded in 96-well plates, performing limiting dilutions with a statistical density of 1 cell/well, in the presence of antibiotic (G418) as selection pressure. After establishment of colonies, the medium was changed every 2 or 3 days after a washing step with sterile PBS. During the selection process, untransfected cells died and positively transfected cells survived and replicated. The 96-well plates were analyzed every 3 or 4 days and the growing clones were monitored for their confluence. When cell confluence was around 70% in the wells with growing cells (41 days after seeding for MSCs and around 14 days for HEK293) a dot blot was performed. The latter, in order to select clones expressing the recombinant proteins, was done using culture medium from each well after 3 days of cultivation. According to the dot blot results, positive clones were transferred into flasks and expanded *in vitro*. The productivity was tested by ELISA, analyzing cell medium from each clone after 3 days of cultivation, seeding the same number of cells. Based on this procedure, the generated cell lines were assumed to be a single cell derived cell lines.

### 2.2.5 Expression and purification of recombinant proteins

#### 2.2.5.1 Periplasmic protein expression in *E. coli* TG1

The scFv fragments were produced and purified from the periplasm of *E. coli* TG1. In particular, a pre-culture of transformed bacteria was grown overnight, at 37 °C and shaking condition (170 rpm), in 20 ml of TY medium with 1 % (w/v) glucose and 100 µg ampicillin/ml. Next, 2 l of TY medium, containing ampicillin and 0.1 % (w/v) glucose, were inoculated with a dilution 1:100 of the overnight culture and cells were grown (37 °C, shaking 170 rpm) until the $OD_{600}$ reached 0.8-1.0. At this time point, IPTG (1 mM) was

added to the cell suspension, in order to induce the protein expression and incubation was performed at 25 °C for 4 h on a shaker (170 rpm). Then, cells were harvested (10 min, 4 °C, 6.000 g) and the cell pellet was resuspended with 100 ml of cold periplasmic preparation buffer (PPB). All the following steps were performed on ice and with chilled liquids and centrifuges. The cell wall was lysed by incubation with lysozyme (50 µg/ml) for 30 min on ice, followed by addition of $MgSO_4$ (10 mM) in order to stabilize the spheroblasts. Then, the periplasmic preparation (supernatant) was collected after centrifugation (10 min, 10.000 g) and dialyzed overnight against 5 l of PBS. After centrifugation (10 min, 10.000 g), in order to remove pellet aggregations, the dialyzed periplasmic preparation was used for purification via Ni-NTA-IMAC (as described in 2.2.5.3).

### 2.2.5.2 Protein expression in mammalian cells

After the selection of stably transfected cell lines, cells were grow in RPMI medium with 5% FCS, until confluence was around 80 %. At this time point, culture medium was exchanged with serum free Opti-MEM, supplemented with $ZnCl_2$ (50 µM). The latter was collected every 2-3 days, after centrifugation (20 min, 2000 g, 4 °C) in order to remove cells from the suspension, and stored at 4 °C. Then, proteins were purified using FLAG affinity chromatography (2.2.5.4) for proteins with FLAG-tag or by Immobilized Metal Affinity Chromatography (2.2.5.3) for 6xHis-tagged proteins.

### 2.2.5.3 Immobilized metal affinity chromatography (IMAC)

IMAC was used as a batch purification method for all recombinant proteins comprising a 6xHis-tag. After equilibration of the Ni-NTA-agarose beads with 8 ml of PBS, the dialyzed periplasmic preparation (2.2.5.1) was incubated with the beads at 4 °C for 2-3 h on a roller mixer. Next, the beads were loaded in an empty column and unspecific bound proteins were removed with 40 column volumes of IMAC wash buffer, containing 25 mM imidazole. Qualitative Bradford assay was performed (90 µl Bradford solution + 10 µl fraction) to test the protein content of wash and elution fractions, and blue color indicated presence of proteins. The specifically bound proteins were eluted from the beads by IMAC elution buffer containing 250 nM imidazole. Each elution fraction (250 µl) was analyzed by Bradford and those fractions containing the highest amount of proteins were pooled and dialyzed overnight against 5 l PBS at 4 °C, followed by SDS-PAGE and Western blot analysis.

### 2.2.5.4 Purification by FLAG affinity chromatography

The anti-FLAG antibody agarose was used for purification of recombinant proteins comprising a FLAG-tag. After loading the anti-FLAG antibody agarose beads (2 ml) into a column, the material was washed first with 3 sequential column volume of low pH buffer (0.1 M glycine-HCl pH 3.5) and then 5 times with PBS in order to neutralize the pH and equilibrate. Next, the material was removed from the column and incubated in a glass bottle with the cell free culture supernatant (1 L), obtained as described in 2.2.5.2, at 4°C for 2 h on a roller mixer. After that, beads were harvested by centrifugation (2000 g, 10 min, 4 °C) and transferred back into the empty column. Several washing steps with PBS were performed until unspecific bound proteins were completely washed away. This was verified by Bradford assay as described in 2.2.5.3. Specifically bound proteins were eluted by applying 10 ml FLAG-peptide (0.1 mg/ml) in PBS in aliquots of 1 column volume. After dialysis of eluates overnight against 5 l of PBS at 4 °C, proteins were concentrated using Vivaspin column concentrators (MW cut-off 30 kDa) and subsequently analyzed by SDS-PAGE and Western blotting.

## 2.2.6 Protein biochemical characterization

### 2.2.6.1 Protein concentration

The protein concentration was determined by using a spectrophotometer (NanoDrop). This latter calculates the amount of protein based on the absorbance of tryptophan and tyrosine residues at a wavelength of 280 nm. The molecular weight (MW [g/mol]) and the molar extinction coefficient ε [l/(mol x cm)] were determined by the online tool 'ProtParam' and the concentration was calculated with the following equation **(** b [cm] represents the path length**)**: $c\ [\mu g/ml] = OD_{280} \times MW / (\varepsilon \times b)$

### 2.2.6.2 SDS-PAGE and Coomassie staining

Equal protein amounts (usually 3 µg for Coomassie staining or 1 µg for Western blotting) were mixed either in reducing or non-reducing 1x Laemmli SDS sample buffer, denaturated for 5 min at 95 °C and loaded, with standard protein for the determination of the molecular mass, on Tris/glycine SDS polyacrylamide gels. The gels consisted of 10%, 12% or 15% polyacrylamide running gel and a stacking gel with 5% polyacrylamide. Electrophoresis was carried out by using a vertical gel electrophoresis chamber and the

gels were run in 1x SDS running buffer for approximately 1h at 50 mA. After washing the gel in water, it was stained with Coomassie solution for 1 hour on a shaker and finally destained in water.

### 2.2.6.3 Western blotting

For Western blot analysis, the proteins separated by SDS PAGE were transferred to polyvinylidene difluoride membrane (PVDF, Roth). The PVDF membrane was hydrated with 100% methanol and then equilibrated with blotting buffer. The proteins were blotted on membrane by semi-dry transfer using a semi-dry blotting chamber (Phase, Lübeck) and a constant current of approximately 150 mA (1.5 - 1.6 mA/$cm^2$) for 1 hour and 30 min at room temperature. The voltage was limited to 15 V. The membrane was blocked with blocking solution (5 % dry milk in 1x PBS) at RT for at least 40 min and incubated overnight at 4 °C with the primary antibody (diluted according to the manufacturer's instructions in blocking solution). The membrane was washed three times with 1x PBS-T and incubated with the appropriate secondary antibody (Horseradish Peroxidase (HRP) conjugate, 1:10000 dilution in blocking solution) for 1 hour at RT. After washing (3 times with 1x PBS-T) the membrane was treated with a peroxidase substrate (enhanced chemiluminescence (ECL) detection system from Pierce) according to the manufacturer's instructions to visualize the signals and exposed to an X-ray film for different time points (5 sec up to 5 min).

### 2.2.6.4 Size exclusion chromatography (SEC)

In order to verify the purity and the integrity of purified proteins high performance liquid chromatography (HPLC) was performed using size exclusion columns. For each sample 20 µl of protein with a concentration between 0.2 and 0.5 µg/µl was injected into the HPLC system and analyzed in a PBS mobile phase with a flow rate of 0.5 ml/min. The following standard proteins were used in order to determine the molecular mass of the purified proteins: thyroglobulin (669 kDa), β-amylase (200 kDa), bovine serum albumin (66 kDa), carbonic anhydrase (29 kDa) and FLAG peptide (1 kDa).

## 2.2.7 Cell death assays

Cells were seeded in 100 µl/well of culture medium in 96-well plates, Colo205 (40.000 cells per well), MSCs (20.000 cells per well) HCT116 and LoVo (30.000 cells per well) and

allowed to grow overnight. The day after, cells were treated with serial dilutions of $Db_{EGFR}$-scTRAIL (starting from 3 nM; titration 1:3), $Db_{CD133}$-scTRAIL and $Db_{LGR5}$-scTRAIL (starting from 10 nM; titration 1:3) or with supernatant from transfected MSCs (dilutions 1:3, 1:9 and 1:27), in triplicates. The neutralizing anti-TRAIL antibody (1 µg/ml) was used in combination with the fusion proteins or the supernatant from transfected MSCs and the sensitizer bortezomib (7.5 ng/ml for HCT116 and 250 ng/ml for all other cell lines) was added 30 min before. After 18 hours of incubation at 37 °C, culture medium was removed and cell viability was analyzed. 50 µl of crystal violet staining solution (20 % (v/v) methanol, 0.5 % (m/v) crystal violet in $dH_2O$) were added in each well and incubated at room temperature for 20 min. After abundant washing of the wells with $H_2O$ and air-drying (1-2 h), crystal violet was dissolved in 50 µl methanol and the absorbance was measured by an ELISA reader at 550 nm.

### 2.2.8 Co-culture of MSCs and Colo205

100.000 Colo205 cells/well were seeded in 24-well plates, in 600µl of MSC medium (alpha-MEM) and allowed to grow at 37°C. After overnight incubation, MSCs were added to the 24-well plate using different ratio of MSCs:Colo205 (1:5, 1:20, 1:50) in a final volume of 1 ml/well. Different treatments with bortezomib (250 or 7.5 ng/ml) and anti-TRAIL antibody (1 µg/ml) were performed and analyzed by crystal violet staining as described in 2.2.7.

### 2.2.9 Migration assay

Into the bottom chamber of a transwell (0.8 µm pore size; Costar), 80.000 Colo205 cells were seeded in RPMI-1640 medium with 10% FCS. After overnight cultivation, medium was removed, transwells were washed three times with PBS, and alpha-MEM with 0.5% FBS was added. Into the upper chamber of the transwell, 15.000 cells for each MSC line, wild type (wt), clone #A1, clone #B12 or Mock, were seeded in medium containing 0,5% FBS and allowed to migrate for 8 hours. The bottom chamber contained Colo205 cells or 30 ng/ml of EGF (R&D) or 30 ng/ml of IGF-1 (R&D). Cells on the top surface of the membrane were removed using a cotton swab and cells on the underside of the membranes were fixed with 4% PFA, stained with 0.2% crystal violet and counted in 5 independent microscopic fields at a 20-fold magnification. Experiments were performed in triplicates.

### 2.2.10 Osteogenic differentiation of mouse MSCs

MSCs were grown to 90-100% confluence in 24-well-plates and the culture medium was then replaced with osteogenic medium (α-MEM supplemented with 15% FBS plus 1% Penicillin/Streptomycin, 100 nM dexamethasone, 50 µg/ml ascorbate-2- phosphate, and 10 mM beta-glycerol phosphate). The medium was changed every 2- 3 days. Osteogenic differentiation was assessed by Alizarin Red staining 21 days after initial osteogenic induction. In brief, cells were washed with PBS and allowed to dry for 5 - 10 min. Next, cells were fixed with 50% ethanol for 20 min. The fixed cells were then stained with 1% Alizarin red (Roth) at pH 6.4 for 30 min under continuous shaking. Finally, cells were rinsed 3 times with $H_2O$, and transmitted light pictures were taken. As a negative control, cells grown in culture medium for 21 days were used.

### 2.2.11 Adipogenic differentiation of mouse MSCs

MSCs were grown to confluence on Permanox 4-well chamber slides (Thermo Scientific). Adipogenic differentiation medium, composed of α-MEM supplemented with 15% FCS plus 1% Penicillin/Streptomycin, 1 µM dexamethasone, 500 µM IBMX, 10 µg/ml human insulin and 100 µM indomethacin, was added and changed every 2-3 days. 12 days after initial adipogenic induction, cells were washed with PBS and fixed for 10 min in 4% Histofix (Roth). Next, cells were rinsed once with $H_2O$ and incubated in 60% isopropanol for 5 min. Subsequently, the cells were incubated for 10 min with Oil Red O. Finally, the cells were washed once with 60% isopropanol followed by $H_2O$. Nuclei were counterstained with hemalaun. As a negative control, cells grown in culture medium for 12 days were used.

### 2.2.12 Immunofluorescence and microscopy

MSCs were seeded on glass coverslips and incubated for 3 h at 37 °C. Then, coverslips were washed with PBS containing $CaCl_2/MgCl_2$, fixed for 10 min with 4% PFA and permeabilized with PBS containing 0.1% Triton X-100 for 5 min. The blocking step was performed by incubating the cells with 5% FCS in PBS for 30 min at room temperature. Next, cells were washed and incubated with primary antibody and DAPI (1 µg/ml) diluted in blocking buffer for 2 h, followed by washing steps with PBS-T. When required, incubation with secondary antibody, diluted in blocking buffer, was performed for 1 h. Coverslips were mounted in Fluoromount G (Southern Biotechnology) and analyzed with

the Spinning Disc using 488 nm, 543 nm and 633 nm excitation and a 20x/0.8 DIC objective lens. Images were processed with ZEN software.

### 2.2.13 Flow Cytometry

#### 2.2.13.1 Propidium iodide staining

After co-culture of MSCs and Colo205, as described in paragraph 2.2.8, the medium from each well was collected in a falcon tube. Then, cells were trypsinized and added to the respective culture medium. After centrifugation (5 min, 500 g), the supernatant was removed, the cell pellet resuspended in 100 µl of PBA and transferred in a 96-well plate. Next, PI (10 µg/ml) was added to the cells and incubated for 5 min, followed by flow cytometry analysis of the stained cells.

#### 2.2.13.2 Cleaved caspase 3 intracellular staining

Colo205 (80.000 cells/well) were seeded in the bottom of a transwell plate (Costar) in RPMI-1640 medium (10% FCS) and incubated at 37 °C overnight. Then, medium was removed and after washing with PBS, changed with alpha-MEM medium with 10% FBS. Bortezomib (250 ng/ml) was added into the culture medium and incubated at 37 °C for 30 min in order to sensitize the cells to TRAIL-induced apoptosis. Next, into the upper chamber of the transwell 16.000 cells for each MSC line, wild type (wt), clone #A1, clone #B12 or Mock, were seeded. After 16 h of incubation at 37°C, the transwell was removed and the culture medium was transferred in a falcon tube. Colo205 from the lower chamber were trypsinized, added to the respective culture medium and after centrifugation (5 min, 3000 g), cell pellet was resuspended in 100 µl of PFA (4%) and transferred into a 96-well plate. After 10 min of fixation with PFA at room temperature, 2 washing steps with PBS (150 µl/well) and subsequent centrifugation (5 min, 1500 rpm) were performed. Next, permeabilization was achieved by incubation of cells for 10 min at RT with permeabilization buffer (0,1% Triton in PBA). Then, primary antibody (dilution 1:1500 in permeabilization buffer) was added and incubated for 1 h at RT with the cells. After two washing steps with PBA, as described above, secondary antibody (anti-rabbit-FITC) was incubated with cells for 45 min at RT (dilution 1:80 in permeabilization buffer). Finally, after two additional washing steps, cells were resuspended in 200 µl/well of PBA and analyzed by flow cytometry.

### 2.2.13.3 Expression of surface markers on cell lines

In order to analyze the expression of surface markers, the cells of interest (MSCs, Caco2, Colo205, HCT116, LoVo) were seeded in a U-bottom 96-well plate (150.000 cell/well) and incubated 1 h at 4 °C with the specific primary antibody (Table 10). After 3 washing steps with 200 µl/well PBA, followed by centrifugation (5.000 g, 5 min, 4 °C), cells were incubated with the secondary antibody, when necessary, for 2 h at 4 °C. Otherwise, after the washing steps, cells were immediately resuspended in 150 µl/well PBA and analyzed by flow cytometry. The respective Isotypes antibodies, for the primary antibody directly conjugated, or the secondary antibodies alone were used as controls.

### 2.2.13.4 Binding assay of fusion proteins

Cells (Colo205, Caco2, HCT116) were seeded in U-bottom 96-well plate and incubated for 1 h at 4 °C, either with scFv proteins ($scFv_{CD133}$, $scFv_{LGR5}$) or with the fusion proteins ($Db_{CD133}$-scTRAIL and $Db_{CD133}$-scTRAIL), in both cases using a titration 1:3 for each protein. After three washing steps with 200 µl/well PBA, as above, cells were incubated for 2 h at 4 °C with the secondary antibody, respectively anti-His-PE for scFv proteins or anti-FLAG-PE for the recombinant proteins. Subsequently, 3 additional washing steps with PBA were performed, then the cells were resuspended in 150 µl/well PBA and immediately analyzed by flow cytometry. For detection control, only PE-conjugated anti-His or anti-FLAG antibodies were incubated with the cells.

## 2.2.14 Enzyme-linked immunosorbent assay (ELISA)

In order to determine the amount of $Db_{EGFR}$-scTRAIL secreted by MSCs in the culture medium or in the serum blood *in vivo* (2.2.15.1), ELISA assays were performed using the kit OptEIA™ human TRAIL ELISA Set (BD), according to the manufacturer's instruction. Briefly, the ELISA plate was coated with 100 µl/well of capture antibody and incubated overnight at 4 °C. Then, after 3 washing steps with ELISA washing solution (0.05 % (v/v) Tween20 in 1x PBS), 200 µl/well of ELISA blocking solution (2 % (w/v) dry milk in PBS) were added and incubated for 1 h at RT. Next, a titration of standard TRAIL protein (start from 2 ng/ml, titration 1:3) and serial dilutions of MSC supernatant or serum blood (dilution 1:20), in duplicate, were added and incubated 2 h at RT. After 5 washing steps, working detector solution (100 µl/well) was incubated 1 h at RT. Next, additional 7 washing steps were performed as above and subsequently 100µl/well of ELISA developing solution (0.1 mg/ml TMB, 100 mM sodium acetate buffer pH 6.0; 0.006 % $H_2O_2$) was added and

incubated 30 min in the dark at RT. Finally, the enzymatic reaction was stopped by adding 50 µl/well of 1 M $H_2SO_4$ and the absorbance at 450 nm was measured in an ELISA reader.

### 2.2.15 *In vivo* studies

All studies with experimental animals were performed according to federal guidelines. Mice were at least 9 weeks old at the beginning of the experiments and were allowed to acclimate for at least two weeks in our animal facilities. All experiments were conducted using female nude NMRI mice obtained from Charles River Laboratories.

#### 2.2.15.1 $Db_{\alpha EGFR}$-scTRAIL serum concentration

Two groups, each composed by five mice, were injected with MSCs expressing $Db_{\alpha EGFR}$-scTRAIL or mock-transfected MSCs. In one case subcutaneous injections were performed using 4 x $10^6$ cells/injection. For the second group, MSCs were intravenously administrated (1 x $10^6$ cell/injection). In both cases 100 µl PBS were used as final volume for each injection, in combination with 100 IU/ml of heparin (Rapp et al., 2015), in order to avoid cell clotting. Next, blood samples were collected from the tail vain 1, 3, 7, 14 and 21 days after the MSC injections and stored at -20 °C. Finally, after centrifugation (10.000 g, 10 min, 4 °C) clotting cells were removed and serum levels of $Db_{EGFR}$-scTRAIL were measured performing a TRAIL ELISA assay as described in 2.2.14.

#### 2.2.15.2 Antitumor activity

Female nude NMRI mice were subcutaneously injected with 3 x $10^6$ Colo205 cells, in a total volume of 100 µl PBS, at both dorsal sides left and right. The treatments with MSCs, expressing $Db_{EGFR}$-scTRAIL, were started when the tumor volumes reached about 100 $mm^3$. In particular, 4 x $10^6$ MSCs were resuspended in 100 µl PBS mixed with 100 IU/ml of Heparin and then peritumorally injected (p.t.). During the injections of all cell lines, mice were anesthetized with isoflurane. The Colo205-bearing mice received three peritumoral injections of MSCs at day 10, 17, 27. While, 5 µg of bortezomib dissolved in 100 µl PBS were injected i.p every second day, starting from day 11 until day 31. Mice in the control groups received either 100 µl PBS i.p injected or MSCs. The mock cell line was p.t injected in combination with bortezomib administrated i.p every other day. Tumor growth was monitored with a caliper and tumor volume was determined as follows (L, longitudinal diameter of tumor; W, transverse diameter of tumor): Tumor volume = $(L * W^2) / 2$

### 2.2.15.3 ALT assay

Nude mice received tumor treatments as described above (2.2.15.2). At day 31, blood samples were collected from the tail vain and after centrifugation (10.000 g, 10 min, 4 °C), the serum fractions were obtained and stored at -20 °C. The alanine transaminase (ALT) activity was analyzed by an enzymatic assay, according to the manufacturer's instruction.

## 2.2.16 Statistical analysis

All values are expressed as means ± SEM (Standard Error of the Mean) while for the analysis of the *in vivo* studies the 95 % confidential interval (95 % CI) was used and the survival rate was measured using a log-rank test based on Kaplan-Meier method. Significances, for each experiment, were calculated with GraphPad prism one-way Anova with Tukey's post-test. In particular: * represents a p-value < 0.05, ** p-value < 0.01 and *** p-value < 0.001.

# 3 Results

In the first part of this study, two novel scFv-scTRAIL fusion proteins selectively targeting the cancer stem markers CD133 and LGR5 were generated. In fact, in the last several years evidence suggested the idea that the driving force behind tumor growth resides in the CSCs, which seem to be also responsible for metastasis formation and tumor relapse after therapy and which are resistant to conventional chemotherapy (Huang et al., 2008). For these reasons I investigated whether a selective targeting of optimized engineered variants of TRAIL to cancer cells, expressing these CSC markers, could be a new therapeutic approach.

## 3.1 Db-scTRAIL fusion proteins targeting CSC markers: CD133 and LGR5

### 3.1.1 Generation of humanized $scFv_{\alpha CD133}$ and $scFv_{\alpha LGR5}$

The first step for the generation of scFv-scTRAIL fusion proteins was the production of specific humanized scFv fragments against CD133 or LGR5, $scFv_{\alpha CD133}$ and $scFv_{\alpha LGR5}$, respectively. For this purpose, from published sequences of CD133 and LGR5 specific antibodies, humanized $scFv_{\alpha CD133}$ and $scFv_{\alpha LGR5}$ fragments were generated, produced (2.2.5.3) and purified by IMAC using the His tag. The analysis of the integrity of both scFv fragments was performed by SDS page, which showed a single band at the expected molecular mass, around 30 kDa for $scFv_{\alpha CD133}$ and 28 kDa for $scFv_{\alpha LGR5}$, both under reducing and non-reducing conditions (Fig. 6).

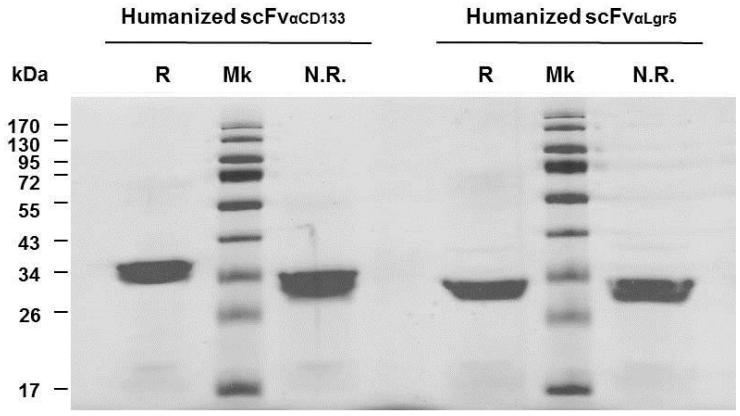


**Figure 6: SDS-PAGE analysis of humanized $scFv_{\alpha CD133}$ and $scFv_{\alpha LGR5}$**
SDS-PAGE analysis of the purified $scFv_{\alpha CD133}$ and $scFv_{\alpha LGR5}$ proteins, under reducing (R) and non-reducing (N.R) conditions. 5 µg of purified protein was loaded for each sample Mk, protein standard marker.

Subsequently, the expression of both CSCs markers, CD133 and LGR5, was analyzed by flow cytometry (2.2.13.3) on four different colon cancer cell lines: Caco2, Colo205, HCT116 and LoVo. For CD133, only Colo205 cells were almost negative, while all the other cell lines were positive with the highest expression observed on Caco2 cells (Fig.7). Concerning LGR5, all cell lines were completely negative for this marker, except for LoVo cells that showed a significant surface expression (Fig 7). The absence of LGR5 expression on three colon cancer cell lines Caco2, Colo205 and HCT116, could be explained by the fact that the expression of this marker is restricted only at the base of the crypts and not in the entire intestinal tissue (Barker et al., 2007).

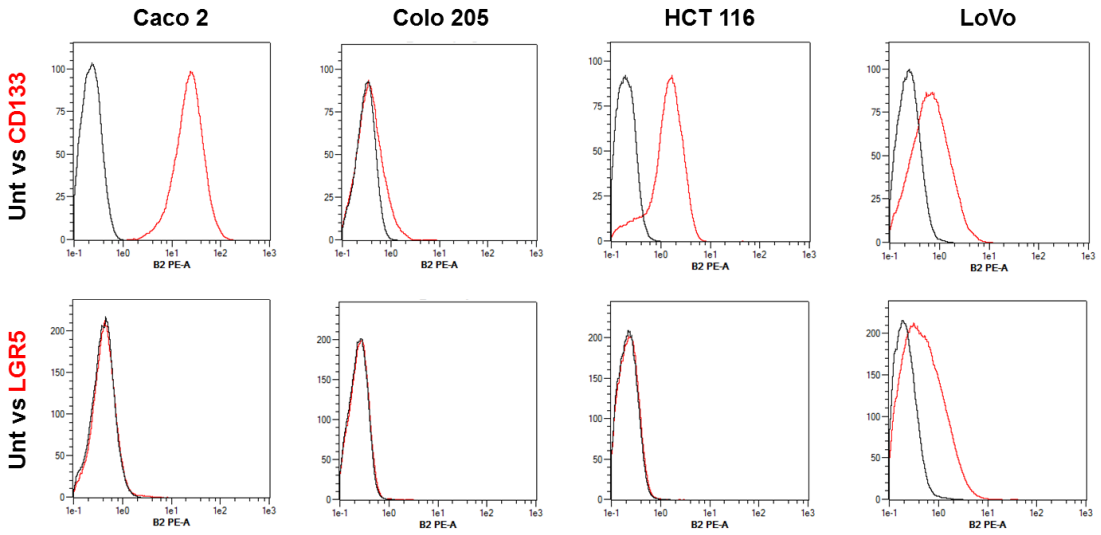


**Figure 7: Surface expression of CD133 and LGR5 on colon cancer cell lines**
Flow cytometry analysis of CD133 and LGR5 expression (red line) on colon cancer cell lines Caco2, Colo205, HCT116 and LoVo. Unstained cells were used as negative control (black line). Y axis: number of events analyzed. Representative experiment out of 4 independent analyses.

According to the results of CSCs marker surface expression, HCT116 and LoVo cells were chosen for further investigations of scFv or fusion proteins for CD133 and LGR5, respectively. These two cell lines were used to perform a quantitative binding study by flow cytometry for both scFv proteins on the respective cell line. Data are shown as mean fluorescence intensity (MFI) and the concentration of half-maximum binding ($EC_{50}$) was calculated. Dose response relationship revealed for both cell lines saturation binding and $EC_{50}$ values in the low nM range with an $EC_{50}$ of 4,7 nM for $scFv_{\alpha CD133}$ and 5,8 nM for $scFv_{\alpha LGR5}$ (Fig. 8). As negative control Colo205 cells, which do not express both markers, were analyzed. No binding was detected in this cell lines for both scFv proteins (data not shown).

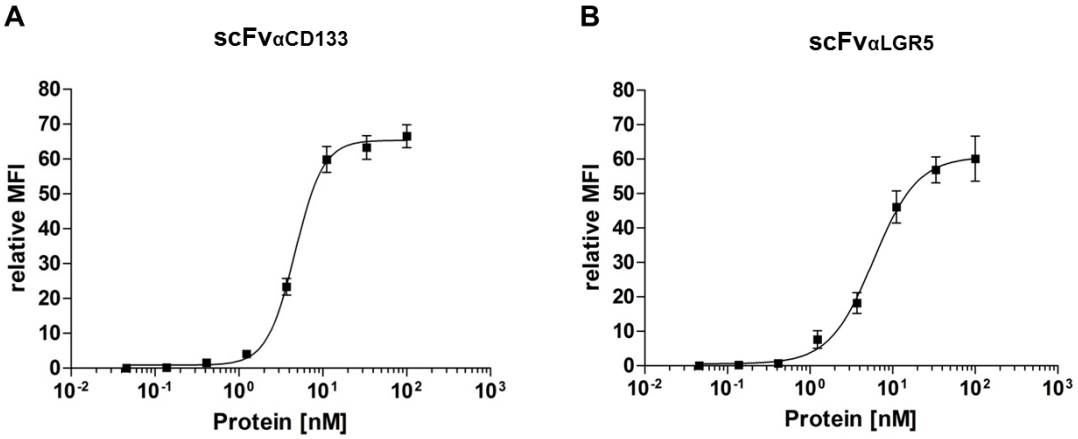


**Figure 8: Binding assay of $scFv_{\alpha CD133}$ and $scFv_{\alpha LGR5}$ on colon cancer cell lines**
Analysis of dose-response relationship of: (A) $scFv_{\alpha CD133}$ binding to HCT116 cells and (B) $scFv_{\alpha LGR5}$ binding to LoVo cells. All proteins were detected, by flow cytometry, via FITC-conjugated anti His-tag antibody and the concentration of half-maximum binding ($EC_{50}$) was measured (mean ± S.E.M., n=4).

### 3.1.2 Fusion proteins: $Db_{\alpha CD133}$-scTRAIL and $Db_{\alpha LGR5}$-scTRAIL

The TRAIL fusion proteins were generated by fusing the humanized scFv fragments directed against CD133 or LGR5 to the N-terminus of human single-chain TRAIL (scTRAIL) comprised of three domains of the extracellular part of wild type TRAIL (aa 118-281) connected via short linkers (Siegemund et al., 2012). The dimerization of the scFv-scTRAIL chain into a functional diabody was accomplished by a short glycine peptide linker (GGG) between $V_H$ (variable domain of immunoglobulin heavy chain) and $V_L$ (variable domain of immunoglobulin light chain), as described by Holliger et al., 1993. The schematic illustration of the fusion proteins is shown in figure 9.

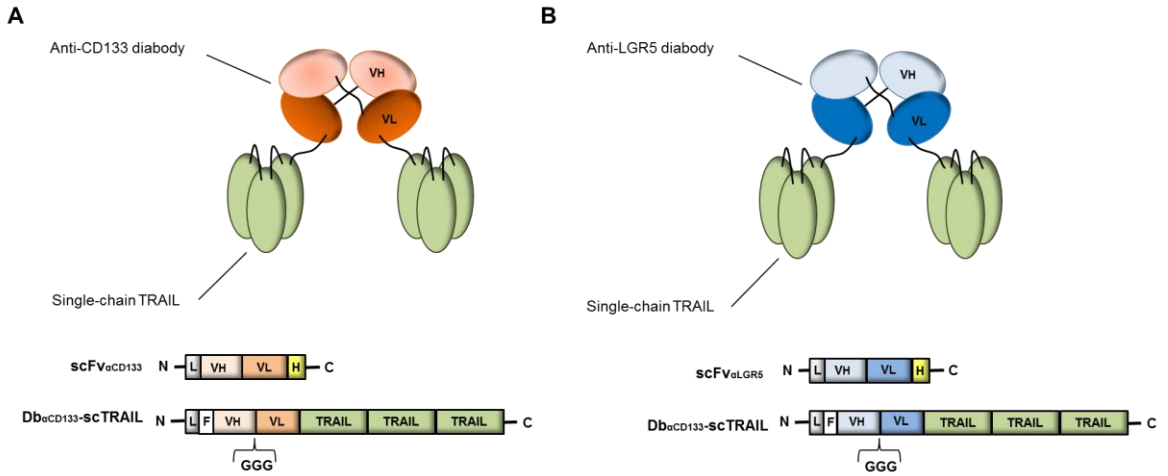


**Figure 9 Schematic illustration of the fusion proteins: $Db_{\alpha CD133}$-scTRAIL and $Db_{\alpha LGR5}$-scTRAIL**
A Schematic illustration of the scFv-scTRAIL fusion proteins. (A) $Db_{\alpha CD133}$-scTRAIL was generated by fusing the $scFv_{\alpha CD133}$, composed by $V_H$ and $V_L$ (show in orange and light orange) with the N-terminus of scTRAIL, comprised of three extracellular TRAIL domains (show in green). (B) For the generation of $Db_{\alpha LGR}$-scTRAIL, the $scFv_{\alpha LGR5}$ fragment, comprising $V_H$ and $V_L$ (show in blue and light blue) connected by a short peptide linker (GGG), was fused to the N-terminus of scTRAIL comprised of three extracellular TRAIL domains (show in green). L: $V_H$ leader; F: FLAG tag; H: His tag.

Both fusion proteins, $Db_{\alpha CD133}$-scTRAIL and $Db_{\alpha LGR5}$-scTRAIL**,** were produced in stably transfected HEK293 cells (2.2.5.2) and purified from serum free cell culture supernatant by FLAG tag (2.2.5.4). The integrity of the purified fusion proteins was analyzed by SDS PAGE, immunoblotting as well as size exclusion chromatography (SEC) (Fig. 10). Both fusion proteins showed, in SDS PAGE and immunoblotting analysis, a single band matching the calculated molecular mass values of 83 kDa for $Db_{\alpha CD133}$-scTRAIL and 85 kDa for $Db_{\alpha LGR5}$-scTRAIL (Fig. 10A, 10B). The size exclusion chromatography confirmed the correct assembly into dimeric molecules under native conditions, for both fusion proteins (Fig. 10C). In particular, $Db_{\alpha LGR5}$-scTRAIL was eluted in a single peak at an apparent molecular mass of approximately 170 kDa, while the fusion protein $Db_{\alpha CD133}$-scTRAIL showed a major peak at the same apparent molecular mass of 170 kDa and a higher molecular weight fraction probably representing tetrameric assembly or other aggregated forms.

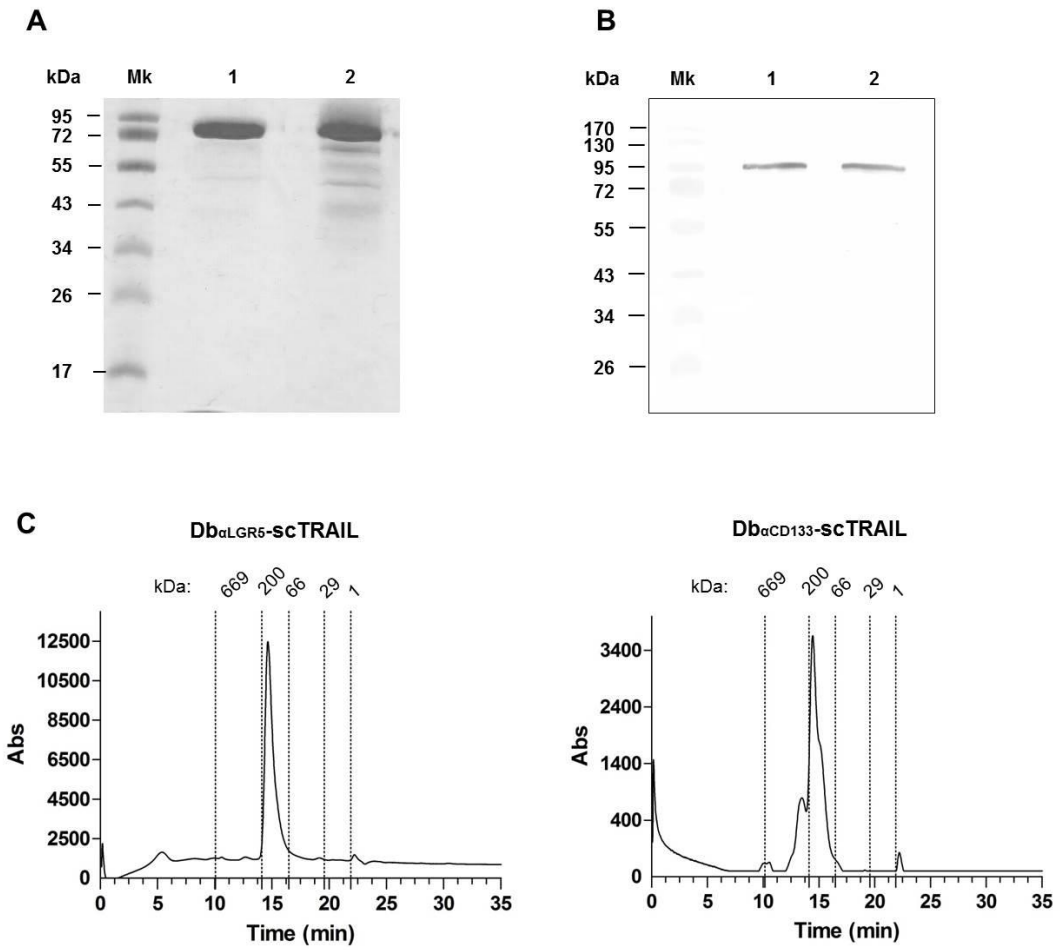


**Figure 10 Biochemical analyses of $Db_{\alpha CD133}$-scTRAIL and $Db_{\alpha LGR5}$-scTRAIL fusion proteins**
Purified $Db_{\alpha LGR5}$-scTRAIL (line 1) and $Db_{\alpha CD133}$-scTRAIL (line 2) fusion proteins were analyzed by: (A) reducing SDS PAGE, 5 µg for each protein; (B) immunoblotting against antibody anti FLAG, loaded 1 µg for each protein and (C) size exclusion chromatography. Thyroglobulin (669 kDa), β-amylase (200 kDa), bovine serum albumin (66 kDa), carbonic anhydrase (29 kDa) and FLAG peptide (1 kDa) were used as standard proteins. Mk protein standard marker.

Although the biochemical analyses confirmed integrity and mostly correct dimeric assembly for both fusion proteins, the yields were very low: 0,3 mg/L for $Db_{\alpha CD133}$-scTRAIL and 0,4 mg/L for $Db_{\alpha LGR5}$-scTRAIL. In order to overcome this problem and to increase the productivity, different experimental approaches were tested. The first one was lowering the culture temperature during HEK293 cultivation, from 37 °C to 32 °C, which enhances protein expression, as described by Chi-Yen et al. 2015. Unfortunately, this method was not successful with these constructs, in fact HEK293 cells did not show significant differences in productivity at 32°C, in comparison with 37°C, for both fusion proteins (data not shown). Then, giving the fact that stably transfected HEK293 represent a pool of transfected cells that likely show large cell selective differences in expression of the transgene, a screening for stable single producer clones was performed applying the limiting dilution method. For this, a cell density of 1 cell/well was used to seed HEK293

cells after transfection, with either $Db_{\alpha CD133}$-scTRAIL or $Db_{\alpha LGR5}$-scTRAIL (2.2.4). Six 96-well plates for each fusion protein were used for the selection and after about two weeks of cultivation under selective pressure of the antibiotic G418, a dot blot assay was performed using culture medium collected from each well (Supplementary figure S1). According to the Dot Blot results the best single clones, nine and six for $Db_{\alpha CD133}$-scTRAIL and $Db_{\alpha LGR5}$-scTRAIL, respectively, were selected and expanded *in vitro*. Next, the productivity was analyzed using an aliquot of cell free culture supernatant for each single clone, with the same seeding cell density, and verified by immunoblotting using an anti-FLAG antibody (Fig. 11).

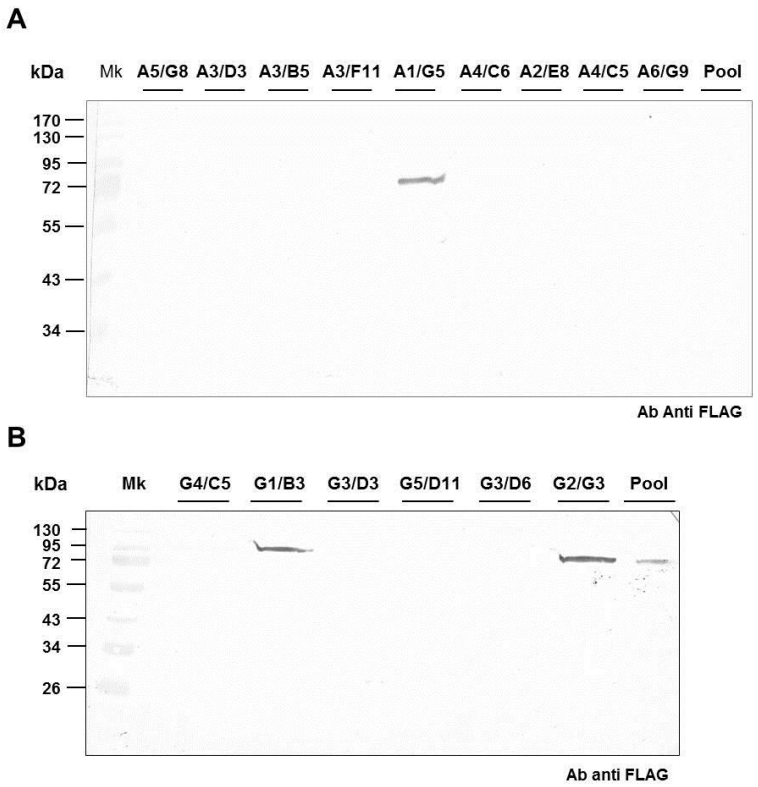


**Figure 11 Single clone selection for $Db_{\alpha CD133}$-scTRAIL and $Db_{\alpha LGR5}$-scTRAIL**
Immunoblotting of cell free culture supernatant from (A), nine single clones of $Db_{\alpha CD133}$-scTRAIL and (B), six single clones of $Db_{\alpha LGR5}$-scTRAIL. 75 µl of cell free culture supernatant, for each line, were loaded and analyzed using an antibody against FLAG. Culture supernatants from $Db_{\alpha CD133}$-scTRAIL and $Db_{\alpha LGR5}$-scTRAIL pools cell lines were used as control. Mk protein standard marker.

Given the results of the immunoblotting assays, the best clones were chosen and expanded for further investigations. In particular, for $Db_{\alpha CD133}$-scTRAIL the clone A1/G5 was selected and named #$Db_{\alpha CD133}$-scTRAIL, while for the fusion protein $Db_{\alpha LGR5}$-scTRAIL the clone G2/G3 showed the highest productivity and named #$Db_{\alpha LGR5}$-scTRAIL. Subsequently, a biochemical analysis of the fusion proteins expressed and purified from each single clone was performed, including SDS PAGE, immunoblotting and size

exclusion chromatography (Fig. 12).The SDS PAGE and the immunoblotting revealed a single band matching the calculated molecular mass values for both fusion proteins: 83 kDa for #Db$_{\alpha CD133}$-scTRAIL and 85 kDa for #Db$_{\alpha LGR5}$-scTRAIL (Fig. 12A, 12B). In addition, the size exclusion chromatography confirmed the protein integrity and tendency to form dimeric molecules (Fig. 12C). It showed, in fact, for the fusion protein #Db$_{\alpha CD133}$-scTRAIL a major peak at an apparent molecular mass of approximately 170 kDa, while the #Db$_{\alpha LGR5}$-scTRAIL fusion protein was eluted as a single peak at the same apparent molecular mass (~170 kDa), indicating a dominant and exclusive dimeric composition for the former and latter, respectively. Finally, the clone selection strategy was also successful concerning the productivity, showing slightly increased yields, in comparison to the pool. The protein production was enhanced ~1,6 fold for #Db$_{\alpha CD133}$-scTRAIL (yield: 0,5 mg/L) and ~ 2,2 fold for #Db$_{\alpha LGR5}$-scTRAIL (yield 0,9 mg/L).

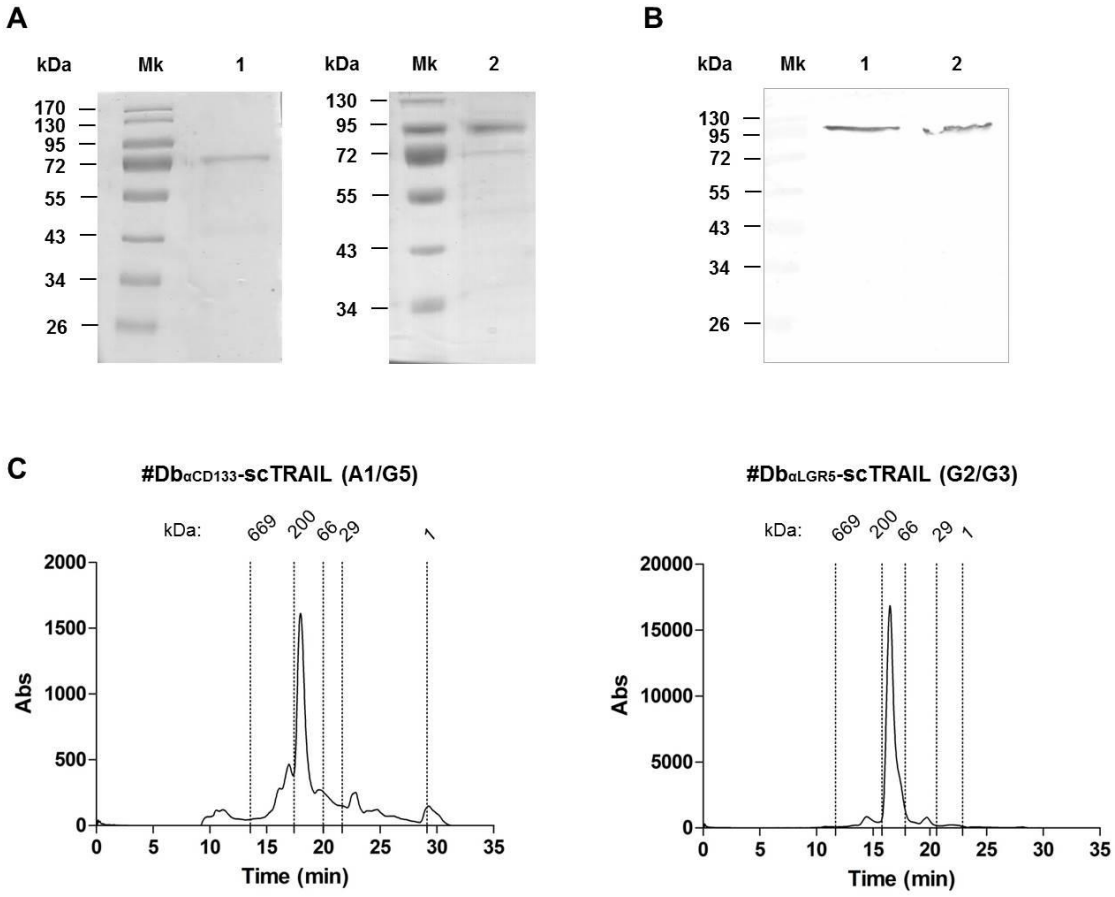


**Figure 12 Biochemical analysis of purified fusion proteins from single clones: #Db$_{\alpha CD133}$-scTRAIL and #Db$_{\alpha LGR5}$-scTRAIL**

Purified #Db$_{\alpha CD133}$-scTRAIL (line 1) and #Db$_{\alpha LGR5}$-scTRAIL (line 2) fusion proteins from single clones (A1/G5 and G2/G3 respectively) were analyzed by: (A) reducing SDS PAGE, 2 µg for each protein; (B) immunoblotting against antibody anti FLAG, loaded 1 µg for each protein and (C) size exclusion chromatography. Thyroglobulin (669 kDa), β-amylase (200 kDa), bovine serum albumin (66 kDa) and carbonic anhydrase (29 kDa) and FLAG peptide (1 kDa) were used as standard proteins. Mk protein standard marker.

### 3.1.3 *In vitro* bioactivity of #Db$_{\alpha CD133}$-scTRAIL and #Db$_{\alpha LGR5}$-scTRAIL

Purified fusion proteins were investigated for their binding functionality by flow cytometry on appropriate target positive cell lines and half-maximum binding ($EC_{50}$) was calculated from dose response curves. As expected, the purified fusion proteins showed binding to their respective target cell line in the low nM range with an $EC_{50}$ of 4,6 nM for the fusion protein targeting CD133 and 6,1 nM for #Db$_{\alpha LGR5}$-scTRAIL (Fig. 13). Again, no binding was detectable on Colo205 cells, lacking these CSC markers (data not shown).

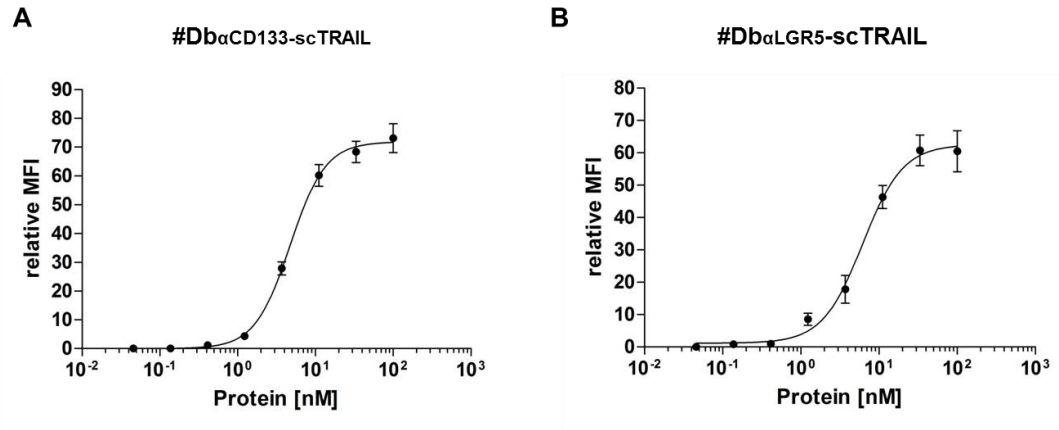


**Figure 13: Binding assay of #Db$_{\alpha CD133}$-scTRAIL and #Db$_{\alpha LGR5}$-scTRAIL on colon cancer cell lines**
Analysis of dose-response relationship of: (A) #Db$_{\alpha CD133}$-scTRAIL binding to HCT116 cells and (B) #Db$_{\alpha LGR5}$-scTRAIL binding to LoVo cells. All proteins were detected, by flow cytometry, via PE-conjugated anti FLAG-tag antibody and the concentration of half-maximum binding ($EC_{50}$) was measured (mean ± S.E.M., n=3).

Next, in order to investigate the bioactivity of the fusion proteins, TRAIL-mediated induction of cell death was analyzed on CD133-expressing HCT116 cell line and on LoVo cells which are positive for LGR5 expression. The cell death induction assays were performed in the presence or absence of two different sensitizers. The proteasome inhibitor bortezomib was used for HCT116 cells, while Smac mimetic was applied for LoVo cells, due to the fact that this cell line showed almost complete resistance to BZB activity (Supplementary figure S2). Both fusion proteins were capable to induce cell death, on the respective cell line, in the absence of sensitizers over the tested concentration range from 1 pM to 10 nM. In particular, for #Db$_{\alpha CD133}$-scTRAIL an $EC_{50}$ value on HCT166 cells of 100 pM was revealed. Similarly, #Db$_{\alpha LGR5}$-scTRAIL showed an $EC_{50}$ value of 140 pM on LoVo cells. The cell death inducing effect of both TRAIL fusion proteins was further increased in the presence of the respective sensitizers (Fig. 14). In fact, #Db$_{\alpha CD133}$-scTRAIL in combination with bortezomib (250 ng/ml) showed an $EC_{50}$ value of 24 pM,

while for #Db$_{\alpha LGR5}$-scTRAIL, in the presence of Smac mimetic (0,1 µM), the $EC_{50}$ value was around 38 pM. These data demonstrate that both TRAIL fusion proteins generated were functional and active in apoptosis induction in a pM range. Furthermore, cell death induction is even stronger in combination with the respective sensitizers, resulting in a ~4-fold increase in activity for both fusion proteins.

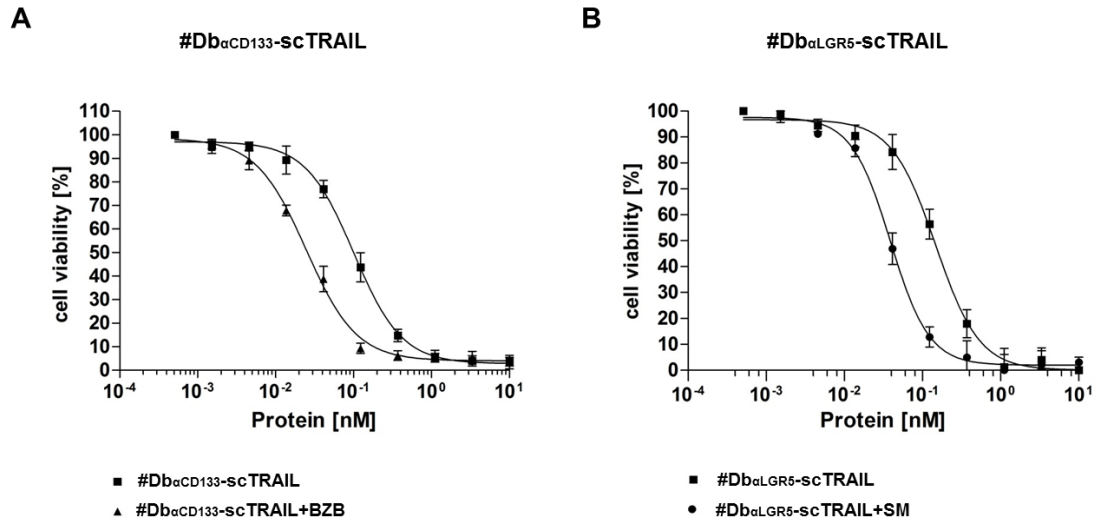


**Figure 14 Cell death induction assay of #Db$_{\alpha CD133}$-scTRAIL and #Db$_{\alpha LGR5}$-scTRAIL on CRC cell lines in the presence or absence of sensitizers *in vitro***
(A) HCT166 cells were sensitized with 250 ng/ml of bortezomib (BZB) and treated with serial dilutions (1:3) of #Db$_{\alpha CD133}$-scTRAIL (starting from 10 nM). (B) LoVo cells were sensitized with Smac Mimetic (SM= 0,1 µM) and treated in combination with a titration 1:3 of the fusion protein #Db$_{\alpha LGR5}$-scTRAIL (starting concentration: 10 nM). After 18 h, cell density was determined using crystal violet staining and data were normalized using bortezomib-treated cells or Smac mimetic-treated cells as control (mean ± S.E.M., n=4).

Subsequently, with the aim of verifying the scFv-receptor targeting capacity of #Db$_{\alpha CD133}$-scTRAIL and #Db$_{\alpha LGR5}$-scTRAIL cell death induction by both fusion proteins was compared with the TRAIL-mediated apoptosis induction of a non-targeting fusion protein Fc-scTRAIL. This latter resembles the hexameric configuration of the Db-scTRAIL molecule, but lacks the specific antigen (CSC marker in this case) binding activity (Fc-scTRAIL protein kindly provided by Dr. Martin Siegemund). As in the experiments above, cell death induction was performed in the presence of the respective sensitizers for the two different cell lines. Surprisingly, the $EC_{50}$ values of non-targeting Fc-scTRAIL were found to be comparable, without any significant differences, with those of #Db$_{\alpha CD133}$-scTRAIL and #Db$_{\alpha LGR5}$-scTRAIL on HCT116 and LoVo cell line, respectively (Fig. 15). In particular, #Db$_{\alpha CD133}$-scTRAIL showed an $EC_{50}$ value of 23 pM and Fc-scTRAIL 25 pM on HCT116 cells, while for #Db$_{\alpha LGR5}$-scTRAIL the $EC_{50}$ value was 34 pM and 38 pM for non-targeting Fc-scTRAIL on LoVo cell line.

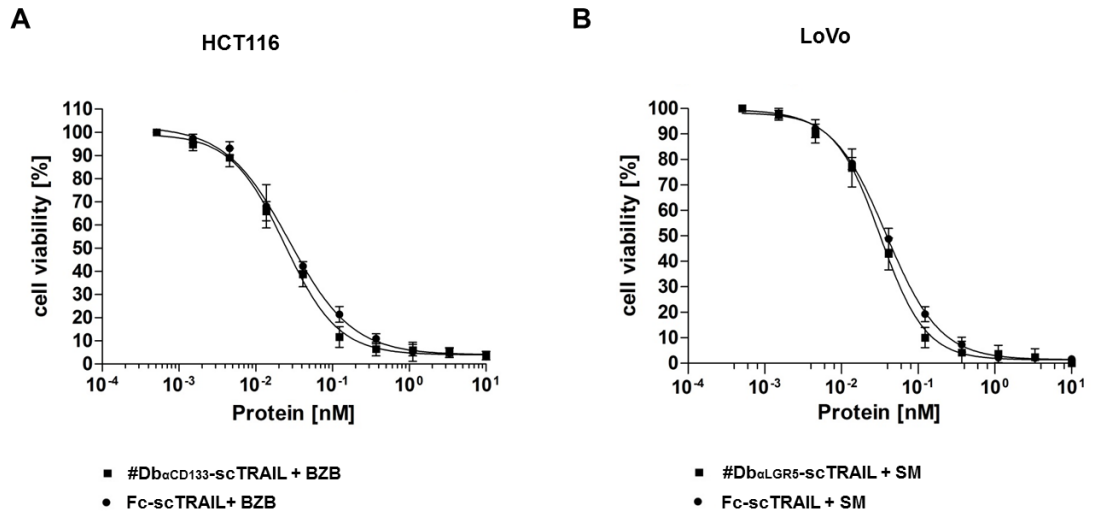


**Figure 15 *In vitro* cell death induction assay of #Db$_{\alpha CD133}$-scTRAIL and #Db$_{\alpha LGR5}$-scTRAIL fusion proteins in comparison with the non-targeting protein Fc-scTRAIL**
(A) HCT166 cells were sensitized with 250 ng/ml of bortezomib (BZB) and treated with a serial dilutions (1:3) of #Db$_{\alpha CD133}$-scTRAIL or Fc-scTRAIL protein (starting from 10 nM). (B) LoVo cells were sensitized with Smac mimetic (SM= 0,1 µM) and treated in combination with a titration (1:3) of #Db$_{\alpha LGR5}$-scTRAIL or the non-targeting protein Fc-scTRAIL (starting concentration: 10 nM). After 18 h, cell density was determined using crystal violet staining and data were normalized using bortezomib-treated cells or Smac mimetic-treated cells as control (mean ± S.E.M., n=4).

Additionally, in order to confirm that the fusion proteins did not improve the TRAIL activity upon binding to the target antigen, competition assays with the respective scFv proteins were performed. In fact, binding conditions under competition with scFv fragments should correspond to those of a scTRAIL protein without antigen targeting. In detail, three different concentrations of the fusion proteins, 1 nM, 0,5 nM and 0,01 nM, were incubated with HCT116 and LoVo cells in the presence or absence of a 100-fold molar excess of either scFv$_{\alpha CD133}$ or scFv$_{\alpha LGR5}$ (Fig. 16). The analysis of the cell viability did not show a significant difference concerning cell death induction between TRAIL fusion proteins alone (#Db$_{\alpha CD133}$-scTRAIL and #Db$_{\alpha LGR5}$-scTRAIL) and in combination with the excess of the respective scFv fragments, for all protein concentrations tested. This confirmed the absence of an increased bioactivity of CSC targeted TRAIL fusion proteins comprising these two specific scFv targeting domains, in comparison with non-targeted TRAIL in this experimental setting.

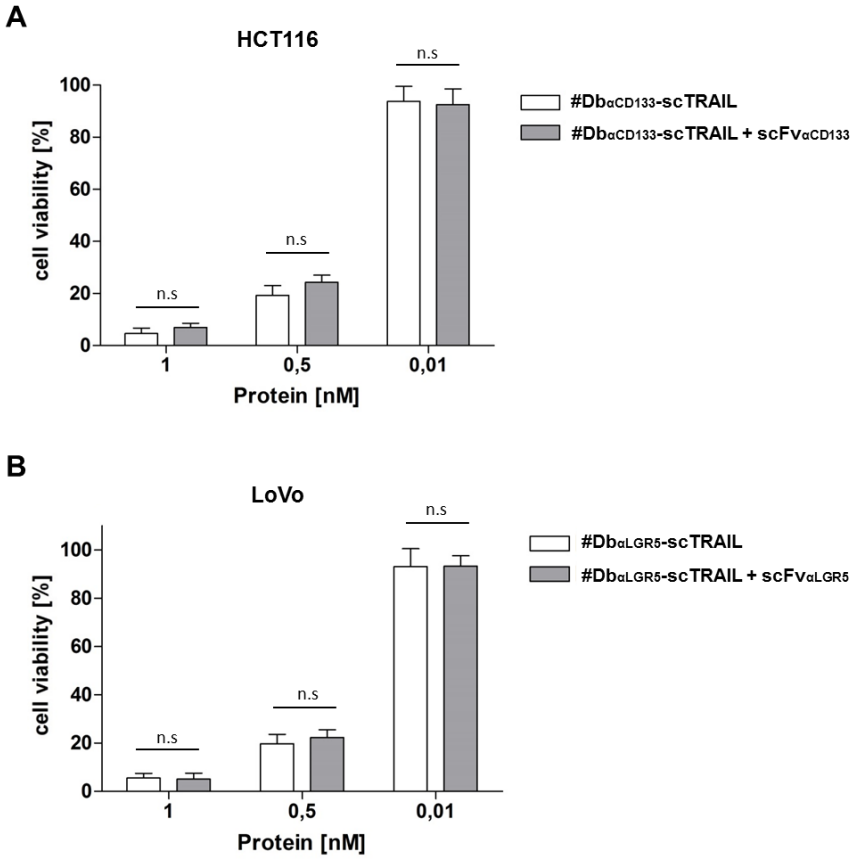


**Figure 16 *In vitro* bioactivity of #Db$_{\alpha CD133}$-scTRAIL and #Db$_{\alpha LGR5}$-scTRAIL fusion proteins in the presence or absence of competition with scFv$_{\alpha CD133}$ and scFv$_{\alpha LGR5}$, respectively**
The fusion proteins were added at concentrations 1 nM, 0,5 nM and 0,01 nM to (A) HCT116 cells for #Db$_{\alpha CD133}$-scTRAIL or (B) to LoVo cells for #Db$_{\alpha LGR5}$-scTRAIL. The scFv proteins were incubated, using a 100-fold molar excess, with the cells 30 min before the respective fusion proteins. After 18 h, cell viability was determined using crystal violet staining (mean ± S.E.M., n=3).

In conclusion, the Db-scTRAIL fusion proteins targeting the CSCs markers CD133 and LGR5, were successfully expressed and produced in the correct dimeric assembly, as confirmed by SEC analysis. Concerning the bioactivity, both constructs, #Db$_{\alpha CD133}$-scTRAIL and #Db$_{\alpha LGR5}$-scTRAIL, exhibited significant TRAIL-mediated apoptosis induction *in vitro* on the respective cell lines. The cell death induction was even stronger when the fusion proteins were used in combination with appropriate sensitizers, resulting in a ~4 fold increase potency .

Nevertheless, with the particular cell lines studied in vitro, the fusion proteins #Db$_{\alpha CD133}$-scTRAIL and #Db$_{\alpha LGR5}$-scTRAIL, despite proven binding to their cognate targets, revealed no positive effect of CSC marker binding on induction of apoptosis when compared to non-targeted TRAIL variants.

## 3.2 MSCs as delivery vector for $Db_{\alpha EGFR}$-scTRAIL expression *in situ*

In the second part of this study I investigated the potential use of MSCs, as an *in situ* cell based delivery system for the expression of a tumor targeting TRAIL fusion protein, both *in vitro* and *in vivo*. Toward this aim, a murine MSC cell line, previously generated at the Institute of Cell Biology and Immunology in Stuttgart (Raeth et al., 2013) was used as a model cell and an activity optimized Db-scTRAIL fusion protein targeting EGFR ($Db_{\alpha EGFR}$-scTRAIL) (Siegemund et al., 2012) was used as a model substance.

### 3.2.1 MSCs insensitivity to $Db_{\alpha EGFR}$-scTRAIL

Several studies reported a significant enhancement of apoptotis on colon cancer cells using combined treatment based on e.g. antibodies and sensitizers, such as bortezomib (Zhu et al., 2005 and Cacan et al., 2015) and Smac mimetic (Lu et al., 2011 and Roesler et al., 2016).

As a prerequisite to study the use of MSCs for a cell based therapy with TRAIL fusion proteins, apoptosis sensitivity of MSCs in comparison to the Colo205 CRC to be used in this tumor model needed to be established. Because the intension for subsequent *in vivo* studies was to investigate combinatorial activity of TRAIL fusion protein with apoptosis sensitizers (bortezomib and smac mimetic), a potential superior apoptotic effect of combined treatment was studied. The combined treatment produced a strong enhancement of cell death induction on Colo205 cells, for both sensitizers, resulting in a ~9-fold increase of TRAIL-mediated apoptosis induction for BZB and ~4-fold for 0,1 µM SM and ~1,4-fold for 0,01 µM. ($EC_{50}$ values: $Db_{\alpha EGFR}$-scTRAIL 19 pM; $Db_{\alpha EGFR}$-scTRAIL + BZB 2,2 pM; $Db_{\alpha EGFR}$-scTRAIL + SM 0,1 µM 4,2 pM and $Db_{\alpha EGFR}$-scTRAIL + SM 0,01µM 13 pM) (Fig. 17).

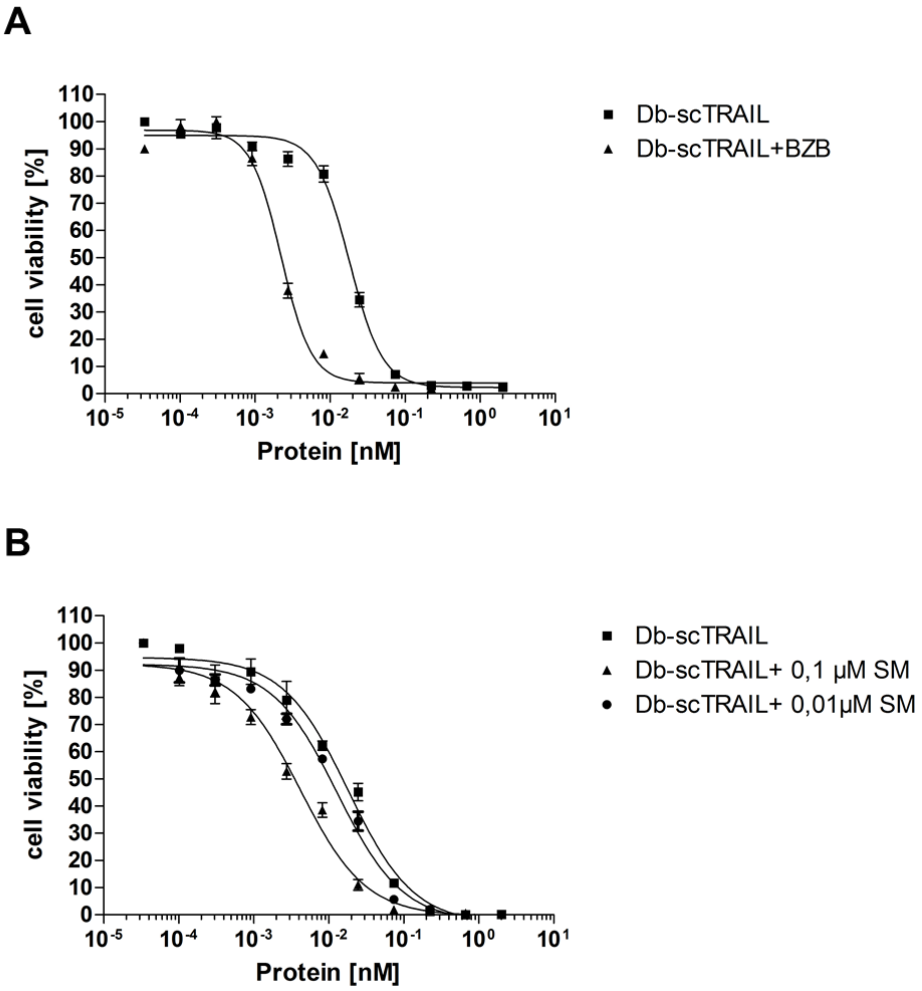


**Figure 17 Cell death induction assay of $Db_{\alpha EGFR}$-scTRAIL on Colo 205 in the presence of sensitizers**
Colo205 were sensitized with 250 ng/ml of bortezomib (BZB) (A) or with Smac Mimetic (SM), using two concentrations 0,1 µM and 0,01 µM (B), in combination with serial dilutions (titration 1:3) of $Db_{\alpha EGFR}$-scTRAIL. After 18 h, cell density was determined using crystal violet staining and data were normalized using bortezomib-treated cells or Smac mimetic-treated cells as control (mean ± S.E.M., n=3).

Next, In order to assess the suitability of MSCs as vehicle for the expression of $Db_{\alpha EGFR}$-scTRAIL, the sensitivity of this stem cell line to Db-scTRAIL activity was analyzed under the same conditions of co-stimulation with apoptosis sensitizers (bortezomib and smac mimetic), as for the CRC line Colo205.

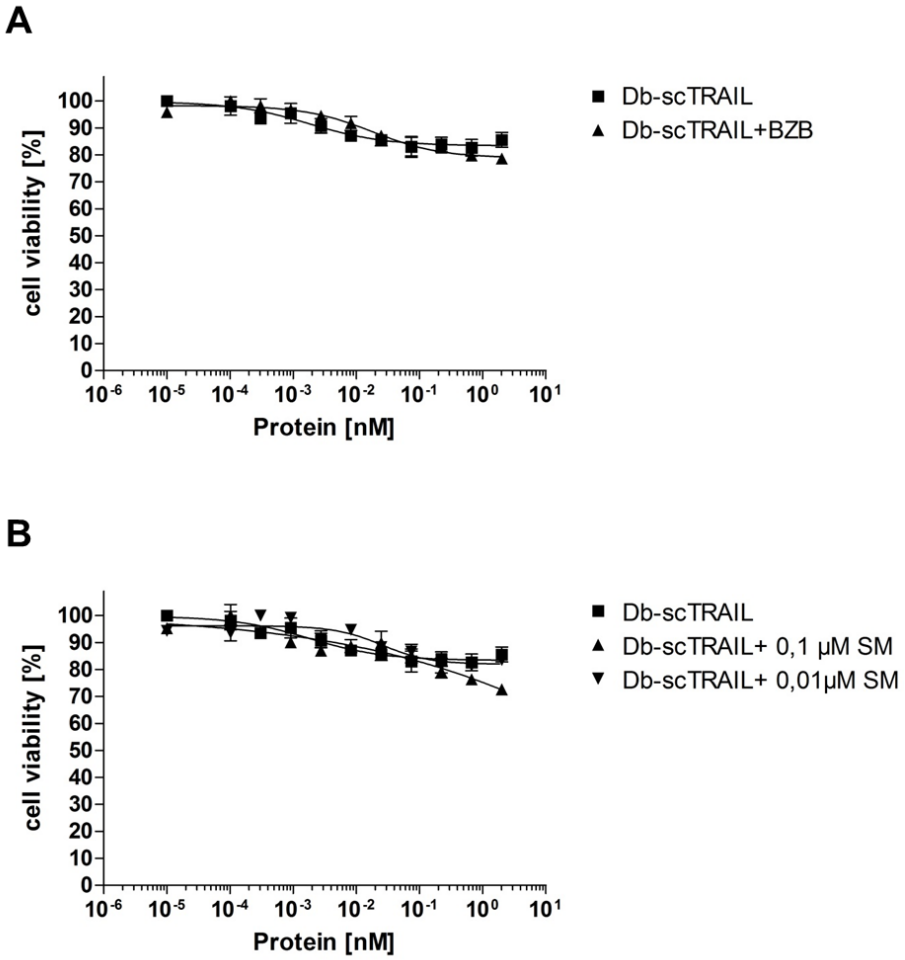


**Figure 18 Cell death induction assay of $Db_{\alpha EGFR}$-scTRAIL on MSCs in the presence of sensitizers**
MSCs were sensitized with 250 ng/ml of bortezomib (BZB) (A) or with Smac mimetic (SM), using two concentrations 0,1µM and 0,01 µM (B), in combination with different concentrations of $Db_{\alpha EGFR}$-scTRAIL. After 18 h, cell density was determined using crystal violet staining and data were normalized using bortezomib-treated cells or smac mimetic-treated cells as control (mean ± S.E.M., n=4).

As shown in figure 18, MSCs were fully resistant to $Db_{\alpha EGFR}$-scTRAIL activity even in the presence of both sensitizers, under which conditions Colo205 cells were completely killed. Taking together these results confirmed that MSCs are potentially suitable cells for generation of a cell based *in situ* delivery system of highly active TRAIL variants for colorectal cancer treatment.

## 3.2.2 Transient transfection of MSCs with $Db_{\alpha EGFR}$-scTRAIL

In order to express $Db_{\alpha EGFR}$-scTRAIL in the murine MSC model cell, different methods were tested. Although several specific kits for stem cells transfection are commercially available, the best results in terms of cell surviving and transfection efficiency were obtained using the Polyethyleneimine (PEI) method.

In a first step, MSCs were transiently transfected with $Db_{\alpha EGFR}$-scTRAIL and the transfection efficiency was verified by ELISA, testing cell culture medium after different time points and through immunoblotting analysis of $Db_{\alpha EGFR}$-scTRAIL purified from culture medium (2.2.5.4). As shown in figure 19A, MSCs were able to secrete the soluble form of the TRAIL fusion protein, the production was monitored daily for five days, revealing a slight, but steady increase for the measured time period, indicative of gradual cessation of expression, yet product accumulation. Western blot of purified TRAIL protein from culture medium, after 5 days of cultivation, confirmed existence of a full length protein, with no evidence for major degradation products (Fig. 19B).

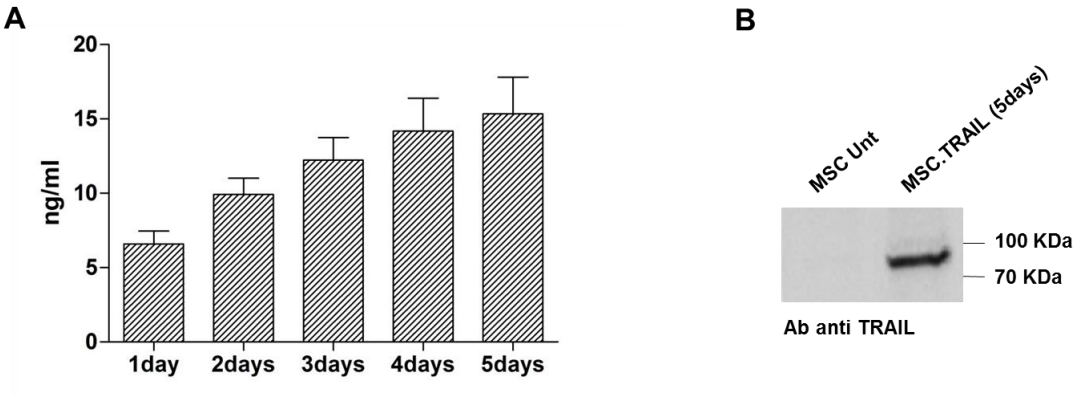


**Figure 19 Expression of $Db_{\alpha EGFR}$-scTRAIL secreted by MSCs after transient transfection**
(A) MSCs were transiently transfected (PEI) and the amount of soluble $Db_{\alpha EGFR}$-scTRAIL released in cell free culture medium was measured by ELISA, every 24 hours (mean ± S.E.M., n=3). (B) After 5 days of transient transfection $Db_{\alpha EGFR}$-scTRAIL secreted in cell medium was purified and analyzed by Western blotting using an antibody against TRAIL.

In order to verify whether $Db_{\alpha EGFR}$-scTRAIL secreted by MSCs is active and functional for apoptosis induction, the cell culture medium was collected every 24 h for five days after transient transfection and tested. In particular, serial dilutions of the daily collected medium were prepared to treat Colo205 cells with or without the sensitizer bortezomib or in combination with a specific blocking anti TRAIL antibody (Ab anti TRAIL-2E5). After 18 hours of treatment, the cell death induction was analyzed by crystal violet assay (Fig. 20A). The latter revealed a strong cell viability reduction, in the presence of bortezomib, which is TRAIL dose-dependent evident from the amount of protein secreted daily, as shown by the ELISA assay (Fig. 20B). In fact, the strongest cell viability reduction, around 85 %, was observed treating Colo205 cells with culture medium collected after one day of transfection, which represents the time point with the highest TRAIL productivity in transient transfection conditions.

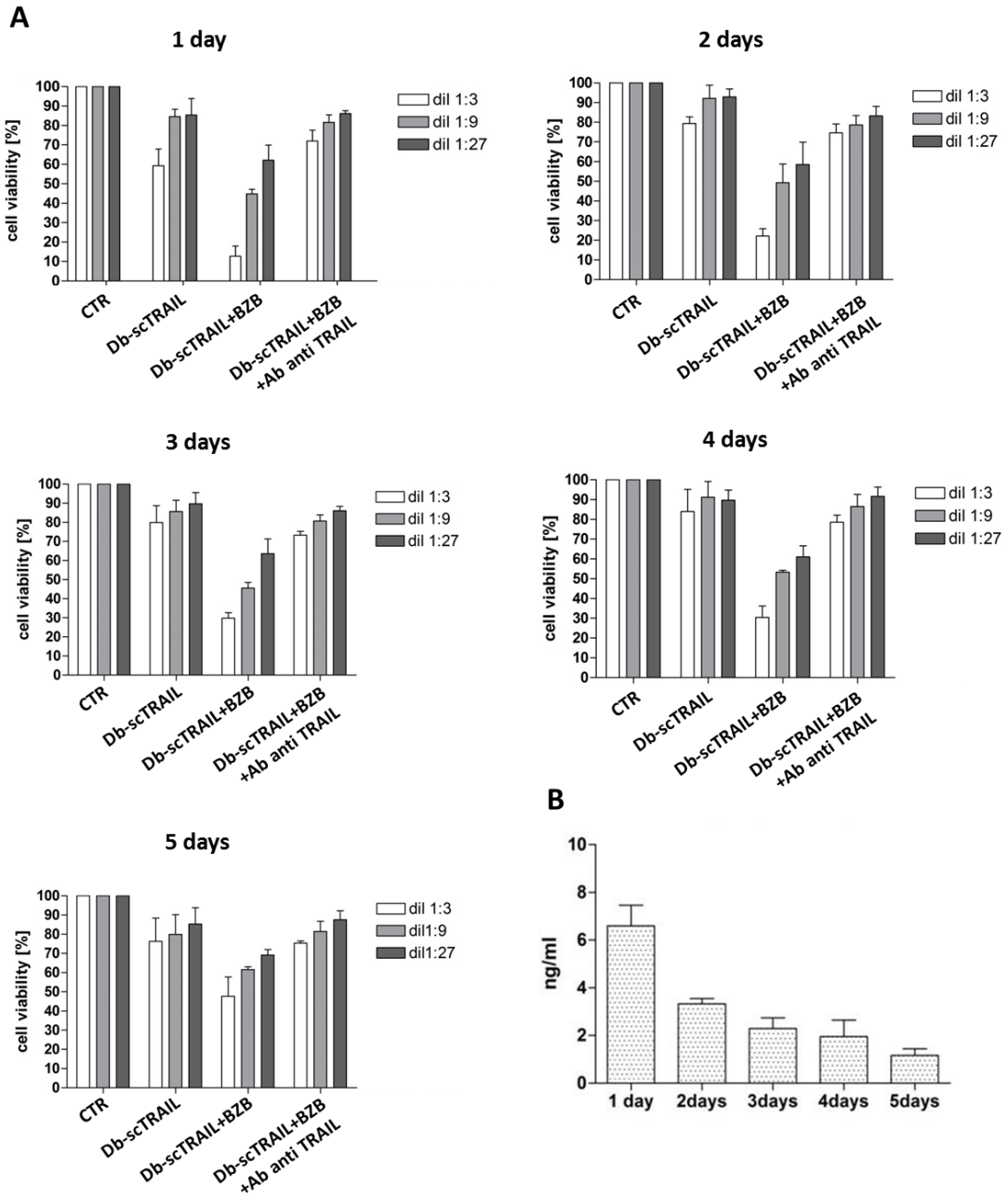


**Figure 20 Cell death induction assay of secreted $Db_{\alpha EGFR}$-scTRAIL on Colo 205**
(A) Colo205 cells were sensitized with bortezomib (BZB, 250 ng/ml) and treated with serial dilutions of daily collected MSCs medium (serial medium dilutions 1:3, 1:9, 1:27) with or without the presence of anti-TRAIL antibody (Ab anti TRAIL, 1 µg/ml). As control (CTR) Colo205 cells were cultivated only with RPMI medium. After 18 h, cell density was determined using crystal violet staining and data were normalized using bortezomib-treated cells as control (mean ± S.E.M., n=4). (B) MSCs were transiently transfected and the daily amount of soluble $Db_{\alpha EGFR}$-scTRAIL released in cell culture medium was measured by ELISA (mean ± S.E.M., n=3).

Furthermore, a nearly complete block of cell death induction was obtained after treatment with the anti-TRAIL antibody, which specifically neutralizes TRAIL. This result confirmed, consequently, that the reduction in cell viability observed after combined treatments was

strictly TRAIL dependent. Of note, Colo205 did not undergo significant apoptotic cell death upon treatment without the sensitizer bortezomib as single agent.

To further investigate the bioactivity of $Db_{\alpha EGFR}$-scTRAIL secreted by MSCs, co-culture experiments were performed. MSCs transiently transfected 24 h before (named MSC.TRAIL) were co-cultured with Colo205 cells for additional 24 hours, in the absence or presence of bortezomib. In this case, cell death was tested with Propidium iodide (PI) staining. As shown in figure 21, mixing of MSCs transiently transfected with colorectal cancer cells gave rise to a significant increase of cell death in combination with bortezomib as compared with the untransfected MSCs or with MSC.TRAIL without sensitizer, in accordance with the previous analysis. Moreover, the co-cultures seem to show induction of apoptosis in a TRAIL dose dependent manner, revealed by the fact that different ratios of MSCs and Colo205 cells (1:5 and 1:50), produced different levels of cell death. Of note, $Db_{\alpha EGFR}$-scTRAIL without the sensitizer did not show a significant cell death induction on Colo205 cells.

These data demonstrated that transiently transfected MSCs are able to secrete a bioactive $Db_{\alpha EGFR}$-scTRAIL.

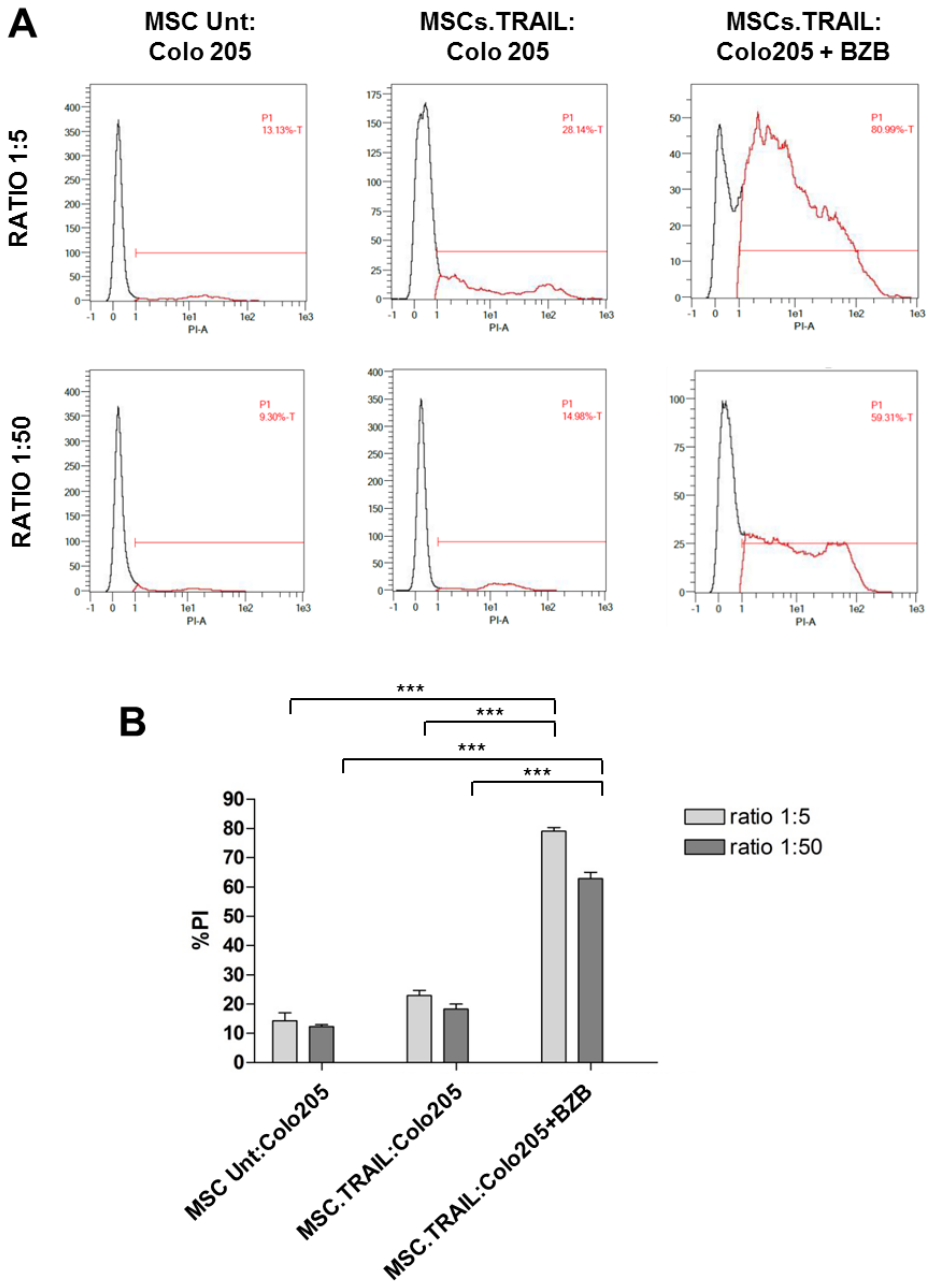


**Figure 21 Analysis of cell death induction after co-culture of Colo 205 with MSCs**
(A) One day after transient transfection MSCs (MSC.TRAIL) were co-cultured with Colo205 cells (100.000 cells) in the presence or absence of BZB (250 ng/ml) for additionally 24 h. Two different ratios of MSCs and Colo205 were tested, 1:5 and 1:50. Y axis: number of events analyzed. (B) The number of dead cells was quantified by PI staining. Colo205 alone were used as PI background signal and Colo205 treated with TritonX100 (10%) as positive cell death signal.

### 3.2.3 Establishment of stable transfected MSC lines

Based on successful transient transfection of MSCs and production of Db-scTRAIL, it was next asked whether transfection can be established for stable production of this fusion protein under retention of their normal stem cell characteristics, i.e. differentiation potential according to the environmental context, to obtain a rational for potential *in vivo* application. So far, the majority of published studies are based on viral transfection, despite all the concerns about the safety of the viral system (Grisendi et al., 2014; Stuckey and Shah 2013). In fact, only few studies had assessed non-viral transfection method for cell-based tumor treatment (Choi et al., 2011 and Hu et al., 2012), that could overcome some of the concerns related to this approach. For these reasons, in this thesis, I chose and tested a non-viral system to establish stable transfected MCS lines, expressing the antitumoral agent $Db_{\alpha EGFR}$-scTRAIL fusion protein, for colorectal cancer treatment.

First, the sensitivity of MSCs to the selection drugs Zeocin (Zeo) and Geneticin (G418), was assessed. Ten different concentrations, up to 800 µg/ml, of both antibiotics were used to treat MSCs and after 7 days the cell viability was analyzed through crystal violet assay (Fig. 22).

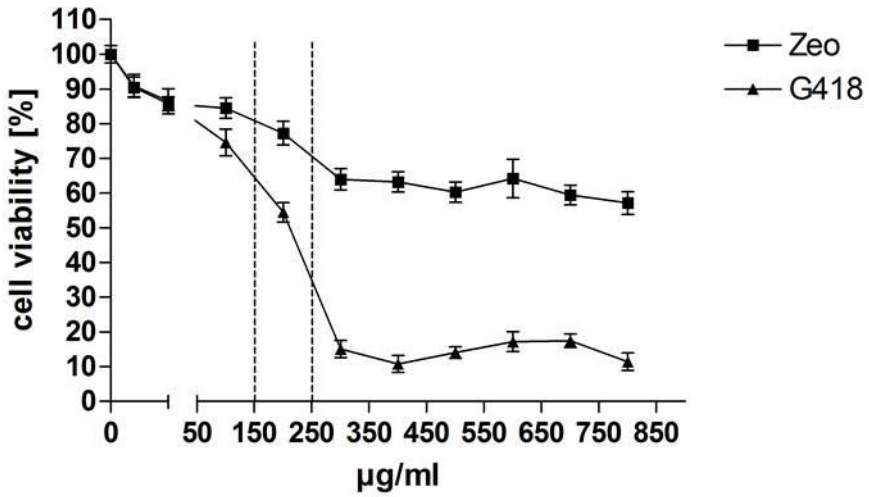


**Figure 22 Analysis of MSCs sensitivity to zeocin and geneticin**
MSCs were treated with different concentrations of Zeocin (Zeo) or Geneticin (G418). After 7 days cell density was determined using crystal violet staining and data were normalized using untreated cells as control (mean ± S.E.M., n=3).

MSCs showed nearly complete resistance to zeocin activity, only 30% of cell death was observed, even at high concentration of the antibiotic. While geneticin induced a strong reduction of cell viability, around 90%, using a range of antibiotic dose between 300 µg/ml

and 800 µg/ml. Based on these results, 150 µg/ml and 250 µg/ml were chosen as subtoxic concentrations for the selection of stable cell lines: M2#1.TRAIL and M2#2.TRAIL which were transfected with EGFR-pCR3-Db-scTRAIL and selected respectively with 150 µg/ml and 250 µg/ml of G418. In addition, the corresponding mock cell lines (Mock#1, Mock#2) were generated using the pCR3 empty vector. All the cell lines, the vectors and the antibiotic concentrations used are listed in Table 18.

| Stable cell line | Vector | Gentamicin (µg/ml) |
|---|---|---|
| M2#1.TRAIL | $Db_{\alpha EGFR}$-scTRAIL | 150 |
| M2#2.TRAIL | $Db_{\alpha EGFR}$-scTRAIL | 250 |
| Mock#1 | Empty vector | 150 |
| Mock#2 | Empty vector | 250 |

**Table 18: List of stable cell lines, vectors and antibiotic concentration used for MSC stable cell lines generation**

Next, the productivity of $Db_{\alpha EGFR}$-scTRAIL secreted by stable MSC lines was tested analyzing cell medium after 4 and 6 days of *in vitro* cultivation by TRAIL ELISA. The M2#2.TRAIL cell line revealed higher productivity as compared to M2#1.TRAIL. As expected, no specific signal was detectable for the controls M2 untransfected and Mock cell lines (Fig. 23A). Co-culture of stable MSC lines with Colo205 as target for Db–scTRAIL revealed strong reduction of cell viability only for the cell line M2#2.TRAIL in combination with the sensitizer (Fig. 23B). These results demonstrate that $Db_{\alpha EGFR}$-scTRAIL secreted by stable cell line M2#2.TRAIL, is functional and can induce cell death in Colo205 cells. While for the other cell line, M2#1.TRAIL, despite detection of fusion protein by ELISA assay, no bioactivity was revealed from the same culture supernatants. This could have been due to a lower productivity of these stable cells, in accordance with the ELISA assay.

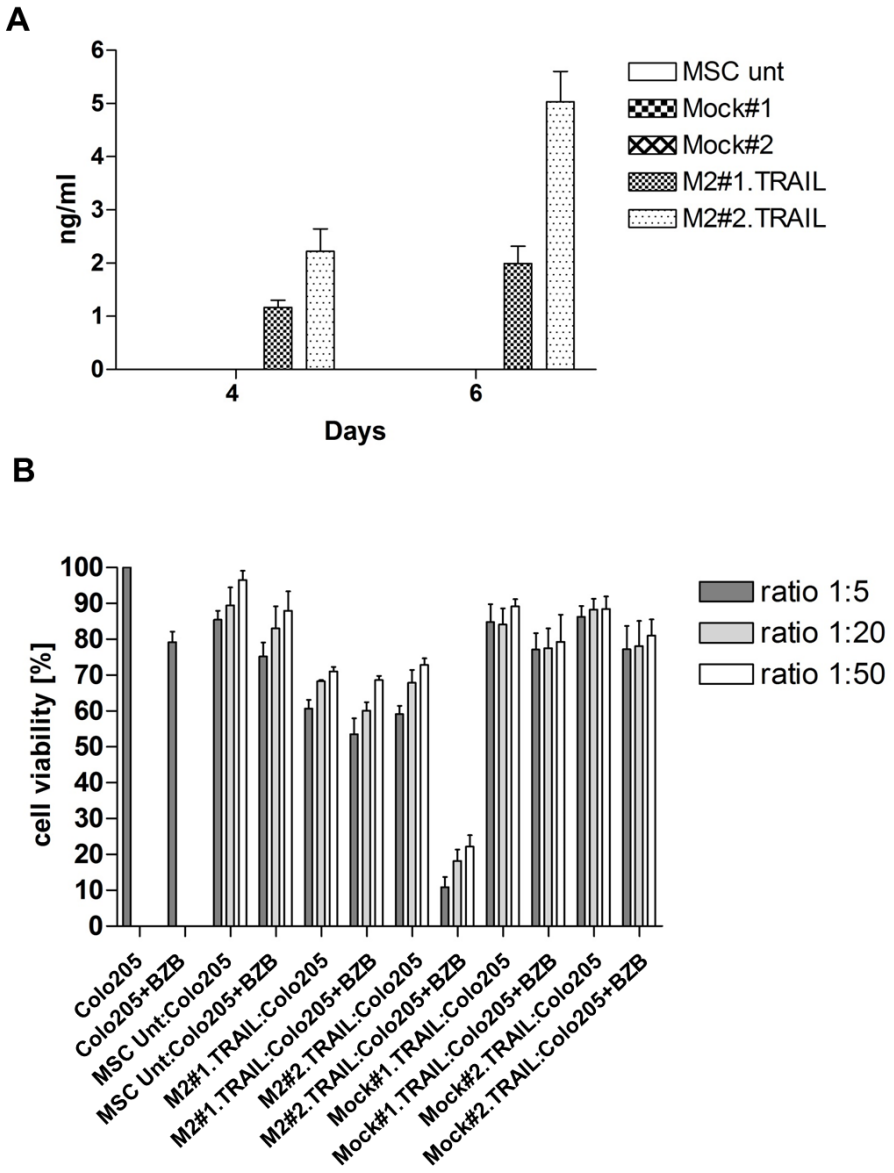


**Figure 23 Analysis of productivity and bioactivity of stable transfected MSC lines**
(A) The amount of soluble $Db_{\alpha EGFR}$-scTRAIL released in the cell culture medium, by stable transfected MSC lines (Table 18), was measured by ELISA after 4 and 6 days of culture (mean ± S.E.M., n=4). (B) The bioactivity of the secreted $Db_{\alpha EGFR}$-scTRAIL was analyzed after 24 h of co-culture seeding different ratios of MSCs and Colo205 cells (ratios 1:5; 1:20 and 1:50). The co-cultures were treated in combination with BZB (250 ng/ml). Cell density was analyzed using crystal violet staining and data were normalized using Colo205 cells treated only with BZB as control (mean ± S.E.M., n=4).

Unfortunately, after long time of *in vitro* cultivation (passage 35) even the M2#2.TRAIL cell line progressively lost $Db_{\alpha EGFR}$-scTRAIL productivity and consequently its bioactivity (data not shown). This phenomenon can be explained by the fact that the selection process has generated a mixed population of drug resistant cells, with different levels of protein secretion, resulting in a heterogeneous pool of cells within the same cell line. In this context, during *in vitro* cultivation the different sub-populations, which compose one cell line, non-producer cells may have proliferation advantages and eventually overgrow the producer cells in such a mixed population.

## 3.2.4 Selection of stable MSC single clones

Having shown that stable transfectants of Db-scTRAIL producing MSCs can, in principle, be established, in a next step, single clone selection was performed by limiting dilution in order to avoid the limitations observed using a pool of transfected cells. The method used in this study is based on limiting serial dilutions in multiwell plates, which allows growing and selection of resistant cells as single cell culture which should show equal features such as productivity.

MSCs were transfected with $Db_{\alpha EGFR}$-scTRAIL and after overnight they were immediately plated, in multiwell plate, performing limiting dilutions (2.2.4) with a statistical density of 1 cell/well (six 96-well plates). After 41 days of cultivation cell confluence of positive wells was around 70%. At this time point, secretion of the proteins into the culture medium was checked and protein concentration estimated semi-quantitatively through dot blot assay, as show in figure 24.

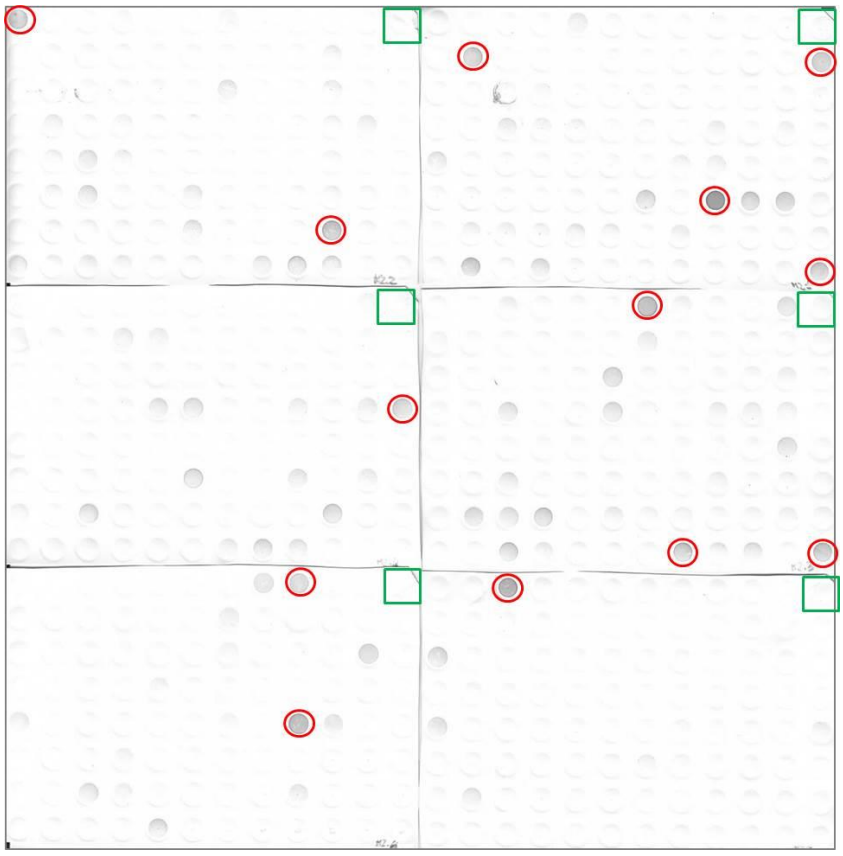

**Fig 24 Dot blot analysis of MSC single cell cultures**
After 41 days of single cell cultivation, culture medium from each well was analyzed by dot blot using a specific antibody against FLAG and 13 single clones were selected (red circles). The pool M2#2.TRAIL cell line was used as control (green squares).

According to the dot blot results thirteen single cell cultures, which showed the highest $Db_{\alpha EGFR}$-scTRAIL expression, were selected and expanded *in vitro*. Next, product concentration was quantitatively analyzed by ELISA after 3 days of cultivation, seeding the same number of cells (Fig. 25A). Surprisingly, only two of thirteen single clone cultures selected showed enhanced levels of proteins in comparison with untransfected cells and with the pool M2#2.TRAIL. The productivity of both best clones, named clone#A1 and clone#B12, was confirmed also by immunoblotting analyzing the purified TRAIL protein from culture medium (Fig. 25B). Additionally, the cell proliferation rates were tested showing comparable levels between the two clones and the untransfected or Mock cell lines during *in vitro* cultivation (Supplementary figure S3).

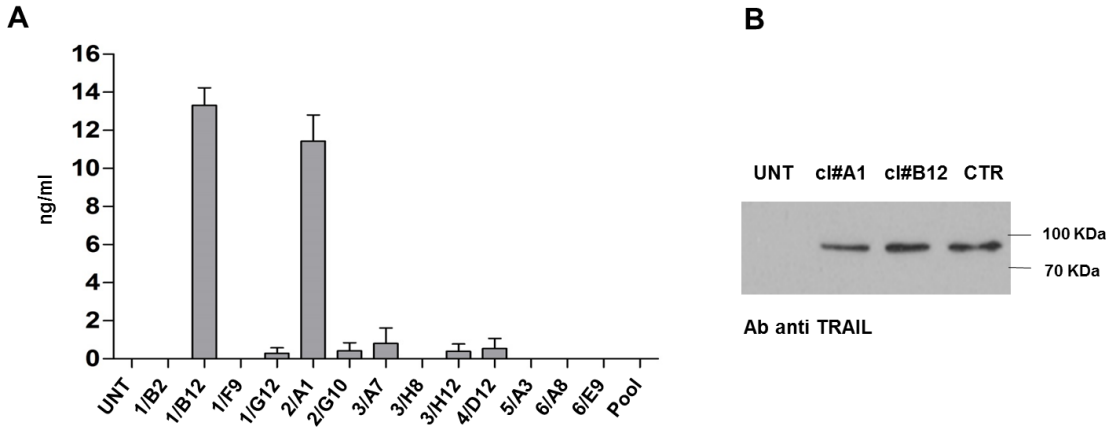


**Figure 25 Single clones selection**
(A) The 13 clones selected after the Dot Blot analysis were seeded ($1x10^6$ cells) and cultured. After 3 days the amount of soluble $Db_{\alpha EGFR}$-scTRAIL released in culture media was measured by ELISA. MSCs untransfected (UNT) and the pool M2#2.TRAIL were used as controls (mean ± S.E.M., n=3). (B) After 5 days of cultivation $Db_{\alpha EGFR}$-scTRAIL secreted in cell media was purified and analyzed by western blotting for each cell line using an anti TRAIL antibody. 3µg of purified $Db_{\alpha EGFR}$-scTRAIL (CTR) was used as control.

A possible reason to explain the discrepancy between the dot blot data, which revealed 13 positives clones, and the ELISA assay is that in the first analysis signals detected were not adjusted to the cell number in each well. In fact, the dot blot was performed from supernatant directly after 41 days of cultivation. While, for the ELISA assay each cell line was plated using the same number of cells and the culture medium was collected and tested after 3 days.

All further experiments were done using the two positive clones selected: clone#A1 and clone#B12. Both showed a cumulative secretion of $Db_{\alpha EGFR}$-scTRAIL up to 5 days of cultivation (Fig. 26A) which was maintained over time *in vitro*, even at late passages (p 44) (data not shown). Next, the bioactivity of proteins secreted by the clones was investigated performing co-culture of Colo205 cells with clone#A1 or clone#B12 in

combination with bortezomib and/or anti-TRAIL antibody. After 24 h cell number was analyzed by crystal violet assay showing, for both clones, a strong reduction in combination with bortezomib (Fig. 26B). Similar results were obtained with pool M2#2.TRAIL cell line. Moreover in the presence of neutralizing TRAIL antibody a nearly complete rescue of cell number was observed. This confirmed that the reduction of cell viability on colon cancer cells is due to a specific TRAIL effect.

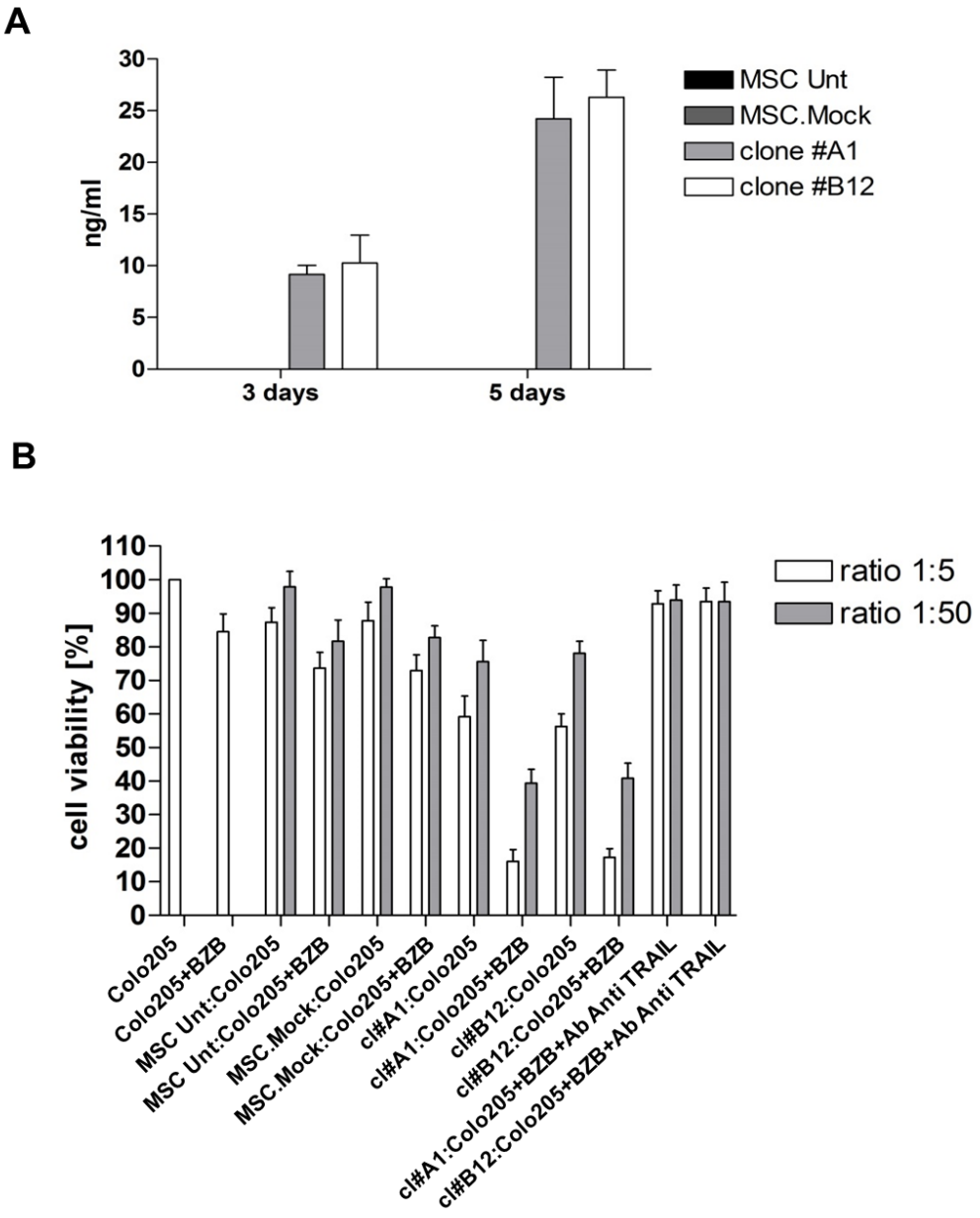


**Figure 26 Analysis of productivity and bioactivity of MSC single clones #A1 and #B12**
(A) The amount of soluble $Db_{\alpha EGFR}$-scTRAIL released in the culture medium, by stable transfected MSC cell line (MSC.Mock, clon#A1, clone #B12) and MSC untransfected (MSC unt), was measured by ELISA after 3 and 5 days of culture (mean ± S.E.M., n=5). (B) The bioactivity of the secreted $Db_{\alpha EGFR}$-scTRAIL by clones was tested after 24 h of co-culture of MSC lines and Colo205 (ratios 1:5 and 1:50). The co-cultures were treated in combination with BZB (250 ng/ml) and or Antibody anti-TRAIL (Ab anti TRAIL; 1 µg/ml). Cell density was analyzed using crystal violet staining and data were normalized using Colo205 cells treated with BZB as control (mean ± S.E.M., n=3).

All the results concerning $Db_{\alpha EGFR}$-scTRAIL bioactivity were obtained performing standard cytotoxicity assays on Colo205 cells, using crystal violet staining as a read-out. In order to confirm that the observed reduction of cell number is due to an apoptotic process, cleaved caspase 3 levels were analyzed as a direct indicator of activation of apoptosis. In particular, a co-culture was performed using a double chamber system with a membrane allowing free exchange of soluble mediators. Colo205 cells were seeded in the bottom chamber and the $Db_{\alpha EGFR}$-scTRAIL producing clones #A1, #B12 or the Mock cells were seeded in the upper chamber. Cleaved caspase 3 levels in Colo205 cells were analyzed by flow cytometry after 18 h of co-culture. A strong increase of cleaved caspase 3 levels were found when Colo205 cells were exposed to either of the $Db_{\alpha EGFR}$-scTRAIL producing clones in combination with the sensitizer BZB, with mock transfected MSC serving as negative control. A weak signal was also noted upon incubation of Colo205 with sensitizer bortezomib only (Fig. 27). These data demonstrate that the strong reduction of cell number observed in the previous analyses is a specific effect of apoptotic pathway activation, induced by $Db_{\alpha EGFR}$-scTRAIL activity, in combination with BZB.

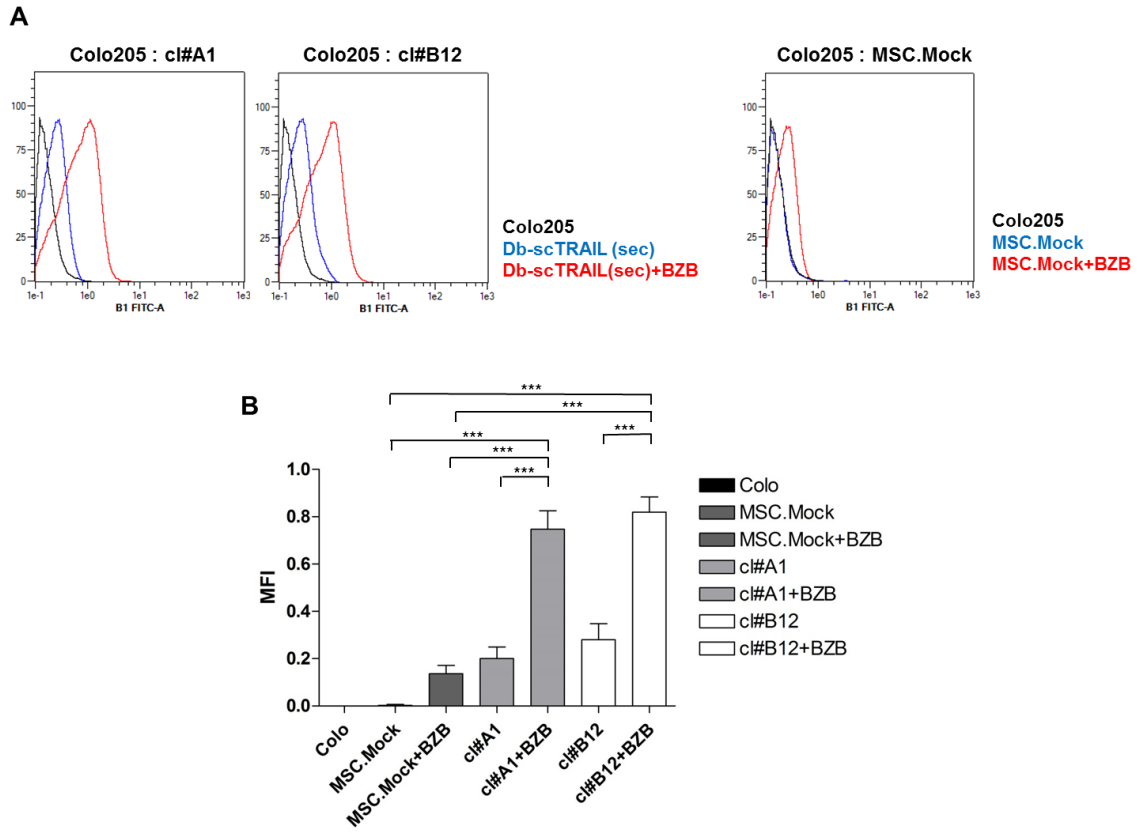


**Figure 27 Analysis of caspase 3 activation after co-culture of Colo 205 with MSC clones**
Colo205 cells were seeded in the lower chamber of a transwell (20.000 cells). After overnight cultivation the stable clones #A1, #B12 and the Mock cells were seeded in the upper chamber (80.000 cells) and BZB (250 ng/ml) was added to the medium. After 18 h of treatment, Colo205 were collected, stained with the specific cleaved caspase 3 antibody (Asp 175) and analyzed by flow cytometry. (A) Y axis: number of events analyzed. (Db-scTRAIL sec: fusion protein secreted by MSCs) (mean ± S.E.M., n=4).

Next, the potential tumor homing ability of wild type and stably transfected MSCs was investigated performing *in vitro* migration assays as a surrogate indicator of directed migration. Even if the factors that mediate this process have yet to be completely clarified, several soluble factors have been reported to exert chemotactic effects on MSCs, including EGF and insulin-like growth factor 1 (IGF-1) (Ponte et al., 2007). In the present work, the ability of these two growth factors to promote MSCs migration was tested. As shown in figure 28, both growth factors induced a significant increase in cell migration in comparison with normal culture medium (Alpha-MEM + 0,5% FBS). Interestingly, both EGF and IGF-1 induced comparable effects in cell motility on untransfected MSC and all the stably transfected cell lines analyzed: clone #A1, clone#B12 and Mock. These results indicated that the stable transfection and the selection of these cells did not interfere with their migration ability, confirming their applicability as drug delivery system. In addition, instead of adding chemotactic factors, Colo205 cells were placed into the bottom wells, but no MSCs migration could be observed under these conditions, suggesting that Colo205 possibly lack production/secretion of suitable chemotactic factors for these MSC lines.

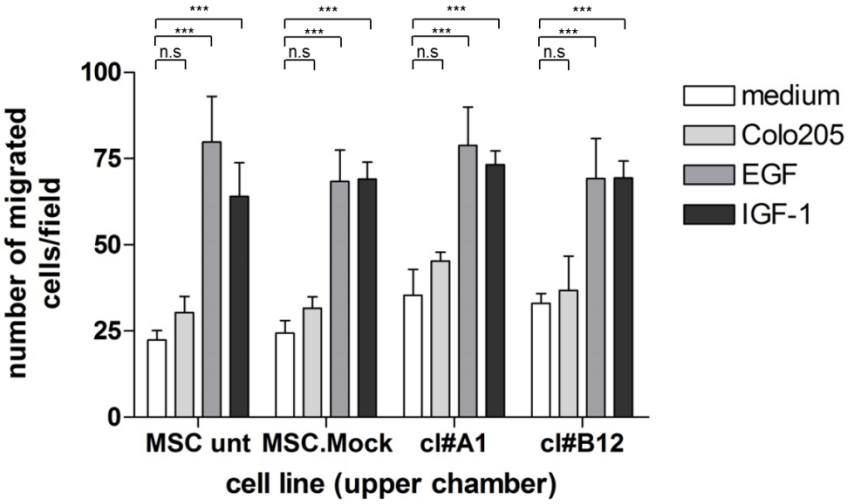


**Figure 28 Analysis of MSC's migration ability**
MSCs untransfected, clone #A1, clone #B12 and Mock cells were seeded (15.000 cells) in medium containing 0,5% FBS into the upper chamber of a transwell. The lower well contained: only medium (0,5% FBS); Colo 205 (80.000 cells) or the following concentrations of soluble growth factors: EGF (30 ng/ml) and IGF-1 (30 ng/ml). Cells that had migrated across the filter after 8 hours were fixed and stained. The number of migrated cells was determined by counting five independent microscopic fields (20-fold magnification) per filter. Data showed the mean of six independent experiments performed with duplicate filters (mean ± S.E.M., n=6).

In summary, these *in vitro* data demonstrate that the established MSC clone derived cell lines are able to maintain over time during cultivation (up to passage 42) the production of the therapeutic protein, which exerts *in vitro* strong apoptotic activity on colon cancer cells in combination with BZB.

### 3.2.5 Characterization of MSC stable clones

In order to investigate whether the stable clones selected maintain mesenchymal stem cell characteristics over time *in vitro*, the properties of these cells were analyzed at different passages. First of all the phenotype of MSCs lines was tested staining the cells with phalloidin to visualize the F-actin. All cell lines analyzed by fluorescence microscopy: MSCs untransfected, clone #A1, clone #B12 and Mock, displayed a typical spindle-shaped phenotype as described for MSCs in literature (Dominici et al., 2006). Remarkably, the phenotype did not change during *in vitro* cultivation up to passage 42 (Fig. 29).

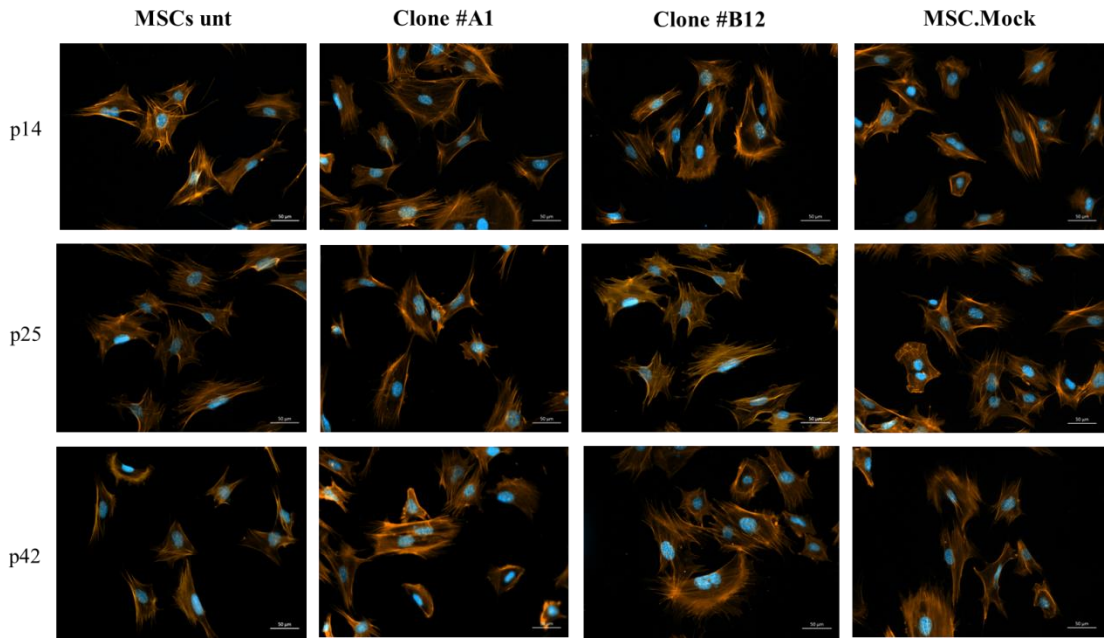


**Figure 29 Phenotype of mesenchymal stem cell lines**
Mesenchymal phenotype for MSCs untransfected (MSCs unt), single clone #A1 (clone #A1), single clone #B12 (clone #B12) and Mock (MSC.Mock) was analyzed at early (p 14), middle (p 25), and late (p 42) passages. Cells were stained with Alexa Fluor568-coupled phalloidin (red/orange). The nuclei were counterstained with DAPI (blue). Scale bar, 50 µm.

Next, the expression of stem cell markers was investigated for all cell lines. In accordance with the International Society of Cellular Therapy (ISCT), all MSC lines analyzed were positive for CD9, CD44, CD71 and CD105 and lack the expression of CD14 and CD34, as show in figure 30. No differences between untransfected MSCs and the stably transfected cell lines were observed. Interestingly, the pattern of marker expression, including CD9, CD44, CD71 and CD105, was maintained from early passage (p 9) up to passage 42

(Supplementary figure S4). Additionally, these results obtained here with MSCs transfected with Db-scTRAIL are in accordance with other studies which described most of the markers also expressed by different murine MSCs lines (reviewed by Boxall and Jones 2012).

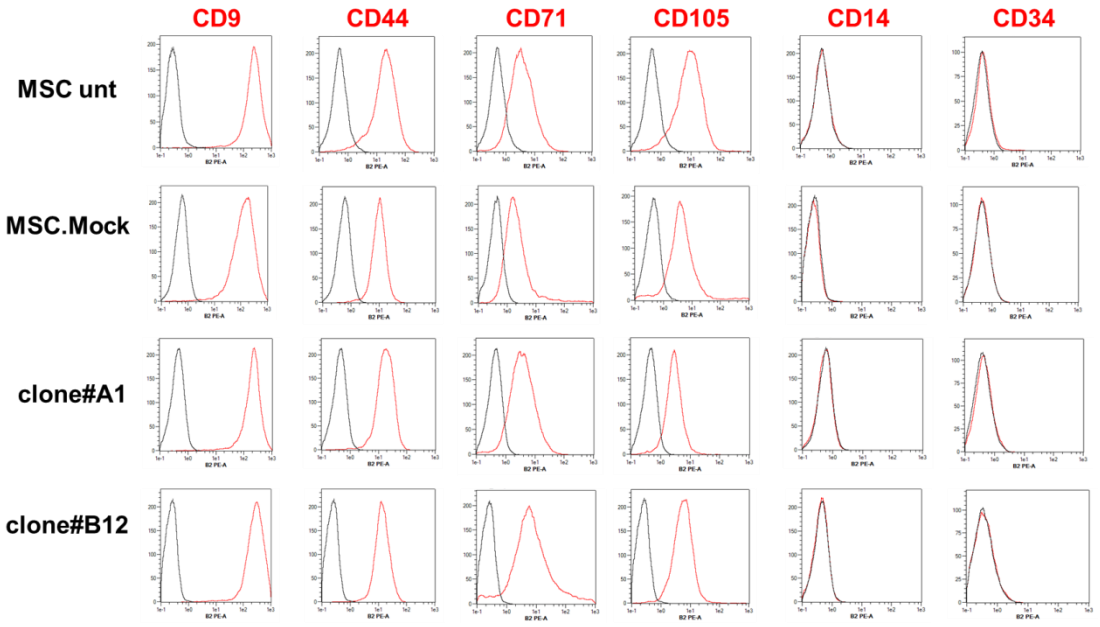


**Figure 30 Surface MSCs marker expression**
Analysis of surface markers expression: CD9, CD44, CD71, CD105, CD14 and CD34 on MSC lines at passage 25. Cells were stained with indicate antibodies and binding was analyzed by flow cytometry (red line). Unstained cells were used as negative control (black line). Y axis: number of events analyzed. Representative experiment out of 5 independent experiments performed.

Nevertheless, the most important characteristic necessary to define MSCs is their multilineage differentiation capability. Towards this end, I verified by the standard differentiation assays their ability to differentiate into adipocytes and osteocytes. All MSCs lines showed, on one hand, the capability to generate lipid droplets which indicate a successful adipogenic differentiation (Fig. 31A). In rare cases a spontaneous adipogenic differentiation was observed, probably due to a high cell density in the differentiation cultures, without a statistically significant frequency. On the other hand, the same cell lines were also able to display mineralization, observed by Alizarin red staining, confirming osteogenic differentiation ability (Fig. 31B). The same results were observed at late passages for all cell lines (data not shown).

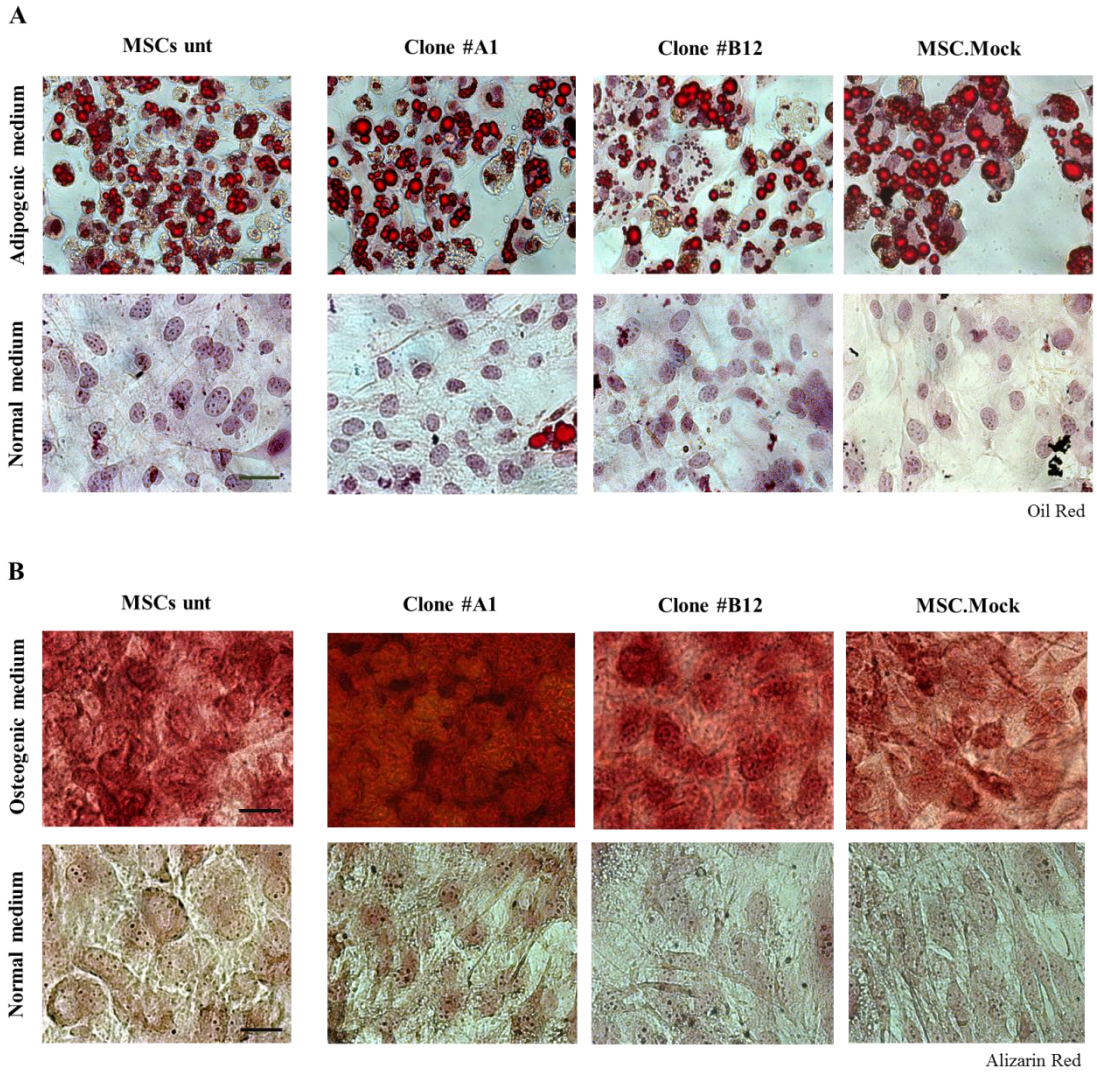


**Figure 31 Multipotency differentiation ability of MSCs**
MSCs untransfected (MSCs unt), clone #A1, clone #B12 and Mock (MSC.Mock) were cultured *in vitro* in (A) adipogenic or (B) osteogenic media, at passage 22. The cells were fixed and stained with Oil Red O (adipogenesis) or Alizarin Red (osteogenesis) for adipocyte or osteoblast differentiation. Cells cultured in normal medium were use as control. Scale bars = 50 µm (adipogenesis) and 100 µm (osteogenesis).

Taken together these data demonstrate that the stable transfection with the selective pressure of the antibiotic G418, and the constitutive Db-scTRAIL secretion do not alter the typical phenotype, the specific markers expression and the multipotency ability of MSCs, even during long-term *in vitro* culture. Consequently, this confirms the advantages and safety of this novel cell based therapeutic approach for tumor treatment.

### 3.2.6 *In vivo* studies: MSC.TRAIL administration for tumor treatment

After completion of the *in vitro* characterization of MSCs.TRAIL clones #A1 and #B12, both were used for *in vivo* studies to assess their potential therapeutic activity. First, MSCs were subcutaneously (s.c.; $4x10^6$ cells) or intravenously (i.v.; $1x10^6$ cells) injected in nude mice, using 4 mice for each group (clone #A1, clone #B12, MSC untransfected, Mock and PBS). The blood was collected from the tail vain after 1, 3, 7, 14 and 21 days and the serum fraction was used in order to test the presence of Db-scTRAIL by ELISA (Fig. 32).

In the intravenous administration approach for both MSC.TRAIL clones, #A1 and #B12, for all the time points analyzed, no fusion protein could be detected in the serum, (data not shown). This negative result probably relates to a technical issue, due to the small number of cells that have been applied using i.v administration. Concerning the subcutaneous administration no TRAIL signals were revealed in the serum after 1 and 3 days whereas after 7 and 14 days fusion protein was detected in the range of 1,5 ng/ml for clone #B12. Surprisingly, despite comparable *in vitro* productivity, s.c. injection of clone #A1 did not result in detectable Db-scTRAIL levels. Whether this was a failure of engraftment or due to others reasons remained unresolved. As expected, all control cell injections gave no positive signal in ELISA. Based on these data clone #B12 was chosen for further *in vivo* experiments.

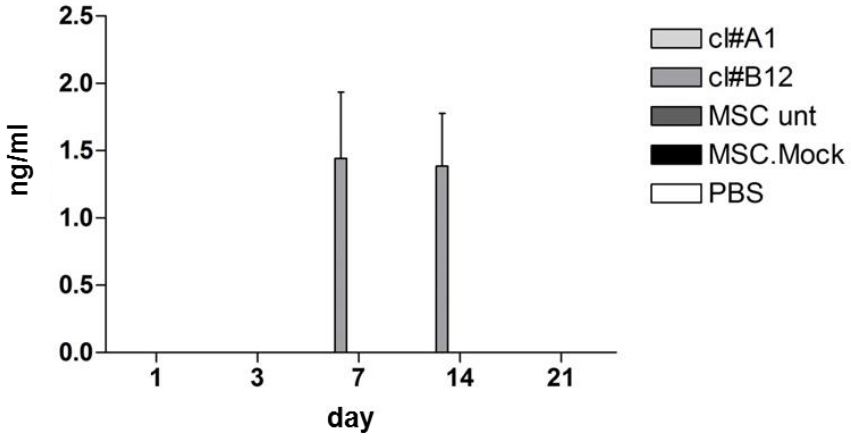


**Figure 32 Analysis of Db-scTRAIL production from MSC clones #A1 and #B12 s.c. injected *in vivo***
MSCs untransfected, clone #A1, clone #B12, MSC.Mock cells ($4x10^6$) were subcutaneously injected in one flank of a nude mouse (n=4 animals for each group, ± 95% CI) or 100 µl of PBS (s.c.) as control. After 1, 3, 7, 14 and 21 days serum concentration of Db-scTRAIL was analyzed by ELISA assay. The groups: clone#A1, MSC unt, MSC.Mock and PBS did not revealed detectable protein levels.

Given the detected Db-scTRAIL concentration in the serum (1,5 ng/ml), and assuming 2 ml as total blood volume in mouse, as reported by Schmidt and Wittrup (Schmidt and Wittrup, 2009), the estimation of total amount of protein in the circulatory system is approximately 3 ng, which corresponds to 32,26 nM. Comparing this result with the $EC_{50}$ values of Db-scTRAIL alone or in combination with BZB obtained *in vitro* on Colo205 cells, respectively 0,019 nM and 0,0022 nM (Fig. 17), the amount of protein in the blood is higher than the range necessary to observe an efficient bioactivity of Db-scTRAIL.

Next, the antitumor activity of clone #B12, in xenograft tumor model, in which #B12 cells were peritumorally (p.t.) injected, was investigated. Figure 33 shows the experimental settings and the different groups of treatments tested. In particular, 4 nude mice for each group were subcutaneously injected with 3 million Colo205 tumor cells at both dorsal sides. The treatments started 10 days post tumor cell inoculation, when tumors were palpable and vascularized, reaching a volume of approximately 100 $mm^3$. At this time point the first MSCs #B12 injection ($4x10^6$ cells in 100µl PBS, single injection) was performed. Mock cells and PBS served as control. In the combination treatment groups (see figure 33, groups 2 and 4), 5 µg of BZB were intraperitoneally (i.p.) co-injected every other day during the entire period of treatments. The second and the third MSCs injections were performed, as described above, after 17 and 27 days respectively. Tumor growth was monitored as described (Schneider at al., 2010 and Kim et al., 2011) every 2 or 3 days.

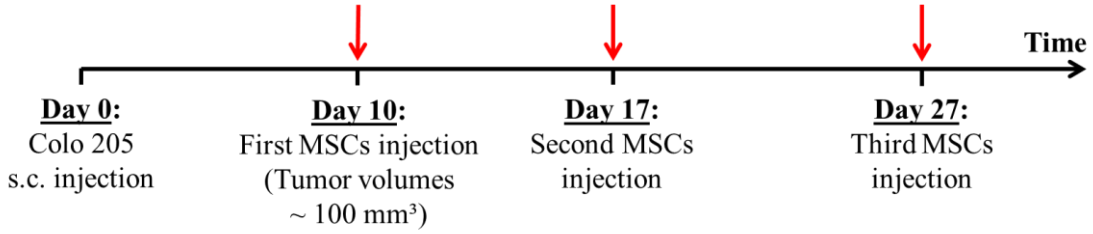


| Groups | Treatments |
|---|---|
| 1) PBS | 100 µl (p.t.) |
| 2) MSC.Mock + BZB | $4x10^6$ cells (p.t.) + 5µg BZB (i.p.) |
| 3) MSC.TRAIL | $4x10^6$ cells (p.t.) |
| 4) MSC.TRAIL + BZB | $4x10^6$ cells (p.t.) + 5µg BZB (i.p.) |

**Figure 33 Scheme of MSC administration for tumor treatment *in vivo***
NMRI nu/nu mice, 9 weeks old, were injected subcutaneously (s.c.) with $3x10^6$ Colo205 cells in 100 µl PBS at left and right dorsal sides. Treatments started 10 days after tumor cell inoculation when tumors reached ~ 100 $mm^3$. Mice received 3 injections of MSCs ($4X10^6$ cells/injection p.t., red arrows), at the indicated time points. After the first MSCs injection mice from groups 2 and 4 received 5 µg Bortezomib (BZB) in 100 µl PBS intraperitoneally (i.p.), every second day.

Up to 2 weeks after the first MSCs injection no differences were observed in tumor growth between the 4 treatment groups. However, from day 17 on, coincident with the second MSCs administration, a slight but increasingly significant reduction of tumor size was observed for the combination treatment group clone#B12 plus BZB, up to day 26 (Fig. 34A). At this time, $Db_{\alpha EGFR}$-scTRAIL was detectable in serum of both animal groups receiving #B12 cells (Fig 35A; 1,5 ng/ml). The second MSC injection was more efficient, probably, due to a cumulative effect with the first one. In fact, this is in accordance with the previous ELISA results *in vivo*, without established tumor (Fig. 32), where serum Db-scTRAIL levels were detectable only 7 and 14 days after s.c. injection.

Next, a third MSCs administration was performed and even if it did not produce a complete remission of tumors, it induced a stronger and more significant tumor size reduction for the group clone#B12 + BZB (Fig. 34B; $p<0,001$; day 31). The combination group Mock + BZB did not significantly interfere with the tumor growth (Fig. 34B), nor did monotherapy with bortezomib at the used dosage as reported by Siegemund et al., 2012.

Of note, mice treated with clone#B12 in the absence of sensitizer BZB did not show any significant antitumoral effect, corroborating the *in vitro* data. This indicates that in the tested experimental conditions *in vitro* and *in vivo* the dosage of Db-scTRAIL secreted by MSCs, is apparently not sufficient to induce a significant antitumoral effect on its own, but is highly active in the presence of the apoptosis sensitizer bortezomib.

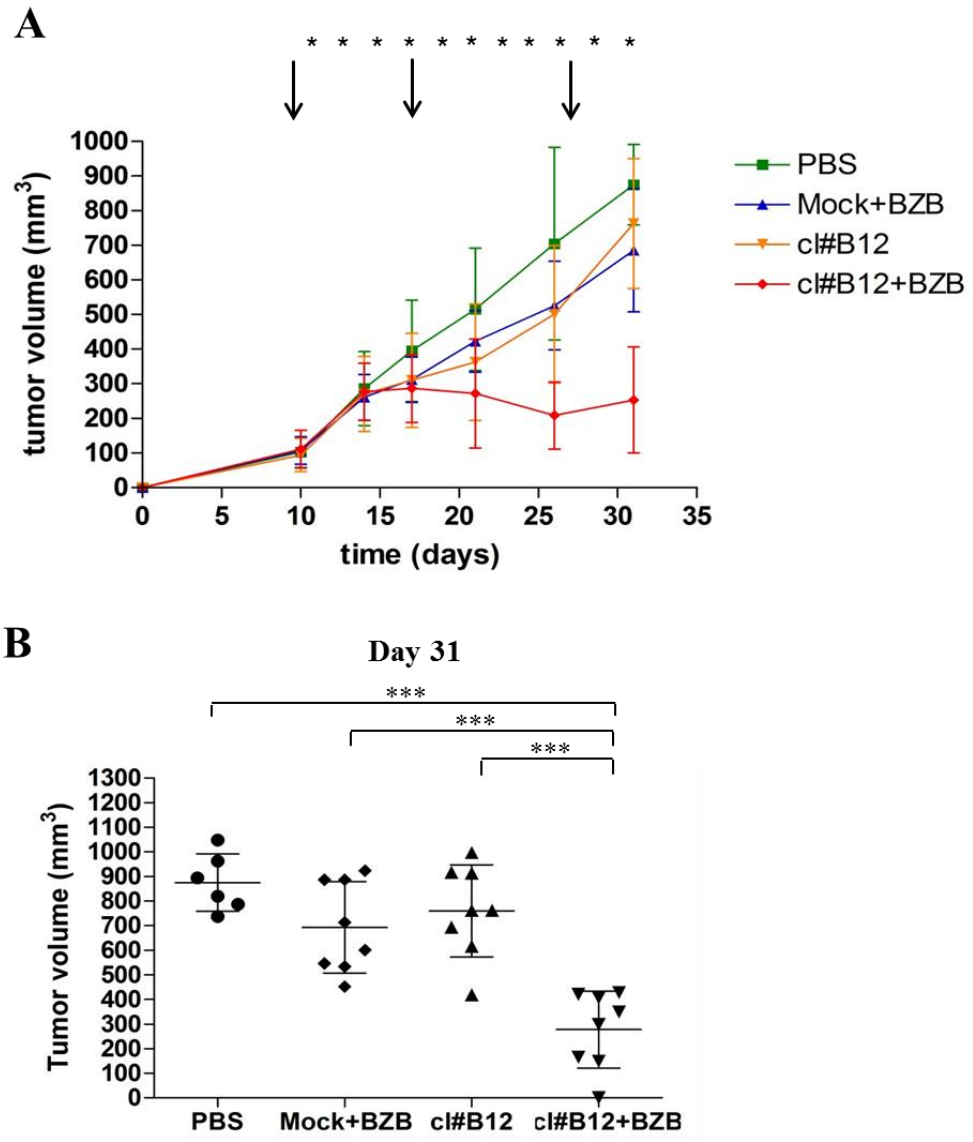


**Figure 34 Antitumoral activity of MSC clone #B12 cells in a Colo205 xenograft tumor model**
(A) Tumor volume was analyzed as a function of time after p.t. injection of: PBS (green line), Mock+BZB (blue line), clone #B12 (orange line) or clone #B12+BZB (red line). Arrows, MSCs p.t. administration; asterisks, Bortezomib application; symbols, mean of tumor volumes ± 95% confidence interval (CI), n=8 tumors/treatment group. (B) Individual tumor volumes at day 31 (n= 6 tumors for PBS group and n=8 tumors for Mock+BZB, cl#B12 and cl#B12+BZB). Bars, mean of tumor volumes ± 95% CI.

Furthermore, in order to get insights into potential off-target, systemic side effects of continuous $Db_{\alpha EGFR}$-scTRAIL expression in tumor bearing animal, liver enzyme values in blood were determined, too, as an established indicator of liver toxicity. Toward this end, serum alanine aminotransaminase (ALT) levels were assayed in tumor bearing mice at day 31, after three MSCs p.t injections (Fig. 34B). The analysis showed for all groups mean serum ALT activities under the baseline (50 U/L), resembling the physiologic level in men (Fig. 35B). Accordingly, this result revealed that MSCs administrations did not induce discernable hepatotoxic effects *in vivo*, in accordance with a recent study from Yan and

colleagues (Yan et al., 2016). Additionally, all the other standard parameters, such as body weight, remained in the normal ranges for the entire period of treatment (data not shown).

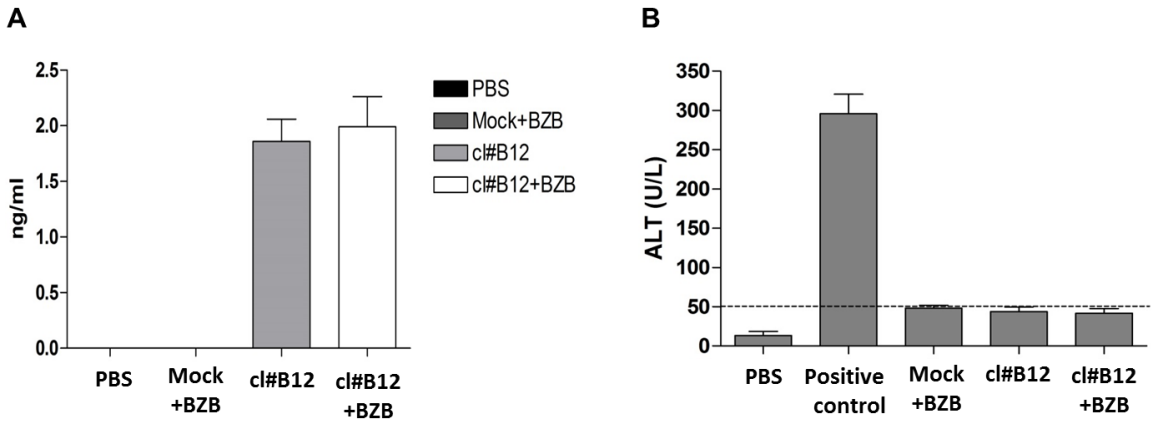


**Figure 35 *In vivo* tolerance of MSCs administration**
(A) $Db_{\alpha EGFR}$-scTRAIL mouse serum levels were analyzed at day 26 by ELISA assay (mean ± S.E.M., n=3). (B) Alanine aminotransaminase (ALT) activity was analyzed in mouse serum, at day 31, after 3 MSCs p.t. injections (mean ± S.E.M., n=3). Positive control, 0.1 nmol Fas ligand fusion protein; negative control, PBS; dotted line, upper normal level (50 U/L).

Finally, the overall survival for each group was followed for up to 52 days. As shown in figure 36, the mice in the control group (PBS) could not survive over 33 days due to fast tumor growth necessitating sacrification when tumor volume reached ~ 1100 $mm^3$. The other two control groups, clone#B12 and MSC.Mock+BZB, showed a survival rate at day 52 of ~50% and ~60%, respectively, indicative of a partial response to each of the drugs when given as monotherapy. In accordance with the direct determination of tumor size at day 31, a higher survival rate of around 80% was observed for the group with the combination treatment clone#B12, secreting Db-scTRAIL, and BZB.

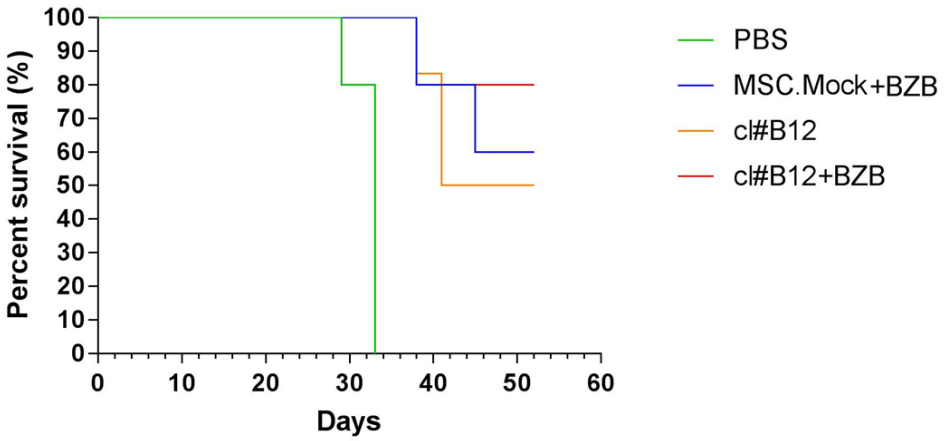


**Figure 36 Analysis of survival rate after MSCs administration**
Analysis of survival rate for all groups of treatment was conducted using a log-rank test based on Kaplan-Meier method. Mice were sacrificed when tumor volume reached ~ 1100 $mm^3$.

In conclusion, together these results demonstrate that stable transfection of MSCs, with $Db_{\alpha EGFR}$-scTRAIL, using a non-viral method is an efficient cell delivery system for anti cancer proteins both *in vitro* and *in vivo*. In particular, multiple injections of MSCs in mouse model did not show hepatotoxic or general side effects, but a significant tumor reduction in combination with bortezomib. Together, the *in vivo* analysis provides proof of concept that *in situ* expression of a tumor targeted TRAIL variant by locally administered stable MSC transfectants is a safe and effective means of combating tumor growth.

# 4. Discussion

Stem cells have generated a great deal of interest, since their first identification in 1963 by McCulloch and Till (Becker et al., 1963 and Siminovitch et al., 1963) due to their unique properties such as multi lineage differentiation potential and immunomodulation ability. The discovery of cancer stem cells (CSCs) (De Maria et al., 2007), which derived from normal SCs after genetic and epigenetic mutations, opened new sceneries in the field of tumor therapy. In fact, several studies have suggested that CSCs are responsible for: tumor initiation, metastasis formation and tumor recurrence after treatment (Todaro et al., 2010). The failure of canonic and standard cancer therapies is attributed to CSCs, which represent only a small fraction of the tumor cell population. Consequently, identification and targeting of these cells, within the tumor mass, is crucial to improve outcomes of current tumor treatments.

Toward this end, in the first part of this study I generated new scFv-scTRAIL fusion proteins targeting CD133 and LGR5, which represent two of the most promising colon CSC markers (Ricci-Vitiani et al., 2007 and Barker et al., 2008). On the other hand, adult stem cells, like MSCs, can be isolated from different sources in the human body such as bone marrow, umbilical cord or adipose tissue (Kern et al., 2006) and applied for clinical treatments. Although, in regenerative and transfusion medicine MSCs are already used and accepted for therapeutic approaches (Lazarus et al., 1995 and Horwitz et al., 1999), additional applications such as in cancer treatment are currently exploited, in part as cell based carrier systems for local expression of peptide or protein therapeutics (reviewed by Stuckey and Shah, 2014). Typically, expression of the therapeutic is upon viral transduction and under control of strong viral promoters (Yu et al., 2013 and Grisendi et al., 2015), which has raised safety concerns. For this reason, in the second part of this work I established a MSC line with non-viral transfection method displaying stable expression of a highly bioactive EGFR targeting Db-scTRAIL fusion protein ($Db_{\alpha EGFR}$-scTRAIL). This cell line showed potent apoptotic induction *in vitro* and retained its mesenchymal characteristics. Furthermore, in xenotransplantation mouse tumor models I could demonstrate a significant antitumoral activity of $Db_{\alpha EGFR}$-scTRAIL produced by MSC, in combination with Bortezomib, when transplanted into the vicinity of established, vascularized tumors. Finally, I showed that the MSCs administration is a safe procedure confirmed by the absence of hepatotoxic effects in the animals.

## 4.1 Db-scTRAIL fusion proteins targeting CSC markers

In oncology TRAIL-based therapies were extensively studied, in clinical trials in a broad range of different tumors, yielding very disappointing results (reviewed by Lemke et al., 2014). There are three major critical aspects that were investigated in order to improve the therapeutic benefits of these therapies. The first one is based on the low *in vivo* bioactivity observed for recombinant TRAIL molecules and their short plasma half-lives (Herbst et al., 2010 and Soria et al., 2010). In order to overcome this limitation, the proapoptotic ligands were engineered to exert stronger antitumor activity by creation of single-chain molecules (Krippner-Heidenreich et al., 2008). The second one is the intrinsic or acquired resistance to TRAIL activity observed in several tumor cell lines (Maksimovic-Ivanic et al., 2012). This obstacle can be overcome by combined therapy based on the sensitization of the tumor cells to TRAIL function by different reagents. The list of TRAIL sensitizers, which showed a significant increase of apoptosis induction, includes the proteasome inhibitor bortezomib (de Wilt et al., 2013) and the small molecule Smac mimetic which mimic the XIAP binding site (Fakler et al., 2009 and Lecis et al., 2010). The last critical aspect that has to be considered to improve the TRAIL anticancer effects, is an active targeted delivery of this proapoptotic protein to the tumor cells, resulting in enhanced local concentration and reduced dilution of the protein in circulation. In fact, several studies reported that TRAIL protein can be engineered to induce a stronger antitumoral activity, *in vitro* and *in vivo*, by targeting specific cell surface-expressed tumor antigens (Seifert et al., 2014 and Siegemund et al., 2016).

Based on these concepts and on the new findings concerning the key role plays by CSCs in tumorigenesis and cancer resistance, I generated two Db-scTRAIL fusion proteins exhibiting target antigen binding domains (scFv) for the cancer stem cell markers CD133 and LGR5 (#$Db_{\alpha CD133}$-scTRAIL and #$Db_{\alpha LGR5}$-scTRAIL). Even if a unique colon cancer stem cell marker is not yet available, CD133 and LGR5 seem to be the most promising candidates to specifically identify CSCs within the tumor as reported by Catalano et al., 2012 and Barker et al., 2013. In particular, CD133 is broadly expressed in colon cancer cells lines as I confirmed by flow cytometry analyses, showing a significant high expression of the marker on 3/4 colon cancer cell lines tested. However, LGR5 expression was detected only in 1/4 cell lines. This difference is probably due to the fact that the expression of LGR5 is restricted only at the base of the intestinal crypts and not in the entire tissue as reported by Barker and colleagues (Barker et al., 2007).
For both fusion proteins a dimeric scTRAIL configuration was designed and achieved, as demonstrated by the size exclusion chromatography. Furthermore, the binding of the

TRAIL fusion proteins to the respective target antigens were tested and confirmed via flow cytometry. In fact, the analysis revealed, for both proteins, a concentration of half-maximum binding ($EC_{50}$) in the pM range. These results are in accordance with other studies which showed a specific CSCs identification using new antibodies targeting either CD133 or LGR5 (Kemper et al., 2012 and Kwiatkowska-Borowczyk et al., 2015).
Additionally, the functional bioactivity of $Db_{\alpha CD133}$-scTRAIL and $Db_{\alpha LGR5}$-scTRAIL in cell death induction was analyzed and confirmed for both proteins. Interestingly, in accordance with previous investigations on colorectal cancer treatments (Siegemund et al., 2012 and Möller et al., 2014), the Db-scTRAIL activity was even more potent in combination with the respective sensitizers (bortezomib and Smac mimetic), resulting in a ~4 fold increase of cell death induction for both fusion proteins.

The targeting antigen effect on apoptosis induction for $Db_{\alpha CD133}$-scTRAIL and $Db_{\alpha LGR5}$-scTRAIL was investigated. Previous studies reported a significant superior bioactivity, both *in vitro* and *in vivo*, for fusion proteins comprising a targeting scFv fragment and scTRAIL domains in comparison with nontargeted TRAIL proteins (Seifert et al., 2014 and Siegemund et al., 2016). This is probably due to the fact that tumor-targeted TRAIL fusion proteins can mimic the natural membrane-bound form of the ligand, allowing the activation of both TRAIL receptors (DR4, DR5) (Bremer et al., 2005 and Schneider et al., 2010). Nevertheless, in this work, a significant increase of TRAIL-mediated apoptosis induction for #$Db_{\alpha CD133}$-scTRAIL and #$Db_{\alpha LGR5}$-scTRAIL in comparison with nontargeted scTRAIL protein was not observed.
This result might be due to two different reasons. The first one is only a moderate affinity of the scFv to the specific target and the second one could be the low antigen expression on the analyzed tumor cell lines. This latter, in particular, was observed for the marker LGR5. Recently, Garg and colleges reported that nontargeted TRAIL fusion protein, compare to targeting TRAIL, showed a much higher cell death induction on tumor cells that lack the antigen expression (Garg et al., 2014). This result suggests that the targeting domain, in this case, exhibits even a negative effect on the protein activity. Additionally, unpublished data, communicated by Meike Hutt (Institute of Cell Biology and Immunology, Stuttgart), revealed for some, but not all xenograft tumor models, only comparable, but not superior bioactivity of targeting vs. structurally similar non-targeting fusion proteins . These data are in accordance with the *in vitro* results of the present study. In conclusion, a superior activity of targeted TRAIL fusion proteins is probably only achieved when the affinity of the fusion protein towards the target antigen or the antigen density at the tumor cell membrane is significantly higher compared to TRAIL receptors.

## 4.2 Mesenchymal stem cell as delivery vector for the expression of Db-scTRAIL therapeutic protein

In this part of the study I investigated and confirmed the potential use of MSCs, isolated from bone marrow, as delivery system for the expression of the pro-apoptotic protein $Db_{\alpha EGFR}$-scTRAIL. Several reports show, in fact, that MSCs can be genetically modified to express different antitumoral agents, such as IL-12 (Shrayer et al., 2002), IFN-β (Studeny et al., 2002) or IL-2 (Stagg et al., 2004). When these MSCs were applied in tumor models, significant tumor growth reduction and even complete remissions were reported.

At the beginning of this work, the MSCs insensitivity to TRAIL activity, even in combination with sensitizers (bortezomib and smac mimetic), was verified. As reported by Szegezdi et al. 2009, apoptosis resistance is not due to a lack of TRAIL receptors expression, but to the fact that DR4 and DR5 are both inactive in MSCs. In this study they examined TRAIL sensitivity testing three MSC lines, isolated from different sources: bone marrow, fetal blood and umbilical cord. All the cell lines resulted insensitive to apoptosis induced by human recombinant TRAIL, despite the expression of DR4 and DR5, suggesting that this is probably a general characteristic for these stem cells lines.

MSCs were transiently transfected and $Db_{\alpha EGFR}$-scTRAIL secreted in the medium showed a significant reduction of cell number in colon cancer cells (Colo205), in a $Db_{\alpha EGFR}$-scTRAIL dose dependent manner. The superior pro-apoptotic activity of TRAIL in the presence of bortezomib is in accordance with several studies revealing synergistic activity in a broad range of different cancer models (reviewed by de Wilt et al., 2013).

Viral vectors are the most used systems to introduce genes into stem cells, even if the safety of these methods, for clinical applications, is still under controversial debate. This is due to the fact that some of these viral vectors, like lentiviruses, are immunogenic and show instability of the transgene, which can cause severe immune responses when introduced into the patients (reviewed by Stuckey and Shah, 2013). Additionally, the specific integration site of the vector DNA into the genome of the cells is crucial and it should not be random, because in case of disruption of genes necessary for essential cellular processes stem cells might themselves generate tumors. Although the existence of all these critical concerns about safety of viral method, probably due to the higher efficiency of this system, only a small number of studies have used non-viral method to transfect SCs (Choi et al., 2011 and Hu et al., 2012).

For this reason, in order to extend knowledge about the potential use of non-viral transfection approach, which can be easily be translated into clinical applications, in this study a non-viral transfection method based on Polyethyleneimine (PEI) was used.

The success of this transfection method in terms of stable and long expression of a bioactive Db-scTRAIL secreted by MSCs was achieved by the selection of MSC clone#A1 and clone#B12. The ELISA analyses confirmed a stable production up to passage 42 while the co-culture of MSC.TRAIL and Colo205 cells demonstrated the bioactivity of the secreted protein. Interestingly, the reduction of cell viability induced by the different ratios of MSC.TRAIL and Colo205 co-cultured was not tightly correlated to the exact number of MSC.TRAIL used, but was generally a bit higher than expected. This is probably due to an intrinsic limitation of the *in vitro* co-culture assay in comparison with application of soluble proteins into the cell medium. In this case, in fact, an equal distribution of the therapeutic molecule in the total culture volume can be reasonably assume. While during co-culture experiment, only a random distribution of "producer" MSCs and cancer cells can be achieved. In this context, consequently, is extremely hard to observe a tight dose-response effect based on the different ratios of the cells. The same effect was also reported in different studies testing the bioactivity of TRAIL molecules, secreted by MSCs, in different tumors such as ovary, lung, colon and pancreas derived cancer cell lines (Yu et al., 2013; Yuan et al., 2015; Grisendi et al., 2015).

In the last several years, the tumor homing ability of MSCs was tested and reported for a broad range of different cancer cell lines including breast cancer (Kidd et al., 2009), melanoma (Studeny et al., 2002), colon cancer (Menon et al., 2007), Kaposis's sarcoma (Khakoo et al., 2006), malignant glioma (Sasportas et al., 2009), ovaric cancer (Kidd et al., 2009) and lung cancer (Loebinger et al., 2009). However, the specific molecular mechanism which regulates the migration of MSCs across the endothelium to reach tumor sites is not yet completely elucidated. Several molecules have been analyzed and proposed as putative candidates which are responsible for integration of MSCs into tumor stroma, in particular chemokines and growth factors (Momin et al., 2010). In the present study I tested the migratory ability of MSCs, transfected and untransfected, in response to EGF, IGF-1 and Colo205 cells. In accordance with Ponte et al., the established clonally derived MSCs lines, clone#A1 and clone#B12, maintained the ability to migrate in response to both growth factors EGF and IGF-1 *in vitro*, in a manner that is comparable with untransfected MSCs (Ponte et al., 2007). While surprisingly all the MSC lines, included the untransfected cells, were not able to migrate when Colo205 cells were seeded in the lower chamber of the transwell. This can be due to the fact that the number of Colo205 cells used in this experimental condition did not secrete a sufficient amount of growth factors in the culture medium. In fact, seeding the same number of Colo205 cells, no detectable levels of EGF after either 8 or 18 h of cultivation were observed (data not shown). However, a comparable migratory (or non-migratory) capacity was observed

between untransfected and transfected MSC lines, demonstrating that the stable transfection did not interfere with this specific MSCs' ability.

Nevertheless, the migratory capacity of the MSCs as well as the bioactivity and the expression rate of the pro-apoptotic protein are not the only aspects that have to be considered and verified in stem cell based gene approach. In fact, MSCs used as cell delivery system must maintain their stemness properties after gene expression. The three minimal criteria to define MSCs were determined in 2006 by the International Society of Cellular Therapy (ISCT) (Dominici et al., 2006). First, MSCs must be adherent to plastic under standard culture condition. According to the second one, MSCs must express certain cell surface markers, including CD9, CD44, CD71, CD90, CD105, and lack expression of other markers like CD14, CD34 or CD11b. The last criterion verifies the multipotency ability of MSCs which must maintain the capacity to differentiate into adipocytes, chondroblasts and osteoblasts *in vitro*. In accordance with the first criteria, both clonal MSC lines (clone#A1 and clone#B12) grown in adherent condition and shown always during the different passages (p 14, p 25, p 42) a typical spindle-shaped phenotype as confirmed by immunofluorescence analysis using phalloidin to visualize F-actin. Furthermore, in line with the second criteria all MSC lines stably transfected maintain the expression of specific cell markers, like CD9, CD44, CD71 and CD105, and on the other hand they didn't express CD14 and CD34. In accordance with these results, most of the surface markers expressed on these MSCs transfected with Db-scTRAIL have been described also by other groups using mouse MSCs (reviewed by Boxall and Jones 2012). Finally, even the last criterion defined by the ISCT was confirmed for all untransfected and transfected MSC lines, which maintained over passages the ability to differentiate into adipocytes and osteocytes. Additionally, all these results, concerning the MSCs characterization, are also in line with the study published by Raeth et al., 2014, who could show that this very same murine MSC line is capable of *in vivo* bone formation.

Taking together these data demonstrate that the MSC lines generated here are characterized by stable, long term expression of the anti-tumoral agent, $Db_{\alpha EGFR}$-scTRAIL, which induces strong apoptotic activation on colon cancer cells in combination with the sensitizer bortezomib. More importantly, expression of the fusion protein did not alter or interfere with the typical MSCs properties, even upon long term cultivation. This is an essential starting point for translation of stem cell based gene therapy in clinical applications.

## 4.3 Mesenchymal stem cell based therapy for cancer treatment *in vivo*

Despite all the extensive studies performed in the past decades in order to improve outcomes of cancer treatments with non-antibody biologics, such as interleukins, proapoptotic and immune-stimulating cytokines, there are still limitations which reduce the potential efficacy of this class of anticancer agents. The major drawbacks of conventional treatments as well as those of new biological reagents include off target actions and potential systemic side effects, and/or inadequate biodistribution/bioavailability due to short plasma half-life and fast renal clearance of the specific agents after administration (Herbst et al., 2010 and Soria et al., 2010). But the discovery of adult stem cells which show intrinsic tumor tropic properties to several cancer types (Sasportas et al., 2009; Loebinger et al., 2009; Kidd et al., 2009), opened new avenues for tumor treatment using stem cell based gene therapy. This novel approach can overcome the major limitations of the conventional treatments like biodistribution and short half-life. In fact, as reported by several studies using different therapeutic agents including IFN-β (Studeny et al., 2002), IFN-α (Ren et al., 2008) and IL-12 (Shrayer et al., 2002), the use of SCs as delivery vector produce a significant increase of local concentration of the antitumoral agents around the tumor. This increased concentration resulted in a more efficient antitumoral activity of the therapeutic agents than the same molecules used in a systemic administration treatment. Importantly, an efficient translation of cell based therapy into clinical application requires the ability to readily administer a safe and efficacious product at the optimal dosage. Toward this aim, two sources of stem cells can be considered, autologous material from the patient and allogeneic material from healthy donors. Despite the fact that allogeneic therapy is, in principle, a disruptive concept in immunology due to the dogma of immune reactions to any foreign tissue, allogeneic MSC based gene therapy potentially offers enormous advantages over autologous systems. It is an efficient way to achieve immediate availability of well characterized cells in appropriate quantities. Strong alloreactivity is clearly a major hurdle in solid organ and hematopoietic transplantation, necessitating strong immunosuppression to protect the allograft from rejection (Chinen et al., 2010). However, MSCs surprisingly evade immune recognition or even actively suppress immune response (van den Akker et al., 2013) suggesting that they can be used as allografts without requiring simultaneous immunosuppression. Moreover a clinical application of autologous MSCs could have some critical limitations compared to an allogeneic, well characterized MSC producer line. In fact, when an autologous source is used, the MSCs derive from a patient that is generally older and with multiple comorbidities and the final product is manufacturing dependent and limited in term of

available healthy cell number. Furthermore, it was recently reported that MSCs derived from elderly donors, revealed decreased biological activities, including regenerative and differentiation potential, resulting in disappointing treatment outcomes (Jung et al., 2014). Isolating allogeneic MSCs from healthy young donors can overcome these issues. The allogeneic MSCs in fact, can be expanded to a larger amount, undergo pre- and post-cryopreservation control of viability and can be immediately available for administration with the necessary cell number. A recent interesting publication, from Lorkeers et al., reported a comprehensive meta-analysis of large animal studies comparing the effects of autologous and allogeneic stem cell therapies, in ischemic heart disease (Lorkeers et al., 2014). Analyzing the 82 publications included in the study, they conclude that stem cell based treatments appear to be safe and that autologous and allogeneic therapy exhibit similar effects. Even if several questions are still open such as the optimal cell delivery method or the cell dosage range, the allogeneic cell therapy represents a promising alternative for clinical treatments of different disease including cancer.

Based on these concepts, I generated stable MSC lines producing the proapoptotic TRAIL fusion protein, clone#A1 and clone#B12, and investigated their usefulness for tumor treatment in a xenograft mouse model. Usually, *in vivo* models for tumor therapy using MSCs as delivery vector requires multiple injections of the cells during the time of treatments. In fact, as recently reported by Grisendi et al., and Yu et al., a significant tumor reduction or a complete remission can be achieved only after multiple injections of MSCs expressing TRAIL, independently on the method of cell administration (Yu et al. 2013 and Grisendi et al. 2015). In contrast, in this work, a significant reduction of tumor volume was observed already after two peritumorally administrations of MSC.TRAIL (clone #B12), in the presence of bortezomib, in comparison with all the other treatments groups. Additionally, the ELISA assay performed after the second administration (day 26), revealed TRAIL levels in the serum of mice injected with MSC.TRAIL cell line. This result suggests a correlation between the significant reduction of tumor size and the TRAIL pro-apoptotic bioactivity.

In the present study the i.v administration of MSCs did not result in detectable TRAIL levels in the serum as observed for the s.c. injection. The main reason is probably the lower number of cells that were applied in this particular experiment due to technical limitations. However, because this approach was performed only once it is not possible to conclude that i.v. is not a feasible approach. In fact, in literature several publications reported an efficient antitumoral effect after i.v. injection of MSCs, even using less than 1 million cells (Yu et al., 2013). Another unexpected finding was that clone#A1, when s.c. injected, showed no detectable production of TRAIL *in vivo*, in contrast to the positive result with clone#B12, despite that in all *in vitro* analyses both clones showed similar

productivity and bioactivity. The reason of this result is unclear, it probably can be due to the fact that the cells were not able to find/establish the proper conditions for an efficient production *in vivo*, or might have been due to a technical problem. Nevertheless, based on this single assay is not reasonable to conclude that the clone#A1 is inactive in vivo, additional experiments are required to clarify this issue.

A critical aspect of the cell based therapy is its safety. In this work, this aspect was investigated by analyzing the alanine transaminase levels in the serum as a measure of acute liver toxicity and by measuring body weight, with no evidence obtained for such adverse, therapy limiting effects. The results are in accordance with other publications that used TRAIL as therapeutic protein, secreted by MSCs, for treatments of different tumors such as lung (Yan et al., 2016) and colon cancer (Yu et al., 2013).

With the applied therapy scheme, after 42 days of treatments tumors started to regrowth, except for 3 tumors in the cl#B12 + BZB group which remain still responding with tumor volumes below 250 $mm^3$ up to day 52, a state classifiable as stable disease. At this time point (42 days) TRAIL was no longer detectable in the serum by ELISA assay (data not shown). This is probably due to different reasons, one could be that the MSCs had differentiated and stopped TRAIL fusion protein production at this time point. This hypothesis would be in accordance with the ELISA results of the previous *in vivo* analysis, where after a single s.c. MSCs injection TRAIL was no longer detectable in the circulation after 21 days. An alternative explanation could be that the MSCs did not survive until day 42. An indication that this hypothesis could be reasonable comes from the immunofluorescence analyses of tumor sections of all groups, even if these were performed at the end of the study (day 52) and not at day 42. Given the fact that NMRI mice express haplotype H-2q as described by Kökény et al. (Kökény et al., 2007), while murine MSCs used in this work are positive for H-2kb, as reported by Raeth et al., 2014. For MSCs detection in tumor sections a specific antibody which binds the H-2kb (MHC class I) alloantigen, and does not cross react with haplotype H-2q, was used. However, no MSCs presence could be identified with certainty in all tumor tissues analyzed, in particular due to a too strong background signal (data not shown). Grisendi and colleagues detected MSCs on tumor sections after three intratumoral injections (Grisendi et al., 2014). But in this case the mice were sacrificed and analyzed 6 days after the last MSC administration. In contrast, in the present study the animals were sacrificed 25 days after the third MSC injection, so the cells had either vanished by this time (more likely explanation) or migrated towards different regions.

Even if further investigations are necessary to address the open questions, the stem cell based therapy appears a promising tool for clinical application in tumor treatment. This method potentially offers, aside from achieving tumor responses, additional benefits for

the patients, for example in terms of frequency of therapeutic injections. In fact, the current standard treatments with purified proteins require daily injections or at least every second day. While based on the obtained results using MSCs, a regimen with a much reduced frequency of applications, weekly or even less frequent, seems achievable. In addition one can assume that the anticipated tumor localized production of the therapeutic is less prone to raise unwanted systemic side effects as noted in systemic clinical application of highly active biologics. This could improve patient compliance very much.

In conclusion, in the preset study proof of concept was revealed that a stable and well characterized MSC line expressing therapeutic protein can be generated and when used in allogeneic transplantation *in vivo* induces a significant tumor response without side effects.
In future studies it would be interesting to detect the biodistribution of transplanted MSCs after systemic injection and their *in vivo* fate, in order to verify the tumor homing ability.

# 5. Supplementary figures

## Dot blot analysis of single cell cultures for $Db_{\alpha CD133}$-scTRAIL and $Db_{\alpha LGR5}$-scTRAIL

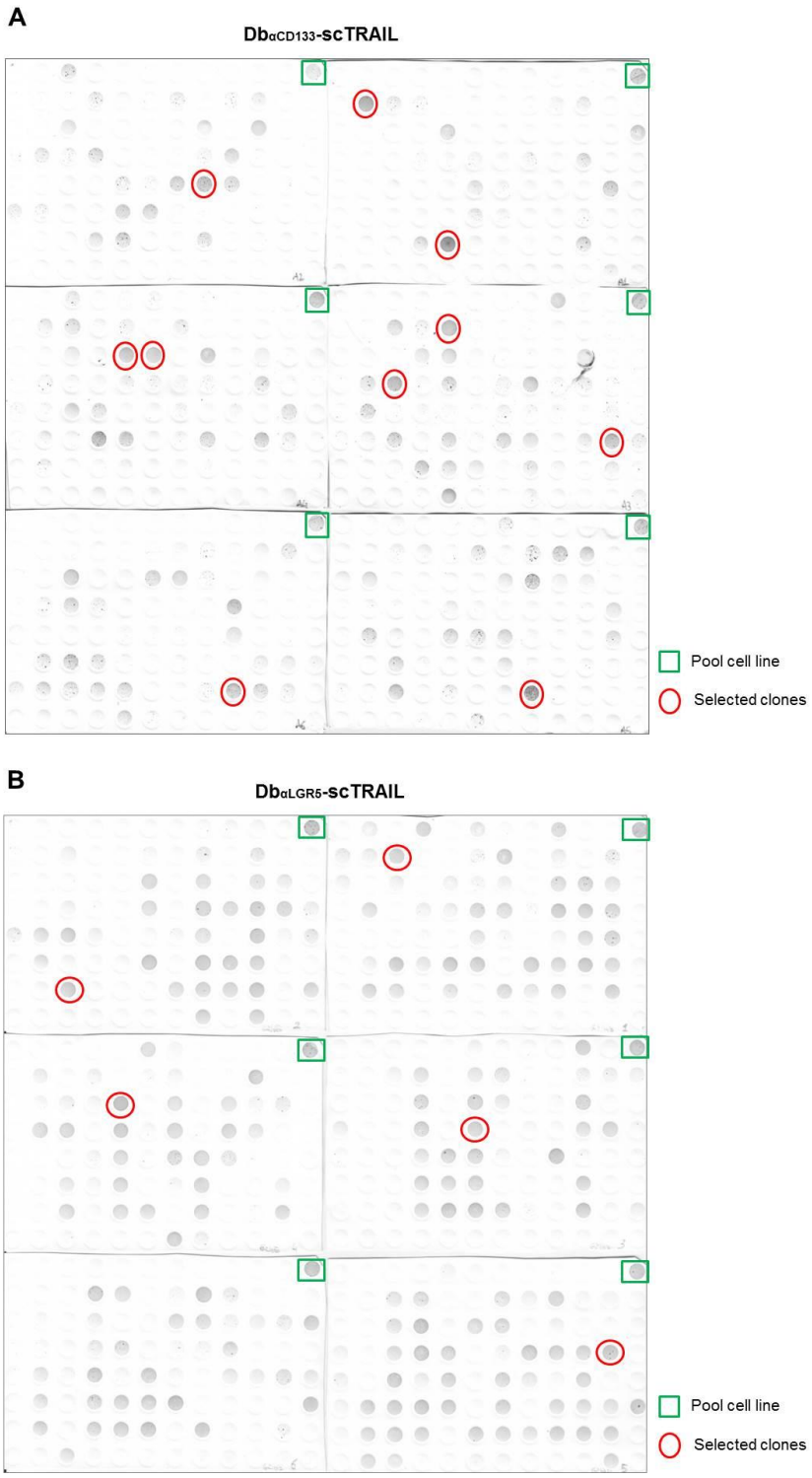


**Figure S1 Dot blot analysis of single cell cultures**
After around 14 days of single cell cultivation, (A) for $Db_{\alpha CD133}$-scTRAIL and (B) for $Db_{\alpha LGR5}$-scTRAIL, culture medium from each well was analyzed by dot blot using a specific antibody against FLAG and single clones were selected (red circles). The pool cell line for each fusion protein was used as negative control (green squares).

## Sensitivity of LoVo cells to smac mimetic and bortezomib

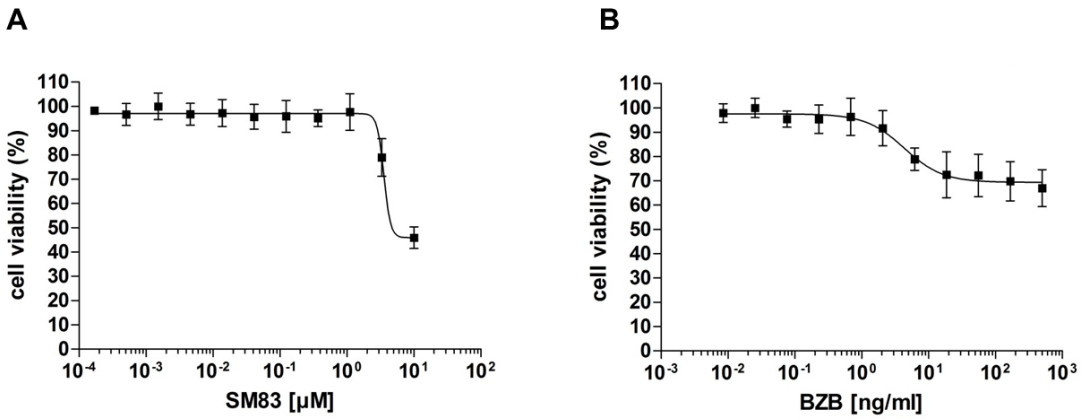


**Figure S2 Analysis of LoVo sensitivity to smac mimetic and bortezomib**
Lovo were treated with serial dilutions of (A) smac mimetic (SM) with a starting concentration of 10 µM (titration 1:3) or (B) with BZB using a starting concentration of 500 ng/ml (titration 1:3). After 18 h, cell viability was determined using crystal violet staining and data were normalized using normal medium treated cells as control (mean ± S.E.M., n=3).

## MSC stable cell lines: proliferation assay

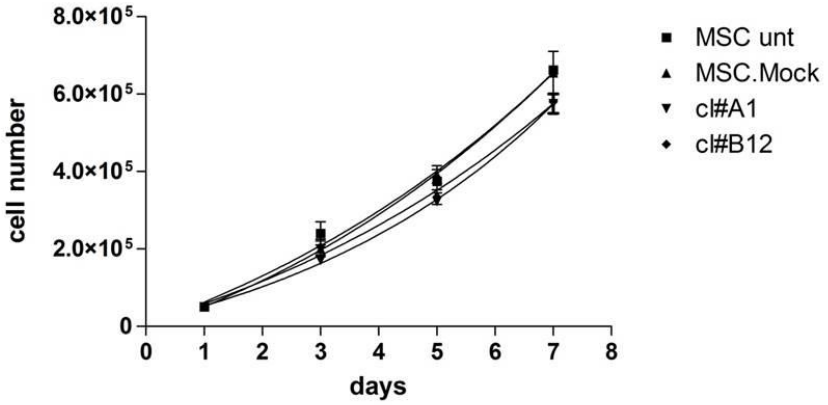


**Figure S3 MSC stable cell lines: proliferation assay**
MSCs untransfected, clone #A1, clone #B12 and Mock cells were seeded at the same cell density and every 48 hours cell number was calculated using the Neubauer chamber and Trypan blue. (mean ± S.E.M., n=5).

## MSCs markers expression

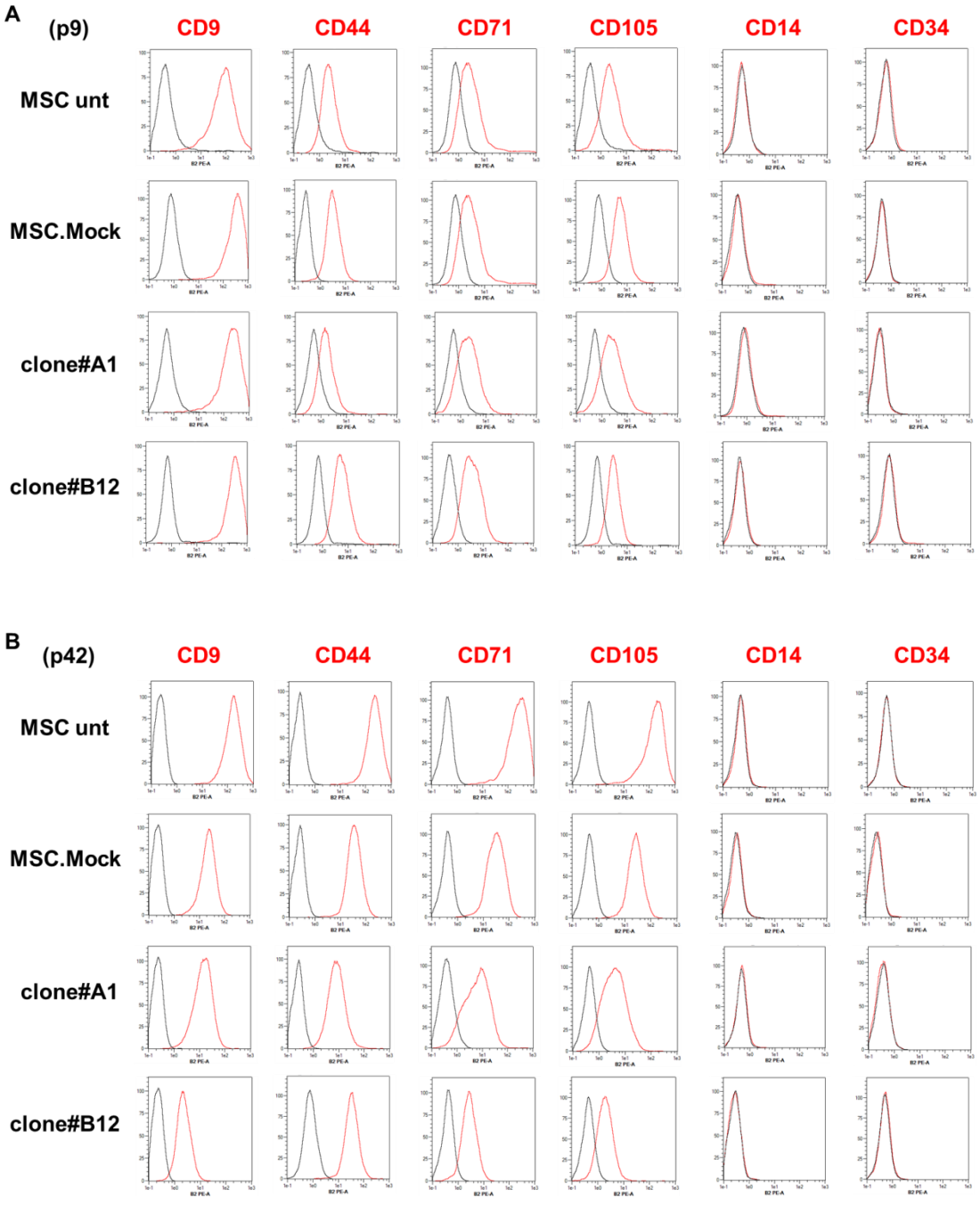


**Figure S4 Surface MSCs markers expression**
Analysis of MSCs markers expression: CD9, CD44, CD71, CD105, CD14 and CD34 at passages (A) 9 and (B) 42. Cells were stained with indicate antibodies and binding was analyzed by flow cytometry (red). Unstained cells were used as negative control (black). Y axis: number of events analyzed.

# References

Aboody, K. S., et al. "Neural Stem Cells Display Extensive Tropism for Pathology in Adult Brain: Evidence from Intracranial Gliomas." *Proc Natl Acad Sci U S A* 97.23 (2000): 12846-51.

Adams, J. "The Proteasome: Structure, Function, and Role in the Cell." *Cancer Treat Rev* 29 Suppl 1 (2003): 3-9.

Andarawewa, K. L., et al. "Stromelysin-3 Is a Potent Negative Regulator of Adipogenesis Participating to Cancer Cell-Adipocyte Interaction/Crosstalk at the Tumor Invasive Front." *Cancer Res* 65.23 (2005): 10862-71.

Aranha, O., and A. B. Benson, 3rd. "Adjuvant Therapy for Colon Cancer." *Curr Gastroenterol Rep* 9.5 (2007): 415-21.

Ashkenazi, A. "Directing Cancer Cells to Self-Destruct with Pro-Apoptotic Receptor Agonists." *Nat Rev Drug Discov* 7.12 (2008): 1001-12.

Ashkenazi, A., P. Holland, and S. G. Eckhardt. "Ligand-Based Targeting of Apoptosis in Cancer: The Potential of Recombinant Human Apoptosis Ligand 2/Tumor Necrosis Factor-Related Apoptosis-Inducing Ligand (Rhapo2l/Trail)." *J Clin Oncol* 26.21 (2008): 3621-30.

Ashkenazi, A., et al. "Safety and Antitumor Activity of Recombinant Soluble Apo2 Ligand." *J Clin Invest* 104.2 (1999): 155-62.

Aslan, H., et al. "Osteogenic Differentiation of Noncultured Immunoisolated Bone Marrow-Derived Cd105+ Cells." *Stem Cells* 24.7 (2006): 1728-37.

Barker, N., S. Tan, and H. Clevers. "Lgr Proteins in Epithelial Stem Cell Biology." *Development* 140.12 (2013): 2484-94.

Barker, N., M. van de Wetering, and H. Clevers. "The Intestinal Stem Cell." *Genes Dev* 22.14 (2008): 1856-64.

Barker, N., et al. "Identification of Stem Cells in Small Intestine and Colon by Marker Gene Lgr5." *Nature* 449.7165 (2007): 1003-7.

Bauer, N., et al. "New Insights into the Cell Biology of Hematopoietic Progenitors by Studying Prominin-1 (Cd133)." *Cells Tissues Organs* 188.1-2 (2008): 127-38.

Becker, A. J., Culloch Ea Mc, and J. E. Till. "Cytological Demonstration of the Clonal Nature of Spleen Colonies Derived from Transplanted Mouse Marrow Cells." *Nature* 197 (1963): 452-4.

Beddington, R. S., and E. J. Robertson. "An Assessment of the Developmental Potential of Embryonic Stem Cells in the Midgestation Mouse Embryo." *Development* 105.4 (1989): 733-7.

Bestor, T. H. "Gene Silencing as a Threat to the Success of Gene Therapy." *J Clin Invest* 105.4 (2000): 409-11.

Booth, C., and C. S. Potten. "Gut Instincts: Thoughts on Intestinal Epithelial Stem Cells." *J Clin Invest* 105.11 (2000): 1493-9.

Boxall, S. A., and E. Jones. "Markers for Characterization of Bone Marrow Multipotential Stromal Cells." *Stem Cells Int* 2012 (2012): 975871.

Brittan, M., and N. A. Wright. "Gastrointestinal Stem Cells." *J Pathol* 197.4 (2002): 492-509.

Brooks, A. D., et al. "Bortezomib Sensitizes Human Renal Cell Carcinomas to Trail Apoptosis through Increased Activation of Caspase-8 in the Death-Inducing Signaling Complex." *Mol Cancer Res* 8.5 (2010): 729-38.

Budinska, E., et al. "Gene Expression Patterns Unveil a New Level of Molecular Heterogeneity in Colorectal Cancer." *J Pathol* 231.1 (2013): 63-76.

Caplan, A. I. "Mesenchymal Stem Cells." *J Orthop Res* 9.5 (1991): 641-50.

Carswell, E. A., et al. "An Endotoxin-Induced Serum Factor That Causes Necrosis of Tumors." *Proc Natl Acad Sci U S A* 72.9 (1975): 3666-70.

Catalano, V., et al. "Cd133 as a Target for Colon Cancer." *Expert Opin Ther Targets* 16.3 (2012): 259-67.

Chawla-Sarkar, M., D. W. Leaman, and E. C. Borden. "Preferential Induction of Apoptosis by Interferon (Ifn)-Beta Compared with Ifn-Alpha2: Correlation with Trail/Apo2l Induction in Melanoma Cell Lines." *Clin Cancer Res* 7.6 (2001): 1821-31.

Chen, S., et al. "Intracoronary Transplantation of Autologous Bone Marrow Mesenchymal Stem Cells for Ischemic Cardiomyopathy Due to Isolated Chronic Occluded Left Anterior Descending Artery." *J Invasive Cardiol* 18.11 (2006): 552-6.

Chen, X. C., et al. "Prophylaxis against Carcinogenesis in Three Kinds of Unestablished Tumor Models Via Il12-Gene-Engineered Mscs." *Carcinogenesis* 27.12 (2006): 2434-41.

Choi, H. Y., et al. "Microparticles from Kidney-Derived Mesenchymal Stem Cells Act as Carriers of Proangiogenic Signals and Contribute to Recovery from Acute Kidney Injury." *PLoS One* 9.2 (2014): e87853.

Choi, S. A., et al. "Therapeutic Efficacy and Safety of Trail-Producing Human Adipose Tissue-Derived Mesenchymal Stem Cells against Experimental Brainstem Glioma." *Neuro Oncol* 13.1 (2011): 61-9.

Coco, C., et al. "Increased Expression of Cd133 and Reduced Dystroglycan Expression Are Strong Predictors of Poor Outcome in Colon Cancer Patients." *J Exp Clin Cancer Res* 31 (2012): 71.

da Silva Meirelles, L., P. C. Chagastelles, and N. B. Nardi. "Mesenchymal Stem Cells Reside in Virtually All Post-Natal Organs and Tissues." *J Cell Sci* 119.Pt 11 (2006): 2204-13.

Dasari, V. R., et al. "Upregulation of Pten in Glioma Cells by Cord Blood Mesenchymal Stem Cells Inhibits Migration Via Downregulation of the Pi3k/Akt Pathway." *PLoS One* 5.4 (2010): e10350.

Dasari, V. R., et al. "Cord Blood Stem Cell-Mediated Induction of Apoptosis in Glioma Downregulates X-Linked Inhibitor of Apoptosis Protein (Xiap)." *PLoS One* 5.7 (2010): e11813.

de Lau, W., et al. "Lgr5 Homologues Associate with Wnt Receptors and Mediate R-Spondin Signalling." *Nature* 476.7360 (2011): 293-7.

de Wilt, L. H., et al. "Bortezomib and Trail: A Perfect Match for Apoptotic Elimination of Tumour Cells?" *Crit Rev Oncol Hematol* 85.3 (2013): 363-72.

Dezawa, M., et al. "Specific Induction of Neuronal Cells from Bone Marrow Stromal Cells and Application for Autologous Transplantation." *J Clin Invest* 113.12 (2004): 1701-10.

Dezawa, M., et al. "Sciatic Nerve Regeneration in Rats Induced by Transplantation of in Vitro Differentiated Bone-Marrow Stromal Cells." *Eur J Neurosci* 14.11 (2001): 1771-6.

Di Ianni, M., et al. "Mesenchymal Cells Recruit and Regulate T Regulatory Cells." *Exp Hematol* 36.3 (2008): 309-18.

Dieter, S. M., et al. "Distinct Types of Tumor-Initiating Cells Form Human Colon Cancer Tumors and Metastases." *Cell Stem Cell* 9.4 (2011): 357-65.

Dimberg, L. Y., et al. "On the Trail to Successful Cancer Therapy? Predicting and Counteracting Resistance against Trail-Based Therapeutics." *Oncogene* 32.11 (2013): 1341-50.

Djouad, F., et al. "Immunosuppressive Effect of Mesenchymal Stem Cells Favors Tumor Growth in Allogeneic Animals." *Blood* 102.10 (2003): 3837-44.

Dominici, M., et al. "Minimal Criteria for Defining Multipotent Mesenchymal Stromal Cells. The International Society for Cellular Therapy Position Statement." *Cytotherapy* 8.4 (2006): 315-7.

Du, W., et al. "Targeting C-Met Receptor Overcomes Trail-Resistance in Brain Tumors." *PLoS One* 9.4 (2014): e95490.

Duda, D. G., et al. "Evidence for Incorporation of Bone Marrow-Derived Endothelial Cells into Perfused Blood Vessels in Tumors." *Blood* 107.7 (2006): 2774-6.

Duiker, E. W., et al. "Development of a Radioiodinated Apoptosis-Inducing Ligand, Rhtrail, and a Radiolabelled Agonist Trail Receptor Antibody for Clinical Imaging Studies." *Br J Pharmacol* 165.7 (2012): 2203-12.

Dwyer, R. M., et al. "Advances in Mesenchymal Stem Cell-Mediated Gene Therapy for Cancer." *Stem Cell Res Ther* 1.3 (2010): 25.

Dwyer, R. M., et al. "Monocyte Chemotactic Protein-1 Secreted by Primary Breast Tumors Stimulates Migration of Mesenchymal Stem Cells." *Clin Cancer Res* 13.17 (2007): 5020-7.

Ehtesham, M., et al. "Induction of Glioblastoma Apoptosis Using Neural Stem Cell-Mediated Delivery of Tumor Necrosis Factor-Related Apoptosis-Inducing Ligand." *Cancer Res* 62.24 (2002): 7170-4.

Fakler, M., et al. "Small Molecule Xiap Inhibitors Cooperate with Trail to Induce Apoptosis in Childhood Acute Leukemia Cells and Overcome Bcl-2-Mediated Resistance." *Blood* 113.8 (2009): 1710-22.

Falschlehner, C., et al. "Trail Signalling: Decisions between Life and Death." *Int J Biochem Cell Biol* 39.7-8 (2007): 1462-75.

Friedenstein, A. J., et al. "Heterotopic of Bone Marrow. Analysis of Precursor Cells for Osteogenic and Hematopoietic Tissues." *Transplantation* 6.2 (1968): 230-47.

Friedenstein, A. J., Shapiro Piatetzky, II, and K. V. Petrakova. "Osteogenesis in Transplants of Bone Marrow Cells." *J Embryol Exp Morphol* 16.3 (1966): 381-90.

Fulda, S., and S. Pervaiz. "Apoptosis Signaling in Cancer Stem Cells." *Int J Biochem Cell Biol* 42.1 (2010): 31-8.

Ganten, T. M., et al. "Preclinical Differentiation between Apparently Safe and Potentially Hepatotoxic Applications of Trail Either Alone or in Combination with Chemotherapeutic Drugs." *Clin Cancer Res* 12.8 (2006): 2640-6.

Gao, P., et al. "Therapeutic Potential of Human Mesenchymal Stem Cells Producing Il-12 in a Mouse Xenograft Model of Renal Cell Carcinoma." *Cancer Lett* 290.2 (2010): 157-66.

Gao, Y., et al. "Chemokine Ccl15 Mediates Migration of Human Bone Marrow-Derived Mesenchymal Stem Cells toward Hepatocellular Carcinoma." *Stem Cells* 34.4 (2016):

1112-22.

Garcia-Olmo, D., et al. "Expanded Adipose-Derived Stem Cells for the Treatment of Complex Perianal Fistula: A Phase Ii Clinical Trial." *Dis Colon Rectum* 52.1 (2009): 79-86.

Garg, A. D., et al. "Immunogenic Cell Death, Damps and Anticancer Therapeutics: An Emerging Amalgamation." *Biochim Biophys Acta* 1805.1 (2010): 53-71.

Garg, G., et al. "Novel Treatment Option for Muc16-Positive Malignancies with the Targeted Trail-Based Fusion Protein Meso-Tr3." *BMC Cancer* 14 (2014): 35.

Giebel, B., et al. "Segregation of Lipid Raft Markers Including Cd133 in Polarized Human Hematopoietic Stem and Progenitor Cells." *Blood* 104.8 (2004): 2332-8.

Greenblatt, M., and P. Shubi. "Tumor Angiogenesis: Transfilter Diffusion Studies in the Hamster by the Transparent Chamber Technique." *J Natl Cancer Inst* 41.1 (1968): 111-24.

Grisendi, G., et al. "Mesenchymal Progenitors Expressing Trail Induce Apoptosis in Sarcomas." *Stem Cells* 33.3 (2015): 859-69.

Gupta, G. P., and J. Massague. "Cancer Metastasis: Building a Framework." *Cell* 127.4 (2006): 679-95.

Gutova, M., et al. "Urokinase Plasminogen Activator and Urokinase Plasminogen Activator Receptor Mediate Human Stem Cell Tropism to Malignant Solid Tumors." *Stem Cells* 26.6 (2008): 1406-13.

Haraguchi, N., et al. "Cd133+Cd44+ Population Efficiently Enriches Colon Cancer Initiating Cells." *Ann Surg Oncol* 15.10 (2008): 2927-33.

Hellwig, C. T., and M. Rehm. "Trail Signaling and Synergy Mechanisms Used in Trail-Based Combination Therapies." *Mol Cancer Ther* 11.1 (2012): 3-13.

Herbst, R. S., et al. "Phase I Dose-Escalation Study of Recombinant Human Apo2l/Trail, a Dual Proapoptotic Receptor Agonist, in Patients with Advanced Cancer." *J Clin Oncol* 28.17 (2010): 2839-46.

Hernanda, P. Y., et al. "Multipotent Mesenchymal Stromal Cells in Liver Cancer: Implications for Tumor Biology and Therapy." *Biochim Biophys Acta* 1846.2 (2014): 439-45.

Ho, I. A., et al. "Matrix Metalloproteinase 1 Is Necessary for the Migration of Human Bone Marrow-Derived Mesenchymal Stem Cells toward Human Glioma." *Stem Cells* 27.6 (2009): 1366-75.

Holliger, P., T. Prospero, and G. Winter. ""Diabodies": Small Bivalent and Bispecific Antibody Fragments." *Proc Natl Acad Sci U S A* 90.14 (1993): 6444-8.

Holmberg, J., et al. "Ephb Receptors Coordinate Migration and Proliferation in the Intestinal Stem Cell Niche." *Cell* 125.6 (2006): 1151-63.

Horwitz, E. M., et al. "Transplantability and Therapeutic Effects of Bone Marrow-Derived Mesenchymal Cells in Children with Osteogenesis Imperfecta." *Nat Med* 5.3 (1999): 309-13.

Hu, Y. L., et al. "Mesenchymal Stem Cells as a Novel Carrier for Targeted Delivery of Gene in Cancer Therapy Based on Nonviral Transfection." *Mol Pharm* 9.9 (2012): 2698-709.

Huang, E. H., and M. S. Wicha. "Colon Cancer Stem Cells: Implications for Prevention and Therapy." *Trends Mol Med* 14.11 (2008): 503-9.

Ichim, T. E., et al. "Placental Mesenchymal and Cord Blood Stem Cell Therapy for Dilated

Cardiomyopathy." *Reprod Biomed Online* 16.6 (2008): 898-905.

Itoh, N., et al. "The Polypeptide Encoded by the Cdna for Human Cell Surface Antigen Fas Can Mediate Apoptosis." *Cell* 66.2 (1991): 233-43.

Javazon, E. H., K. J. Beggs, and A. W. Flake. "Mesenchymal Stem Cells: Paradoxes of Passaging." *Exp Hematol* 32.5 (2004): 414-25.

Jemal, A., et al. "Global Cancer Statistics." *CA Cancer J Clin* 61.2 (2011): 69-90.

Jiang, Y., et al. "Pluripotency of Mesenchymal Stem Cells Derived from Adult Marrow." *Nature* 418.6893 (2002): 41-9.

Johns, T. G., et al. "Antiproliferative Potencies of Interferons on Melanoma Cell Lines and Xenografts: Higher Efficacy of Interferon Beta." *J Natl Cancer Inst* 84.15 (1992): 1185-90.

Karnieli, O., et al. "Generation of Insulin-Producing Cells from Human Bone Marrow Mesenchymal Stem Cells by Genetic Manipulation." *Stem Cells* 25.11 (2007): 2837-44.

Karnoub, A. E., et al. "Mesenchymal Stem Cells within Tumour Stroma Promote Breast Cancer Metastasis." *Nature* 449.7162 (2007): 557-63.

Kawada, H., et al. "Nonhematopoietic Mesenchymal Stem Cells Can Be Mobilized and Differentiate into Cardiomyocytes after Myocardial Infarction." *Blood* 104.12 (2004): 3581-7.

Kelley, S. K., et al. "Preclinical Studies to Predict the Disposition of Apo2l/Tumor Necrosis Factor-Related Apoptosis-Inducing Ligand in Humans: Characterization of in Vivo Efficacy, Pharmacokinetics, and Safety." *J Pharmacol Exp Ther* 299.1 (2001): 31-8.

Kemper, K., et al. "Monoclonal Antibodies against Lgr5 Identify Human Colorectal Cancer Stem Cells." *Stem Cells* 30.11 (2012): 2378-86.

Kendall, S. E., et al. "Neural Stem Cell Targeting of Glioma Is Dependent on Phosphoinositide 3-Kinase Signaling." *Stem Cells* 26.6 (2008): 1575-86.

Kern, S., et al. "Comparative Analysis of Mesenchymal Stem Cells from Bone Marrow, Umbilical Cord Blood, or Adipose Tissue." *Stem Cells* 24.5 (2006): 1294-301.

Khakoo, A. Y., et al. "Human Mesenchymal Stem Cells Exert Potent Antitumorigenic Effects in a Model of Kaposi's Sarcoma." *J Exp Med* 203.5 (2006): 1235-47.

Khanbolooki, S., et al. "Nuclear Factor-Kappab Maintains Trail Resistance in Human Pancreatic Cancer Cells." *Mol Cancer Ther* 5.9 (2006): 2251-60.

Kharaziha, P., et al. "Improvement of Liver Function in Liver Cirrhosis Patients after Autologous Mesenchymal Stem Cell Injection: A Phase I-Ii Clinical Trial." *Eur J Gastroenterol Hepatol* 21.10 (2009): 1199-205.

Kidd, S., et al. "Mesenchymal Stromal Cells Alone or Expressing Interferon-Beta Suppress Pancreatic Tumors in Vivo, an Effect Countered by Anti-Inflammatory Treatment." *Cytotherapy* 12.5 (2010): 615-25.

Kidd, S., et al. "Direct Evidence of Mesenchymal Stem Cell Tropism for Tumor and Wounding Microenvironments Using in Vivo Bioluminescent Imaging." *Stem Cells* 27.10 (2009): 2614-23.

Kim, T. H., et al. "Pegylated Tnf-Related Apoptosis-Inducing Ligand (Trail) Analogues: Pharmacokinetics and Antitumor Effects." *Bioconjug Chem* 22.8 (2011): 1631-7.

Klopp, A. H., et al. "Concise Review: Dissecting a Discrepancy in the Literature: Do Mesenchymal Stem Cells Support or Suppress Tumor Growth?" *Stem Cells* 29.1 (2011): 11-9.

Knoop, K., et al. "Mesenchymal Stem Cell-Mediated, Tumor Stroma-Targeted Radioiodine Therapy of Metastatic Colon Cancer Using the Sodium Iodide Symporter as Theranostic Gene." *J Nucl Med* 56.4 (2015): 600-6.

Kokeny, G., et al. "Skin Disease Is Prevented but Nephritis Is Accelerated by Multiple Pregnancies in Autoimmune Mrl/Lpr Mice." *Lupus* 16.7 (2007): 465-77.

Kontermann, R. E., et al. "Enzyme Immunoassays Using Bispecific Diabodies." *Immunotechnology* 3.2 (1997): 137-44.

Koschny, R., et al. "Bortezomib Sensitizes Primary Human Astrocytoma Cells of Who Grades I to Iv for Tumor Necrosis Factor-Related Apoptosis-Inducing Ligand-Induced Apoptosis." *Clin Cancer Res* 13.11 (2007): 3403-12.

Kreso, A., et al. "Variable Clonal Repopulation Dynamics Influence Chemotherapy Response in Colorectal Cancer." *Science* 339.6119 (2013): 543-8.

Kreuz, S., et al. "Nf-Kappab Inducers Upregulate Cflip, a Cycloheximide-Sensitive Inhibitor of Death Receptor Signaling." *Mol Cell Biol* 21.12 (2001): 3964-73.

Kruyt, F. A. "Trail and Cancer Therapy." *Cancer Lett* 263.1 (2008): 14-25.

Kwiatkowska-Borowczyk, E. P., et al. "Immunotargeting of Cancer Stem Cells." *Contemp Oncol (Pozn)* 19.1A (2015): A52-9.

Lampropoulos, P., et al. "Tgf-Beta Signalling in Colon Carcinogenesis." *Cancer Lett* 314.1 (2012): 1-7.

Lazarus, H. M., et al. "Ex Vivo Expansion and Subsequent Infusion of Human Bone Marrow-Derived Stromal Progenitor Cells (Mesenchymal Progenitor Cells): Implications for Therapeutic Use." *Bone Marrow Transplant* 16.4 (1995): 557-64.

Lecis, D., et al. "Novel Smac-Mimetics Synergistically Stimulate Melanoma Cell Death in Combination with Trail and Bortezomib." *Br J Cancer* 102.12 (2010): 1707-16.

Lemke, J., et al. "Selective Cdk9 Inhibition Overcomes Trail Resistance by Concomitant Suppression of Cflip and Mcl-1." *Cell Death Differ* 21.3 (2014): 491-502.

Lemke, J., et al. "Getting Trail Back on Track for Cancer Therapy." *Cell Death Differ* 21.9 (2014): 1350-64.

Levin, I. "Changes in the Tissue Surrounding a Growing Tumor and the Significance of the "Precancerous State."." *J Exp Med* 16.2 (1912): 149-54.

Levin, I. "The Mechanisms of Metastasis Formation in Experimental Cancer." *J Exp Med* 18.4 (1913): 397-405.

Li, L., et al. "A Small Molecule Smac Mimic Potentiates Trail- and Tnfalpha-Mediated Cell Death." *Science* 305.5689 (2004): 1471-4.

Liang, J., et al. "Allogenic Mesenchymal Stem Cells Transplantation in Refractory Systemic Lupus Erythematosus: A Pilot Clinical Study." *Ann Rheum Dis* 69.8 (2010): 1423-9.

Lin, C. Y., et al. "Enhancing Protein Expression in Hek-293 Cells by Lowering Culture Temperature." *PLoS One* 10.4 (2015): e0123562.

Lin, Y., and W. J. Hogan. "Clinical Application of Mesenchymal Stem Cells in the Treatment and Prevention of Graft-Versus-Host Disease." *Adv Hematol* 2011 (2011): 427863.

Liu, J., et al. "Bortezomib Synergizes Trail-Induced Apoptosis in Gastric Cancer Cells." *Dig Dis Sci* 55.12 (2010): 3361-8.

Liu, L., et al. "Exogenous Marker-Engineered Mesenchymal Stem Cells Detect Cancer and Metastases in a Simple Blood Assay." *Stem Cell Res Ther* 6 (2015): 181.

Loebinger, M. R., et al. "Mesenchymal Stem Cell Delivery of Trail Can Eliminate Metastatic Cancer." *Cancer Res* 69.10 (2009): 4134-42.

Loebinger, M. R., et al. "Magnetic Resonance Imaging of Mesenchymal Stem Cells Homing to Pulmonary Metastases Using Biocompatible Magnetic Nanoparticles." *Cancer Res* 69.23 (2009): 8862-7.

Lyden, D., et al. "Impaired Recruitment of Bone-Marrow-Derived Endothelial and Hematopoietic Precursor Cells Blocks Tumor Angiogenesis and Growth." *Nat Med* 7.11 (2001): 1194-201.

Madec, A. M., et al. "Mesenchymal Stem Cells Protect Nod Mice from Diabetes by Inducing Regulatory T Cells." *Diabetologia* 52.7 (2009): 1391-9.

Maestroni, G. J., E. Hertens, and P. Galli. "Factor(S) from Nonmacrophage Bone Marrow Stromal Cells Inhibit Lewis Lung Carcinoma and B16 Melanoma Growth in Mice." *Cell Mol Life Sci* 55.4 (1999): 663-7.

Maksimovic-Ivanic, D., et al. "Resistance to Trail and How to Surmount It." *Immunol Res* 52.1-2 (2012): 157-68.

Marisa, L., et al. "Gene Expression Classification of Colon Cancer into Molecular Subtypes: Characterization, Validation, and Prognostic Value." *PLoS Med* 10.5 (2013): e1001453.

Markowitz, S. D., and M. M. Bertagnolli. "Molecular Origins of Cancer: Molecular Basis of Colorectal Cancer." *N Engl J Med* 361.25 (2009): 2449-60.

Meacham, C. E., and S. J. Morrison. "Tumour Heterogeneity and Cancer Cell Plasticity." *Nature* 501.7467 (2013): 328-37.

Medema, J. P., and L. Vermeulen. "Microenvironmental Regulation of Stem Cells in Intestinal Homeostasis and Cancer." *Nature* 474.7351 (2011): 318-26.

Menon, L. G., et al. "Differential Gene Expression Associated with Migration of Mesenchymal Stem Cells to Conditioned Medium from Tumor Cells or Bone Marrow Cells." *Stem Cells* 25.2 (2007): 520-8.

Merlos-Suarez, A., and E. Batlle. "Eph-Ephrin Signalling in Adult Tissues and Cancer." *Curr Opin Cell Biol* 20.2 (2008): 194-200.

Moller, Y., et al. "Egfr-Targeted Trail and a Smac Mimetic Synergize to Overcome Apoptosis Resistance in Kras Mutant Colorectal Cancer Cells." *PLoS One* 9.9 (2014): e107165.

Momin, E. N., et al. "The Oncogenic Potential of Mesenchymal Stem Cells in the Treatment of Cancer: Directions for Future Research." *Curr Immunol Rev* 6.2 (2010): 137-48.

Moolten, F. L., and J. M. Wells. "Curability of Tumors Bearing Herpes Thymidine Kinase Genes Transferred by Retroviral Vectors." *J Natl Cancer Inst* 82.4 (1990): 297-300.

Moretta, A., et al. "Activating Receptors and Coreceptors Involved in Human Natural Killer Cell-Mediated Cytolysis." *Annu Rev Immunol* 19 (2001): 197-223.

Mueller, L. P., et al. "Trail-Transduced Multipotent Mesenchymal Stromal Cells (Trail-Msc) Overcome Trail Resistance in Selected Crc Cell Lines in Vitro and in Vivo." *Cancer Gene Ther* 18.4 (2011): 229-39.

Muller, N., et al. "Superior Serum Half Life of Albumin Tagged Tnf Ligands." *Biochem Biophys Res Commun* 396.4 (2010): 793-9.

Muraglia, A., R. Cancedda, and R. Quarto. "Clonal Mesenchymal Progenitors from Human Bone Marrow Differentiate in Vitro According to a Hierarchical Model." *J Cell Sci* 113 ( Pt 7) (2000): 1161-6.

Mylotte, L. A., et al. "Metabolic Flexibility Permits Mesenchymal Stem Cell Survival in an Ischemic Environment." *Stem Cells* 26.5 (2008): 1325-36.

Nakamizo, A., et al. "Human Bone Marrow-Derived Mesenchymal Stem Cells in the Treatment of Gliomas." *Cancer Res* 65.8 (2005): 3307-18.

Naumann, I., et al. "Bortezomib Primes Neuroblastoma Cells for Trail-Induced Apoptosis by Linking the Death Receptor to the Mitochondrial Pathway." *Clin Cancer Res* 17.10 (2011): 3204-18.

Nemeth, K., et al. "Bone Marrow Stromal Cells Use Tgf-Beta to Suppress Allergic Responses in a Mouse Model of Ragweed-Induced Asthma." *Proc Natl Acad Sci U S A* 107.12 (2010): 5652-7.

Newsom-Davis, T., S. Prieske, and H. Walczak. "Is Trail the Holy Grail of Cancer Therapy?" *Apoptosis* 14.4 (2009): 607-23.

Niess, H., et al. "Treatment of Advanced Gastrointestinal Tumors with Genetically Modified Autologous Mesenchymal Stromal Cells (Treat-Me1): Study Protocol of a Phase I/Ii Clinical Trial." *BMC Cancer* 15 (2015): 237.

O'Brien, C. A., et al. "A Human Colon Cancer Cell Capable of Initiating Tumour Growth in Immunodeficient Mice." *Nature* 445.7123 (2007): 106-10.

O'Donoghue, K., et al. "Microchimerism in Female Bone Marrow and Bone Decades after Fetal Mesenchymal Stem-Cell Trafficking in Pregnancy." *Lancet* 364.9429 (2004): 179-82.

Ogasawara, J., et al. "Lethal Effect of the Anti-Fas Antibody in Mice." *Nature* 364.6440 (1993): 806-9.

Ohlsson, L. B., et al. "Mesenchymal Progenitor Cell-Mediated Inhibition of Tumor Growth in Vivo and in Vitro in Gelatin Matrix." *Exp Mol Pathol* 75.3 (2003): 248-55.

Orlowski, R. Z., and D. J. Kuhn. "Proteasome Inhibitors in Cancer Therapy: Lessons from the First Decade." *Clin Cancer Res* 14.6 (2008): 1649-57.

Otsu, K., et al. "Concentration-Dependent Inhibition of Angiogenesis by Mesenchymal Stem Cells." *Blood* 113.18 (2009): 4197-205.

Oyagi, S., et al. "Therapeutic Effect of Transplanting Hgf-Treated Bone Marrow Mesenchymal Cells into Ccl4-Injured Rats." *J Hepatol* 44.4 (2006): 742-8.

Ozoren, N., and W. S. El-Deiry. "Defining Characteristics of Types I and Ii Apoptotic Cells in Response to Trail." *Neoplasia* 4.6 (2002): 551-7.

Pilati, P., et al. "Prognostic Value of Putative Circulating Cancer Stem Cells in Patients Undergoing Hepatic Resection for Colorectal Liver Metastasis." *Ann Surg Oncol* 19.2 (2012): 402-8.

Pittenger, M. F., et al. "Multilineage Potential of Adult Human Mesenchymal Stem Cells." *Science* 284.5411 (1999): 143-7.

Pitti, R. M., et al. "Induction of Apoptosis by Apo-2 Ligand, a New Member of the Tumor Necrosis Factor Cytokine Family." *J Biol Chem* 271.22 (1996): 12687-90.

Ponte, A. L., et al. "The in Vitro Migration Capacity of Human Bone Marrow Mesenchymal Stem Cells: Comparison of Chemokine and Growth Factor Chemotactic Activities." *Stem Cells* 25.7 (2007): 1737-45.

Potten, C. S., et al. "Measurement of in Vivo Proliferation in Human Colorectal Mucosa Using Bromodeoxyuridine." *Gut* 33.1 (1992): 71-8.

Prockop, D. J. "Marrow Stromal Cells as Stem Cells for Nonhematopoietic Tissues." *Science* 276.5309 (1997): 71-4.

Pulkkanen, K. J., and S. Yla-Herttuala. "Gene Therapy for Malignant Glioma: Current Clinical Status." *Mol Ther* 12.4 (2005): 585-98.

Qiao, L., et al. "Suppression of Tumorigenesis by Human Mesenchymal Stem Cells in a Hepatoma Model." *Cell Res* 18.4 (2008): 500-7.

Qiao, L., et al. "Dkk-1 Secreted by Mesenchymal Stem Cells Inhibits Growth of Breast Cancer Cells Via Depression of Wnt Signalling." *Cancer Lett* 269.1 (2008): 67-77.

Raab, M. S., et al. "Multiple Myeloma." *Lancet* 374.9686 (2009): 324-39.

Raeth, S., et al. "A Mouse Bone Marrow Stromal Cell Line with Skeletal Stem Cell Characteristics to Study Osteogenesis in Vitro and in Vivo." *Stem Cells Dev* 23.10 (2014): 1097-108.

Rapp, A. E., et al. "Systemic Mesenchymal Stem Cell Administration Enhances Bone Formation in Fracture Repair but Not Load-Induced Bone Formation." *Eur Cell Mater* 29 (2015): 22-34.

Ren, C., et al. "Therapeutic Potential of Mesenchymal Stem Cells Producing Interferon-Alpha in a Mouse Melanoma Lung Metastasis Model." *Stem Cells* 26.9 (2008): 2332-8.

Ren, C., et al. "Cancer Gene Therapy Using Mesenchymal Stem Cells Expressing Interferon-Beta in a Mouse Prostate Cancer Lung Metastasis Model." *Gene Ther* 15.21 (2008): 1446-53.

Ricci-Vitiani, L., et al. "Identification and Expansion of Human Colon-Cancer-Initiating Cells." *Nature* 445.7123 (2007): 111-5.

Rich, J. N., and S. Bao. "Chemotherapy and Cancer Stem Cells." *Cell Stem Cell* 1.4 (2007): 353-5.

Ringe, J., et al. "Towards in Situ Tissue Repair: Human Mesenchymal Stem Cells Express Chemokine Receptors Cxcr1, Cxcr2 and Ccr2, and Migrate Upon Stimulation with Cxcl8 but Not Ccl2." *J Cell Biochem* 101.1 (2007): 135-46.

Roberts, N. J., et al. "Systemic Use of Tumor Necrosis Factor Alpha as an Anticancer Agent." *Oncotarget* 2.10 (2011): 739-51.

Roepman, P., et al. "Colorectal Cancer Intrinsic Subtypes Predict Chemotherapy Benefit, Deficient Mismatch Repair and Epithelial-to-Mesenchymal Transition." *Int J Cancer* 134.3 (2014): 552-62.

Sasportas, L. S., et al. "Assessment of Therapeutic Efficacy and Fate of Engineered Human Mesenchymal Stem Cells for Cancer Therapy." *Proc Natl Acad Sci U S A* 106.12 (2009): 4822-7.

Sayers, T. J., et al. "The Proteasome Inhibitor Ps-341 Sensitizes Neoplastic Cells to Trail-Mediated Apoptosis by Reducing Levels of C-Flip." *Blood* 102.1 (2003): 303-10.

Schaffert, D., and E. Wagner. "Gene Therapy Progress and Prospects: Synthetic Polymer-Based Systems." *Gene Ther* 15.16 (2008): 1131-8.

Schmidt, M. M., and K. D. Wittrup. "A Modeling Analysis of the Effects of Molecular Size and Binding Affinity on Tumor Targeting." *Mol Cancer Ther* 8.10 (2009): 2861-71.

Schneider, B., et al. "Potent Antitumoral Activity of Trail through Generation of Tumor-Targeted Single-Chain Fusion Proteins." *Cell Death Dis* 1 (2010): e68.

Schneider, P. "Production of Recombinant Trail and Trail Receptor: Fc Chimeric Proteins."

*Methods Enzymol* 322 (2000): 325-45.

Scopelliti, A., et al. "Therapeutic Implications of Cancer Initiating Cells." *Expert Opin Biol Ther* 9.8 (2009): 1005-16.

Seifert, O., et al. "Tetravalent Antibody-Sctrail Fusion Proteins with Improved Properties." *Mol Cancer Ther* 13.1 (2014): 101-11.

Seki, N., et al. "Bortezomib Sensitizes Human Esophageal Squamous Cell Carcinoma Cells to Trail-Mediated Apoptosis Via Activation of Both Extrinsic and Intrinsic Apoptosis Pathways." *Mol Cancer Ther* 9.6 (2010): 1842-51.

Shrayer, D. P., et al. "Capacity of Murine Il-12 to Inhibit the Development of Primary Melanoma Tumors and to Prevent Lung Metastases in the Melanoma-Challenged Mice." *J Exp Ther Oncol* 2.2 (2002): 93-9.

Siegel, R., et al. "Cancer Statistics, 2014." *CA Cancer J Clin* 64.1 (2014): 9-29.

Siegemund, M., et al. "Superior Antitumoral Activity of Dimerized Targeted Single-Chain Trail Fusion Proteins under Retention of Tumor Selectivity." *Cell Death Dis* 3 (2012): e295.

Siegemund, M., et al. "An Optimized Antibody-Single-Chain Trail Fusion Protein for Cancer Therapy." *MAbs* 8.5 (2016): 879-91.

Siminovitch, L., E. A. McCulloch, and J. E. Till. "The Distribution of Colony-Forming Cells among Spleen Colonies." *J Cell Physiol* 62 (1963): 327-36.

Simons, K., and D. Toomre. "Lipid Rafts and Signal Transduction." *Nat Rev Mol Cell Biol* 1.1 (2000): 31-9.

Song, C., et al. "Thymidine Kinase Gene Modified Bone Marrow Mesenchymal Stem Cells as Vehicles for Antitumor Therapy." *Hum Gene Ther* 22.4 (2011): 439-49.

Soria, J. C., et al. "Phase 1b Study of Dulanermin (Recombinant Human Apo2l/Trail) in Combination with Paclitaxel, Carboplatin, and Bevacizumab in Patients with Advanced Non-Squamous Non-Small-Cell Lung Cancer." *J Clin Oncol* 28.9 (2010): 1527-33.

Spaeth, E., et al. "Inflammation and Tumor Microenvironments: Defining the Migratory Itinerary of Mesenchymal Stem Cells." *Gene Ther* 15.10 (2008): 730-8.

Sprick, M. R., et al. "Fadd/Mort1 and Caspase-8 Are Recruited to Trail Receptors 1 and 2 and Are Essential for Apoptosis Mediated by Trail Receptor 2." *Immunity* 12.6 (2000): 599-609.

Stagg, J., et al. "Marrow Stromal Cells for Interleukin-2 Delivery in Cancer Immunotherapy." *Hum Gene Ther* 15.6 (2004): 597-608.

Steeg, P. S. "Tumor Metastasis: Mechanistic Insights and Clinical Challenges." *Nat Med* 12.8 (2006): 895-904.

Stuckey, D. W., and K. Shah. "Trail on Trial: Preclinical Advances in Cancer Therapy." *Trends Mol Med* 19.11 (2013): 685-94.

Studeny, M., et al. "Bone Marrow-Derived Mesenchymal Stem Cells as Vehicles for Interferon-Beta Delivery into Tumors." *Cancer Res* 62.13 (2002): 3603-8.

Sun, L. Y., et al. "Abnormality of Bone Marrow-Derived Mesenchymal Stem Cells in Patients with Systemic Lupus Erythematosus." *Lupus* 16.2 (2007): 121-8.

Szegezdi, E., et al. "Stem Cells Are Resistant to Trail Receptor-Mediated Apoptosis." *J Cell Mol Med* 13.11-12 (2009): 4409-14.

Todaro, M., et al. "Colon Cancer Stem Cells: Promise of Targeted Therapy." *Gastroenterology* 138.6 (2010): 2151-62.

Tomchuck, S. L., et al. "Toll-Like Receptors on Human Mesenchymal Stem Cells Drive Their Migration and Immunomodulating Responses." *Stem Cells* 26.1 (2008): 99-107.

Tracey, K. J., S. F. Lowry, and A. Cerami. "Cachetin/Tnf-Alpha in Septic Shock and Septic Adult Respiratory Distress Syndrome." *Am Rev Respir Dis* 138.6 (1988): 1377-9.

Tracey, K. J., et al. "Cachectin/Tumor Necrosis Factor Induces Lethal Shock and Stress Hormone Responses in the Dog." *Surg Gynecol Obstet* 164.5 (1987): 415-22.

Trauth, B. C., et al. "Monoclonal Antibody-Mediated Tumor Regression by Induction of Apoptosis." *Science* 245.4915 (1989): 301-5.

Uchibori, R., et al. "Cancer Gene Therapy Using Mesenchymal Stem Cells." *Int J Hematol* 99.4 (2014): 377-82.

Vaiopoulos, A. G., et al. "Colorectal Cancer Stem Cells." *Stem Cells* 30.3 (2012): 363-71.

Vallabhaneni, K. C., et al. "Urokinase Receptor Mediates Mobilization, Migration, and Differentiation of Mesenchymal Stem Cells." *Cardiovasc Res* 90.1 (2011): 113-21.

Vousden, K. H., and X. Lu. "Live or Let Die: The Cell's Response to P53." *Nat Rev Cancer* 2.8 (2002): 594-604.

Wahl, K., et al. "Increased Apoptosis Induction in Hepatocellular Carcinoma by a Novel Tumor-Targeted Trail Fusion Protein Combined with Bortezomib." *Hepatology* 57.2 (2013): 625-36.

Walczak, H., and P. H. Krammer. "The Cd95 (Apo-1/Fas) and the Trail (Apo-2l) Apoptosis Systems." *Exp Cell Res* 256.1 (2000): 58-66.

Walczak, H., et al. "Tumoricidal Activity of Tumor Necrosis Factor-Related Apoptosis-Inducing Ligand in Vivo." *Nat Med* 5.2 (1999): 157-63.

Wang, S., and W. S. El-Deiry. "Trail and Apoptosis Induction by Tnf-Family Death Receptors." *Oncogene* 22.53 (2003): 8628-33.

Waterman, R. S., S. L. Henkle, and A. M. Betancourt. "Mesenchymal Stem Cell 1 (Msc1)-Based Therapy Attenuates Tumor Growth Whereas Msc2-Treatment Promotes Tumor Growth and Metastasis." *PLoS One* 7.9 (2012): e45590.

Waterman, R. S., et al. "A New Mesenchymal Stem Cell (Msc) Paradigm: Polarization into a Pro-Inflammatory Msc1 or an Immunosuppressive Msc2 Phenotype." *PLoS One* 5.4 (2010): e10088.

Wiley, S. R., et al. "Identification and Characterization of a New Member of the Tnf Family That Induces Apoptosis." *Immunity* 3.6 (1995): 673-82.

Winner, M., et al. "Amplification of Tumor Hypoxic Responses by Macrophage Migration Inhibitory Factor-Dependent Hypoxia-Inducible Factor Stabilization." *Cancer Res* 67.1 (2007): 186-93.

Woods, A. E., and J. M. Papadimitriou. "The Effect of Inflammatory Stimuli on the Stroma of Neoplasms: The Involvement of Mononuclear Phagocytes." *J Pathol* 123.3 (1977): 165-74.

Wu, M., et al. "Differentiation Potential of Human Embryonic Mesenchymal Stem Cells for Skin-Related Tissue." *Br J Dermatol* 155.2 (2006): 282-91.

Wurm, F. M. "Production of Recombinant Protein Therapeutics in Cultivated Mammalian Cells." *Nat*

*Biotechnol* 22.11 (2004): 1393-8.

Yan, C., et al. "Human Umbilical Cord Mesenchymal Stem Cells Delivering Strail Home to Lung Cancer Mediated by Mcp-1/Ccr2 Axis and Exhibit Antitumor Effects." *Tumour Biol* 37.6 (2016): 8425-35.

Ye, Z., et al. "Immunosuppressive Effects of Rat Mesenchymal Stem Cells: Involvement of Cd4+Cd25+ Regulatory T Cells." *Hepatobiliary Pancreat Dis Int* 7.6 (2008): 608-14.

Yin, A. H., et al. "Ac133, a Novel Marker for Human Hematopoietic Stem and Progenitor Cells." *Blood* 90.12 (1997): 5002-12.

Yu, R., et al. "Delivery of Strail Variants by Mscs in Combination with Cytotoxic Drug Treatment Leads to P53-Independent Enhanced Antitumor Effects." *Cell Death Dis* 4 (2013): e503.

Yuan, Z., et al. "Mesenchymal Stromal Cell Delivery of Full-Length Tumor Necrosis Factor-Related Apoptosis-Inducing Ligand Is Superior to Soluble Type for Cancer Therapy." *Cytotherapy* 17.7 (2015): 885-96.

Yuan, Z., et al. "Cryopreservation of Human Mesenchymal Stromal Cells Expressing Trail for Human Anti-Cancer Therapy." *Cytotherapy* 18.7 (2016): 860-9.

Zappia, E., et al. "Mesenchymal Stem Cells Ameliorate Experimental Autoimmune Encephalomyelitis Inducing T-Cell Anergy." *Blood* 106.5 (2005): 1755-61.

Zeinaloo, A., et al. "Intracoronary Administration of Autologous Mesenchymal Stem Cells in a Critically Ill Patient with Dilated Cardiomyopathy." *Pediatr Transplant* 15.8 (2011): E183-6.

Zhang, S. S., et al. "Cd133(+)Cxcr4(+) Colon Cancer Cells Exhibit Metastatic Potential and Predict Poor Prognosis of Patients." *BMC Med* 10 (2012): 85.

Zhu, Y., et al. "Human Mesenchymal Stem Cells Inhibit Cancer Cell Proliferation by Secreting Dkk-1." *Leukemia* 23.5 (2009): 925-33.

Zuk, P. A., et al. "Multilineage Cells from Human Adipose Tissue: Implications for Cell-Based Therapies." *Tissue Eng* 7.2 (2001): 211-28.

# Declaration

I hereby assure that I performed the present study independently without further help or other materials than stated.

Irene Marini

Stuttgart

# Curriculum vitae

## Personal data


| | |
|---|---|
| **Name** | Irene Marini |
| **Date of birth** | 08-04-1987 |
| **Place of birth** | Rome (Italy) |
| **Nationality** | Italian |
| **Email address** | irenemarini87@gmail.com |


## Education

**Zentrum für Klinische Transfusionsmedizin (ZKT) - Tübingen** ***Jun. 2016 – present***

Researcher in the group of Prof. M.D. Tamam Bakchoul.

**Universität Stuttgart -** ***Institute für Zellbiologie und Immunologie*** ***Mar. 2013 – Mar. 2016***

*PhD in Cellular and Molecular Biology*

PREDICT project in the research group of Prof. Klaus Pfizenmaier.

**University of Rome** ***"Tor Vergata"*** ***Oct. 2009 – May 2012***

*Master of Science in Cellular and Molecular Biology* Final grade: 110/110 with honors

**Relevant courses:** Signal transduction, Neoplastic transformation, Gene expression regulation, Redox signaling, Macromolecules structure and function, Cell differentiation and cell death, Biochemistry and Metabolism, Drug design, Molecular microbiology and virology, Molecular bioinformatics.

**University of Rome** ***"Tor Vergata"*** ***Sept. 2006 – Oct. 2009***

*Bachelor of Science in Cellular and Molecular Biology* Final grade: 110/110

**Relevant courses:** Molecular biology, Genetics, Cytology, Histology, Cytogenetics, Developmental Biology, Biochemistry, Biophysics, Virology, Microbiology, Immunology, Pathology, Clinical Biochemistry, Bioinformatics, Genetic Engineering, Organic chemistry.

**Scientific High School "*Francesco Severi*", Frosinone** ***Sept. 2001 – Jun. 2006***

*Scientific High School leaving Certificate* Final grade: 95/100

# Acknowledgements

First of all I want to express my deep gratitude to Professor Dr. Klaus Pfizenmaier for the chance to be involved in such an interesting research project, as the PREDICT, and for his constant motivation and encouraging support. He was an amazing supervisor and I like to thank him for all the scientific and critical discussions as well as for reviewing this thesis.

I like to express my sincere appreciation to Prof. Dr. Roland Kontermann for his interest and helpful inputs during lab meetings and talks for my studies throughout the whole time.

Many thanks also to Prof. Dr. Steffen Rupp for taking over the second opinion of this thesis.

I also want to thank Dr. Angelika Hausser for all her knowledge about mesenchymal stem cells and because she really was available and helpful at any time for me.

Special thanks to Dr. Martin Siegemund who supported me in the everyday work with critical discussions and to Nathalie Peters who was not only a great help in lab but was also extremely patient with me and my poor German.

I wish to extend my thanks to all people who sheared with me good time in and outside the lab, in particular to Simona, Caterina, Filipa and Nicole.

Finally, I would especially like to thank my friends: Silvia, Lidia, Ludovica, Nakia, Cinzia, Ilenia, Cristina, Fabio, Moro, Endi, Alessio, Bomb, Wob, Papitto.

Most important, I want to thank Andrea for his love, support and patience during the last 11 years.

My deepest and eternal thanks to my wonderful family: mum, dad, my sister Marta and my twin brother Guido (Pito) for the continuous support and care, not only during the time of my thesis.